# Investigation of Polybromides, Non-Classical Polyinterhalides Based on ICl and IBr, and Fluorinated $[PPN]^+$-Salts

Inaugural-Dissertation
to obtain the academic degree
Doctor rerum naturalium (Dr. rer. nat.)

submitted to the Department of Biology, Chemistry and Pharmacy
of Freie Universität Berlin

by
Lisa Mann
from Kirchheimbolanden

2018

The present work was carried out under the supervision of Prof. Dr. Sebastian Hasenstab-Riedel from May 2014 to June 2018 at Freie Universität Berlin in the Institute of Chemistry and Biochemistry.

First Referee: Prof. Dr. Sebastian Hasenstab-Riedel

Second Referee: Prof. Dr. Christian Müller

Date of Defense: 28.09.2018

# Acknowledgement

First, I would like to express my sincere gratitude to Prof. Dr. Sebastian Riedel for the opportunity to do my Ph.D. thesis in his group. Thanks for the exciting varied topic, his scientific support and guidance during my Ph.D. time.

I would like to acknowledge Prof. Dr. Christian Müller, who accepted to invest his valuable time for reviewing this thesis.

My special thanks go to Dr. Heike Haller, for her guidance, encouragement, her creative advices, and everything she taught me about single-crystal X-ray diffraction measurements in the first year of my Ph.D.

I would like to thank Dr. Simon Steinhauer for his good suggestions, the scientific discussions, his help with the NMR and the preparation of my publications. All this have contributed greatly to the success of this work.

I am grateful to Dr. habil. Helmut Beckers for the valuable advices and support with Raman spectroscopy.

At this point I would like to thank all former and present group members of the Riedel group for their support and the nice atmosphere. I will remember the funny but also discussion-rich coffee breaks, the wonderful time at conferences, GRK meetings, group excursions and barbecues. My thanks go especially to Karsten Sonnenberg and Sebastian Hämmerling for academic support and nice discussions. I thank them and Maximilian Stahnke for the good mood during our daily lab work. In addition, I would like to thank Anja Wiesner for introduction in the synthesis of pentafluoroorthotellurates. I thank her and Mathias Ellwanger for good advices.

My students Maxim Gawrilow, Gene Senges, Patrick Voßnacker, Elisabeth Hornberger and Lars Hoffmann are kindly acknowledged for their great work and dedication.

Furthermore, I would like to thank Dr. habil. Helmut Beckers, Dr. Simon Steinhauer, Karsten Sonnenberg and Tyler Gully for proof-reading and language polishing of parts of this work.

I would like to acknowledge Prof. Dr. Dieter Lentz and his former group members, namely Michael Kathan, Dr. Darina Heinrich, Dr. Annika Meyer, Dr. Juliane Krüger, and Dr. Blazej Duda for providing me laboratory space as well as chemicals and glass ware at the beginning of my Ph.D. time. I appreciate all the help and the nice welcome in Berlin.

My further thanks go to the Seppelt group for discussions and ideas, especially to Dr. Moritz Malischewski, who showed me how to work with anhydrous HF.

I would like to thank Dr. Carsten Müller for his contribution to my first paper and his support within the research training network "Fluorine as a Key Element".

I am grateful to Dr. Günther Thiele and Dr. Adelheid Hagenbach for their help in interpreting crystal data.

I thank the core facility BioSupraMol, especially Thomas Kolrep and Xuan Pham for the MS-ESI measurements and the High-Performance Computing facilities of the Zentral-einrichtung für Datenverarbeitung (ZEDAT) for computer resources and support. Furthermore, my thanks go to the administrative and technical stuff in the chemistry department.

I am grateful to my family and friends for their manifold support, their encouragement and understanding over all these years. Last but certainly not least, I want to thank Leon for his loving support, all the patience, and the wonderful time.

# Contents

List of Abbreviations ..... 2
1 Introduction ..... 5
1.1 Polyhalogen Anions ..... 5
1.1.1 General Bonding Situation ..... 5
1.1.2 Polybromide Monoanions ..... 7
1.1.3 Polybromide Dianions ..... 11
1.1.4 Polychlorides and -fluorides ..... 13
1.2 Polyinterhalides ..... 15
1.3 Bis(triphenylphosphoranylidene)iminium Cations ..... 26
1.4 References ..... 31
2 Aims and Objectives ..... 39
3 Publications ..... 40
3.1 Polybromide Dianions and Networks Stabilized by Fluorinated Bromo(triaryl)-phosphonium Cations ..... 40
3.2 $[NMe_4][I_4Br_5]$: A new Iodobromide from an Ionic Liquid with Halogen–Halogen Interactions ..... 65
3.3 Further Development of Weakly Coordinating Cations: Fluorinated Bis(triaryl-phosphoranylidene)iminium Salts ..... 79
4 Further Investigations on Polyhalides and Polyinterhalides ..... 121
4.1 Investigation of Polyhalides and Polyinterhalides of the Cobaltocenium Cation ..... 121
4.2 Iodobromide Synthesized from Tetraethylammonium Bromide in an Ionic Liquid ..... 128
4.3 Investigation of $[PPN\text{-}3^F]Cl$ in the Synthesis of a Polyhalide and a Polyinterhalide ..... 131
4.4 Reaction of $[PPh_4]Cl$ with ICl ..... 134
4.5 Overview of the Stretching Vibrations of Non-Classical Iodochlorides and -bromides ..... 141
4.6 Experimental Section ..... 143
4.6.1 Methods ..... 143
4.6.2 Crystallographic Data ..... 144
4.6.3 Syntheses ..... 146
4.7 References ..... 150
5 Summary ..... 153
6 Zusammenfassung ..... 155
7 Publications and Conference Contributions ..... 157
8 Curriculum Vitae ..... 159

# List of Abbreviations

| | |
|---|---|
| Alk | alkyl |
| Ar | aryl |
| a.u. | atomic units |
| bcp | bond critical point |
| $B_{15}K_5$ | benzo-15-crown-5 |
| BEDT-TTF | bis(ethylenedithio)tetrathiofulvalene |
| B3LYP | Becke, three-parameter, Lee-Yang-Parr |
| BMDIM | 1,12-bis((1-methylbenzimidazolium)3-yl)dodecane |
| BMP / $C_4$MPyr | *N*-butyl-*N*-methylpyrrolidinium |
| BPH / BHP | 2,2'-bipyridylium |
| btmgn | 1,8-bis(tetramethylguanidinyl)naphthalene |
| Bu | butyl |
| Bz | benzyl |
| CCDC | The Cambridge Crystallographic Data Centre |
| CCSD(T) | Coupled Cluster with Single, Double and perturbative Triple excitations |
| CSD | Cambridge Structural Database |
| Cp | cyclopentadienyl |
| Cp* | pentamethylcyclopentadienyl |
| dafone | 4,5-diazafluoren-9-one |
| $DB_{24}K_8$ | dibenzo-24-crown-8 |
| DCM | dichloromethane |
| DFB | difluorobenzene |
| DFT | Density Functional Theory |
| DMSO | dimethyl sulfoxide |
| $E_h$ | Hartree energy |
| ESI | Electrospray Ionization |
| Et | ethyl |

| | |
|---|---|
| FIA | Fluoride Ion Affinity |
| FIR | Far Infrared |
| FT | Fourier Transform |
| HF | Hartree-Fock |
| HMET | 1,6-bis(trimethylammonium)hexane |
| HMIM | 1-hexyl-3-methyl-imidazolium |
| HOMO | Highest Occupied Molecular Orbital |
| $I_2b_{15}c_5$ | diiodobenzo-15-crown-5 |
| IR | Infrared |
| IUPAC | International Union of Pure and Applied Chemistry |
| LUMO | Lowest Unoccupied Molecular Orbital |
| Me | methyl |
| MP2 | Second-order Møller-Plesset perturbation theory |
| NMR | Nuclear Magnetic Resonance |
| NPA | Natural Population Analysis |
| NTf | bis(trifluoromethylsulfonyl)imide |
| $N(Tf)_2$ | bis(trifluoromethylsulfonyl)amide |
| OTf | triflate |
| $P_{4,4,4,4}$ | tetrabutylphosphonium |
| $P_{6,6,6,14}$ | tetradecyltrihexylphosphonium |
| Pip | 1,1,3,3,5,5-hexamethylpiperidinium |
| phen | phenanthroline |
| $[PPN]^+$ | bis(triphenylphosphoranylidene)iminium |
| $[PPN\text{-}1^F]^+$ | bis[tris(4-fluorophenyl)phosphoranylidene]iminium |
| $[PPN\text{-}2^F]^+$ | bis[tris(3,5-difluorophenyl)phosphoranylidene]iminium |
| $[PPN\text{-}3^F]^+$ | bis[tris(3,4,5-trifluorophenyl)phosphoranylidene]iminium |
| $[PPN\text{-}5^F]^+$ | bis[tris(perfluorophenyl)phosphoranylidene]iminium |
| Pr | propyl |
| Py | pyridine |
| SCS | Spin-Component Scaled |

| | |
|---|---|
| SI | Supporting Information |
| TG | Thermogravimetry |
| TGA | Thermogravimetric Analysis |
| $T_{min}/T_{max}$ | minimum/ maximum transmission factor |
| tppz | tetra(2-pyridyl)pyrazine |
| tptz | 2,4,6-tris(2-pyridyl)-1,3,5-triazine |
| ttmgn | 1,2,4,5-tetrakis(tetramethylguanidyl)naphthalene |
| TZVPP | Valence triple-zeta with two sets of polarization functions |
| UV/Vis | Ultraviolet-visible |
| WCA | Weakly Coordinating Anion |
| WCC | Weakly Coordinating Cation |
| X, Y, Z | halogen atom |

# 1 Introduction

## 1.1 Polyhalogen Anions

A wide range of poly- and polyinterhalide compounds are known. Starting with polyhalogen anionic species the polyiodides are the most investigated class ranging from $[I_3]^-$ to $[I_{26}]^{4-}$.[1–3] The tendency to form polyhalides decreases the lighter the halogens are.

First, the general bonding situation of polyhalogen anions will be described, thereafter the polybromides are discussed in more detail and then briefly compared with the polychlorides and -fluorides.

### 1.1.1 General Bonding Situation

Polyhalides are formed of three building blocks $[X]^-$, $[X_3]^-$, and $X_2$. $[X]^-$ and $[X_3]^-$ are usually located in the polyhalide molecule center and act as Lewis bases donating electron density from their HOMO into the LUMO of one or more Lewis acids, $X_2$. This results in an elongation of the X–X bond of coordinated $X_2$, which can be detected via vibrational spectroscopy as a shift of the corresponding stretching mode to lower wavenumbers. A distinction is made for the trihalide anion $[X_3]^-$ depending on whether it is linear and symmetric, and can therefore be described as a 4-electron 3-center bonding system, which is isoelectronic to e.g. $XeF_2$, or shows an asymmetric structure represented by a donor-acceptor or charge-transfer complex as described above.[4] Figure 1-1 shows the Rundle-Pimentel model for 4-electron 3-center bonding systems in comparison to a donor-acceptor interaction.[5–8]

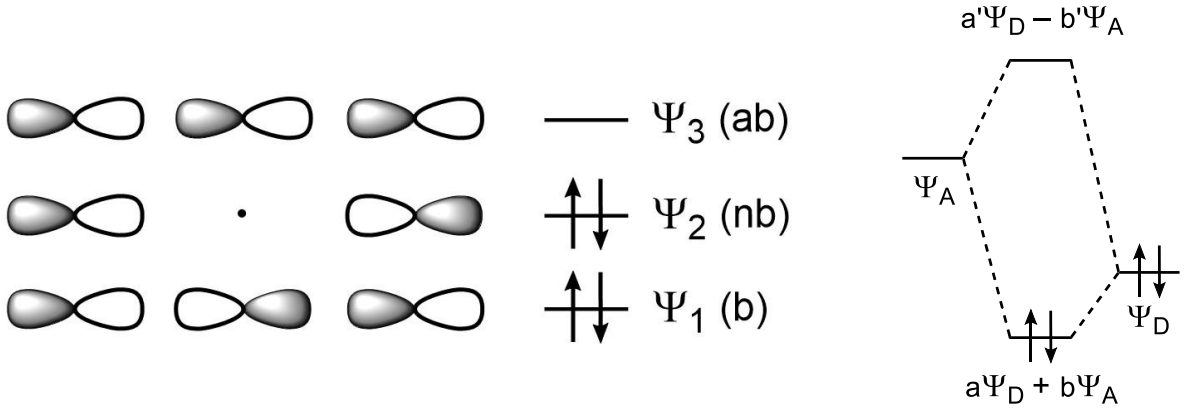


Figure 1-1: Different bonding situations in $[X_3]^-$. *Left:* Rundle-Pimentel scheme for the description of a 4-electron 3-center bonding system. *Right:* Simplified diagram of a donor-acceptor complex. (graphic: based on [8])

Hoffmann and Aragoni investigated these two bonding concepts for $[X_3]^-$ on basis of theoretical calculations as well as structural data from the Cambridge Structural Database (CSD). While the donor-acceptor model, as already mentioned above, is particularly suitable for the description of very asymmetric systems due to the consideration of two stable fragments the Rundle-Pimentel model explains well the charge distribution of symmetric trihalide anions. Thus, the two terminal halogen atoms show a much more negative charge than the central atom in $[X_3]^-$, since they are the largest contributors to the HOMO.[7,8] For example, the NPA (Natural Population Analysis) charges of a tribromide anion are –0.451 for the two terminal and –0.098 for the central bromine atom as calculated in quantum-chemical calculations at CCSD(T)/aug-cc-pVTZ//B3LYP/aug-cc-pVTZ level.[4]

Furthermore, the concept of halogen bonding is used to describe the bonding situation in polyhalogen anions. This concept and related nomenclature have recently been a topic of an IUPAC recommendation.[9] The noncovalent interaction is largely driven by electrostatic forces and generally built between a R–X unit in which the halogen atom X shows a region of positive electrostatic potential, namely the σ-hole, and a negative site like the lone pair of a Lewis base or a halide anion. Beside the σ-hole, that lies in extension of the covalent bond, the anisotropic charge distribution of R–X also leads to a belt of negative electrostatic potential around the central region due to the three unshared electron pairs.[10–17] Figure 1-2 shows the electrostatic potential plotted for a $Br_2$ molecule.

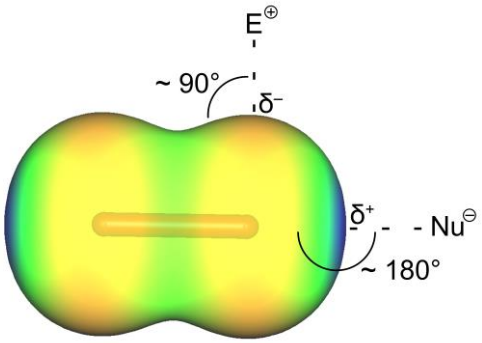


Figure 1-2: Electrostatic potential of $Br_2$ mapped on the total electron density isosurface of 0.005 a.u. in the range from –0.02 a.u. (red) to 0.08 a.u. (blue); calculated at the B3LYP-D3/def2-TZVPP level. Halogen close contacts with another atom show an angle of approximately 180° to a nucleophile and around 90–120° to an electrophile.

Halogen bonding is highly directional with bond angles of approximately 180° for R–X···B with the halogen X acting as electron acceptor and 90–120° for a contact with electrophiles in which X acts as an electron donor (see Figure 1-2).[12,15] The electrostatic potential at the σ-hole decreases in the order X = I > Br > Cl > F. Its value also depends on electron-withdrawing properties of the R substituent.[11,14] Therefore, Politzer et al.

observed a σ-hole for the chlorine atom in $CF_3Cl$, but not for $CH_3Cl$. Even the fluorine atom in $CF_3F$ does not show a σ-hole, its high electronegativity and *sp*-hybridization result in the cancellation of the σ-hole.[11]

### 1.1.2 Polybromide Monoanions

First investigations on polybromide anions were reported in 1923 by Chattaway and Hoyle. They reacted tetramethylammonium bromide with bromine in two different ways, either by dissolving them in small amounts of acetic acid and alcohol or by absorption in a desiccator. For the latter, they determined the highest amount of absorbed bromine to be 5.7 eq.[18]

Today, the polybromide monoanions $[Br_3]^-$, $[Br_5]^-$, $[Br_7]^-$, $[Br_9]^-$ and $[Br_{11}]^-$ are structurally known, see Figure 1-3 for schematic representations.

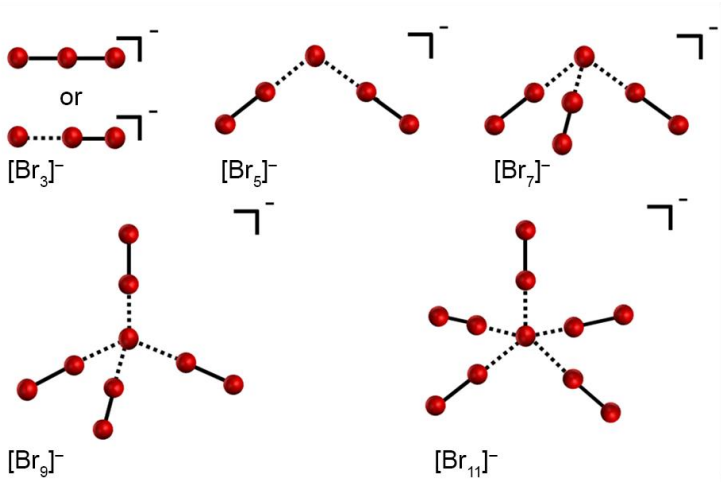


Figure 1-3: Schematic representation of the polybromide monoanion structures $[Br_3]^-$, $[Br_5]^-$, $[Br_7]^-$, $[Br_9]^-$ and $[Br_{11}]^-$.

In 2011 Pichierri compared all high-resolution crystal structures containing $[Br_3]^-$ anions (R factor ≤0.05) found in the CSD. This analysis showed 12 compounds with a symmetric $[Br_3]^-$ revealing the same bond lengths that range from 252.3–255.1 pm as well as 30 compounds that contain an asymmetric $[Br_3]^-$ anion.[19] The asymmetry is usually due to the presence of cations or other positively charged groups like in the most asymmetric example adamantylidene-adamantane bromonium tribromide.[20] In this case the bromonium cation interacts both with the central and one of the terminal bromine atoms resulting in an elongation of one Br–Br bond to 271.8(1) pm while the other distance is only 241.2(1) pm.[19] These interactions are consistent with *ab initio* calculations for $KBr_3$,

where the cation in side-on position also induces a distortion of the $[Br_3]^-$ anion with a difference in the Br–Br bond lengths of 50 pm.[21]

After initial evidence of $[Br_5]^-$ anions in UV/Vis[22] and Raman spectra[23], the first structural proofs were reported by Himmel et al. for $[(ttmgn\text{-}Br_4)(BF_2)_2][Br_5]_2$ (ttmgn = 1,2,4,5-tetrakis(tetramethylguanidyl)naphthalene) and $[(btmgn\text{-}Br_4)(BF_2)][Br_5]$ (btmgn = 1,8-bis-(tetramethylguanidinyl)naphthalene). In both structures the asymmetric V-shaped $[Br_5]^-$ anions interact with each other to form dimeric units or polymeric chains.[24] Polymeric $[Br_5]^-$ zig-zag chains, which are in contrast to the $[Br_5]^-$ described above, formed by alternating $[Br_3]^-$ anions and $Br_2$ molecules, are recently reported for $[p\text{-}MeOPy_2Br][Br_5]$ (*p*-$MeOPy_2Br$ = bis(4-methoxypyridine)bromonium)[25], $[Cu(dafone)_3][Br_3][Br_5]$ and $[Cu(dafone)_3][Br_5][Br_8]_{0.5} \cdot CH_3CN$ (dafone = 4,5-diazafluoren-9-one).[26]

The behavior to interact with adjacent ions is also found for $[Br_7]^-$. Feldmann et al. obtained the compound $[PPh_3Br][Br_7]$ in an eutectic mixture of the ionic liquids $[C_{10}MPyr]Br$ ($C_{10}MPyr$ = *N*-decyl-*N*-methylpyrrolidinium) and $[C_4MPyr][OTf]$ ($C_4MPyr$ = *N*-butyl-*N*-methylpyrrolidinium). The $[Br_7]^-$ anion, that consists of a central $Br^-$ coordinating three bromine molecules in a distorted trigonal pyramidal structure, weakly interacts with the bromine atom of the phosphonium cation as well as with neighboring $[Br_7]^-$ anions, see Figure 1-4A.[27] When working in a $HBr/Br_2$ medium Gorokh et al. obtained the 2D supramolecular polymer $[NEt_4][(Br_3)(Br_2)_2]$ in which each $[Br_3]^-$ anion interacts with four $Br_2$ molecules, see Figure 1-4B.[28]

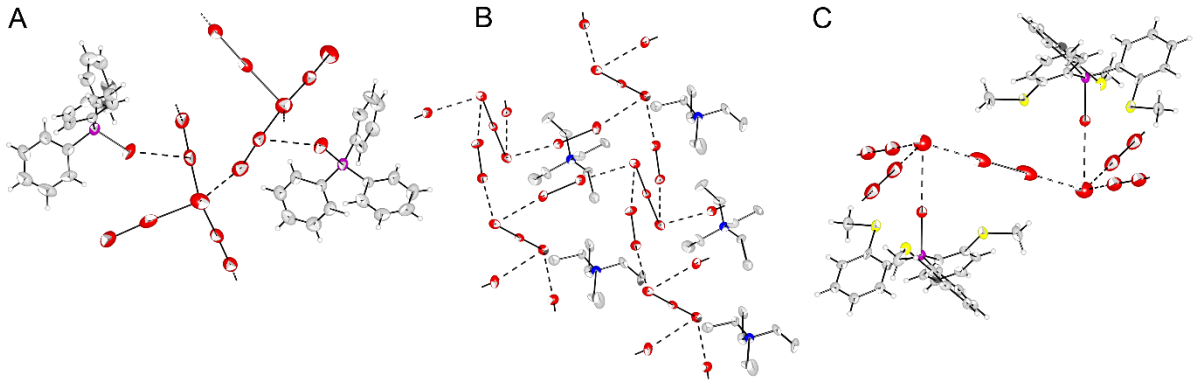


Figure 1-4: Crystal packing in the solid state structures of $[PPh_3Br][Br_7]$ (A), $[NEt_4][(Br_3)(Br_2)_2]$, where the hydrogen atoms are omitted for clarity (B), and $\{[o\text{-}SCH_3C_6H_4)_3PBr][Br] \cdot 0.5(\mu\text{-}Br_2)_3\}_n$ (C). (graphic: based on [27–29])

A compound that does not formally contain any $[Br_7]^-$ anion, but nevertheless shows many of the already mentioned structural motifs is $\{[o\text{-}SCH_3C_6H_4)_3PBr][Br] \cdot 0.5(\mu\text{-}Br_2)_3\}_n$, see Figure 1-4C. Here, the central $Br^-$ anions are coordinated by three bromine molecules. Each $Br_2$ molecule interacts with two $Br^-$ anions, forming a polybromide network.[29]

Chen et al. studied the reactions of tetraethylammonium bromide with bromine forming polybromides from $[Br_3]^-$ to $[Br_9]^-$. With the exception of the $[Br_7]^-$ anion, the measured Raman spectra agree well with quantum-chemical calculations at the MP2/6-31G(d) ($[Br_3]^-$, $[Br_5]^-$, $[Br_7]^-$) and the HF/6-31G(d) level ($[Br_9]^-$).[30] The first nonabromide crystal structure $[NPr_4][Br_9]$ was obtained from a reaction mixture of tetrapropylammonium bromide in an excess of bromine. The $[Br_9]^-$ anion is almost tetrahedrally coordinated with additional intermolecular contacts that form a 3D-network. According to quantum-chemical calculations at MP2 and HF level, the most stable $[Br_9]^-$ isomer shows $T_d$ symmetry.[31] However, depending on the used cation the $[Br_9]^-$ structures differ in the series of $[NEt_4][Br_9]$ (Alk = Me, Et, Pr, Bu). Analogous to $[NPr_4][Br_9]$, the $[Br_9]^-$ anions of $[NMe_4]^+$ and $[NEt_4]^+$ also consist of the two building blocks $[Br]^-$ and $Br_2$ forming different networks of T- and Z-shaped wires or layers in a zipper-like motif. $[NBu_4][Br_9]$ displays two different structural motifs for the $[Br_9]^-$ anion, see Figure 1-5. In the first one, the central $Br^-$ is coordinated by four bridging and two terminal $Br_2$ units and is comparable to the structural motif in $[NEt_4][Br_9]$. With the building block $[Br_3]^-$ that coordinates at each side three $Br_2$ molecules, the second structural motif in $[NBu_4][Br_9]$ deviates from all other described $[Br_9]^-$ anions.[32]

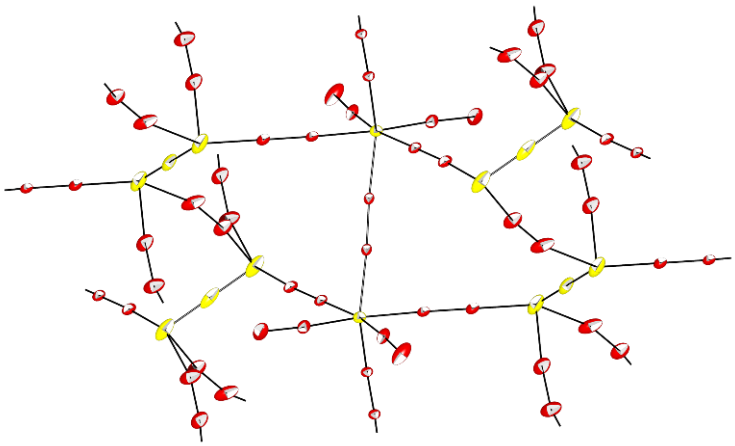

Figure 1-5: Excerpt from the polybromide network in the solid state structure of $[NBu_4][Br_9]$. The building blocks $Br^-$ and $[Br_3]^-$ are yellow colored, $Br_2$ is red colored. (CCDC: 845161)[32]

This $[Br_3]^-$ building block is also observed in the Raman spectrum as an additional band at 219 $cm^{-1}$. The other two bands of the $[Br_9]^-$ anion are shifted to lower wavenumbers (254 and 268 $cm^{-1}$) in contrast to all other described $[Br_9]^-$ anions that show bands at approximately 260 and 275 $cm^{-1}$.[32] The nonabromides show surprisingly high conductivities[31–33], especially $[HMIM][Br_9]$ (HMIM = 1-hexyl-3-methylimidazolium), the first nonabromide ionic liquid, shows a conductivity of 52.1 $mS \cdot cm^{-1}$ at 25.6 °C, while for [HMIM]Br the conductivity of 54.2 $\mu S \cdot cm^{-1}$ at 26.6 °C is considerably lower.[33] A Grotthuss-type hopping mechanism was proposed for the conductivity of $Br^-/Br_2$

systems.[34] Nowadays, even higher polybromides are tested in redox-flow batteries[35,36] and $Br^-/[Br_3]^-$ electrolyte solutions in dye-sensitized solarcells.[37,38] In addition to some tribromides[39–41] the nonabromide $[NPr_4][Br_9]$ can also be used as a bromination reagent that is easier to handle and shows in some cases a higher selectivity than elemental bromine.[42]

The polybromide monoanion with the highest bromine content obtained so far is $[PPN][Br_{11} \cdot Br_2]$ (PPN = bis(triphenylphosphoranylidene)iminium).[43] The $[Br_{11}]^-$ anion consists of a central $Br^-$ coordinating five $Br_2$ molecules in an almost square-pyramidal structure. The additional embedded $Br_2$ molecule has a short bond length of 227.3(1) pm and shows distances to the neighboring $[Br_{11}]^-$ anions of 328.8(1) and 366.9(1) pm that are below twice the van der Waals radius of bromine (370 pm). The formed chains are pictured in Figure 1-6.

Figure 1-6: Chain-like structure in $[PPN][Br_{11} \cdot Br_2]$ formed by $[Br_{11}]^-$ anions and $Br_2$ molecules. (CCDC: 906333)[43]

### 1.1.3 Polybromide Dianions

In the series of polybromide dianions $[Br_4]^{2-}$, $[Br_6]^{2-}$, $[Br_8]^{2-}$, $[Br_{10}]^{2-}$, $[Br_{16}]^{2-}$, $[Br_{20}]^{2-}$ and $[Br_{24}]^{2-}$ are known. Schematic representations for the four first mentioned dianions are presented in Figure 1-7.

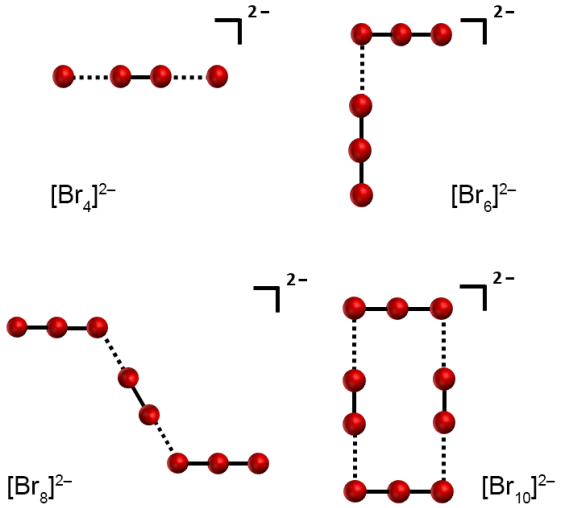


Figure 1-7: Schematic representation of the polybromide dianion structures $[Br_4]^{2-}$, $[Br_6]^{2-}$, $[Br_8]^{2-}$ and $[Br_{10}]^{2-}$.

The $[Br_4]^{2-}$ dianion was already investigated by X-ray crystallography in 1959.[44] The nearly linear chains are formed by treating dimethylammonium bromide with elemental bromine in chloroform. They show an angle of 173.0° and Br–Br distances of 242 pm between the two central and 303 pm to the terminal bromine atoms. Further $[Br_4]^{2-}$ dianions are known for $W_6Br_{16}$ in which $[W_6Br_8]^{6+}$ cations and $[Br_4]^{2-}$ dianions are linked to repeating units of angled chains[45], $[(CH_3)_2SBr^+][Br^-_{0.5}(Br_4^{2-})_{0.25}]$[46] and $[H_4ttpz^{4+}][(Br^-)_2(Br_4^{2-})]$ (tppz = tetra(2-pyridyl)pyrazine]. For the latter bands at 167 and 74 $cm^{-1}$ are observed in the Raman spectrum that agree well with predicted bands at 176 and 70 $cm^{-1}$ in quantum-chemical calculations at the MP2/LanL2DZ level.[47]

Recently, the first structure of a $[Br_6]^{2-}$ dianion was reported for the reaction of 1,3-dimethylimidazolidinone with oxalyl bromide. The dianion shows a hockey-stick like structure (see Figure 1-7) that consists of two asymmetric tribromides connected in a L-shaped geometry by halogen-halogen interaction with an angle of 87.7(1)°. The interaction of the two $[Br_3]^-$ units is facilitated by another interaction of the $[Br_3]^-$ units with the bromoamidinium cation. In contrast, quantum-chemical calculations at the RI-MP2/aug-cc-pVTZ level predict a T-shaped minimum structure.[48]

The $[Br_8]^{2-}$ dianion is built of two $[Br_3]^-$ anions connected by a $Br_2$ molecule in a roughly planar Z-shaped structure (see Figure 1-7). Many examples containing a $[Br_8]^{2-}$ dianion are known. The angles of the linked building blocks range from 76.8(1)° to 117.7(1)°.[27,49–53]

The reaction of 1,5-diphenylformazan and bromine yielded a salt of the rectangular $[Br_{10}]^{2-}$ dianion. It consists of two asymmetric $[Br_3]^-$ anions that are linked by two $Br_2$ molecules (see Figure 1-7).[54]

$[PPN]_2[Br_{16}] \cdot Br_2$ contains the only known $[Br_{16}]^{2-}$ dianion so far. $[Br_{16}]^{2-}$ consists of two nearly T-shaped $[Br_7]^-$ whose central $Br^-$ anions are interconnected by a $Br_2$ molecule. An additional $Br_2$ links these $[Br_{16}]^{2-}$ dianions to chains.[55]

All reported $[Br_{20}]^{2-}$ dianions $[(n\text{-}Bu_3)_3MeN]_2[Br_{20}]$, $[C_4MPyr]_2[Br_{20}]$ ($C_4MPyr$ = *N*-butyl-*N*-methylpyrrolidinium) (see Figure 1-8) and $[P(C_6F_5)_3Br]_2[Br_{20}] \cdot Br_2$ consist of the two building blocks $Br^-$ and $Br_2$. They all show different structural motifs forming 3D-networks. While the first two compounds were obtained from ionic liquids, the latter was observed when $P(C_6F_5)_3$ was treated with 5 or 10 equivalents of elemental bromine.[27,55,56]

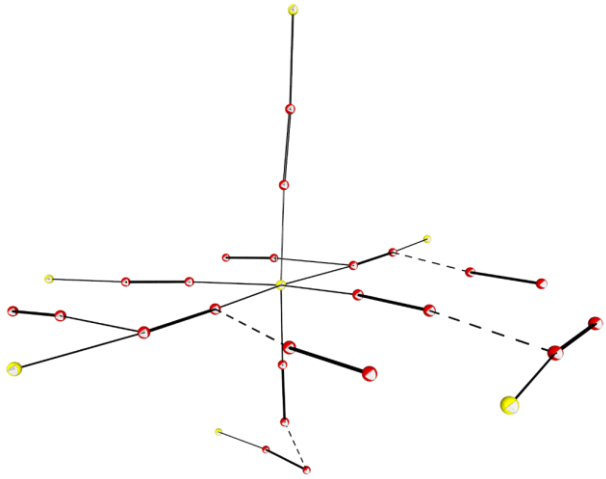

Figure 1-8: Solid state structure of the $[Br_{20}]^{2-}$ dianion in $[C_4MPyr]_2[Br_{20}]$ (B) (CCDC: 811451). The central $Br^-$ are yellow colored. (graphic based on [27,56])

The largest known polybromide $[Br_{24}]^{2-}$ was obtained by the reaction of an equimolar mixture of $[P_{4,4,4,4}]Br$ and $[P_{6,6,6,14}][NTf]$ with 10 equivalents of elemental bromine, see Figure 1-9 for the obtained structure.[57] Maschmeyer et al. compared the obtained structural motif to the roughly square pyramidal $[Br_{11} \cdot Br_2]^-$ anion.[43]

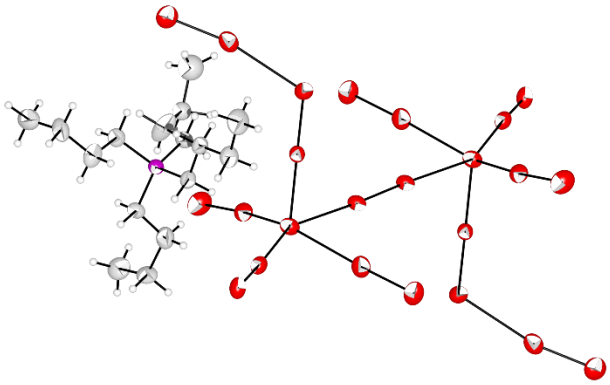

Figure 1-9: Solid state structure of $[P_{4,4,4,4}]_2[Br_{24}]$ containing the largest known polybromide. (CCDC: 1059043)[57]

### 1.1.4 Polychlorides and -fluorides

Again, Chattaway and Hoyle reported on the first polychlorides in 1923. They obtained pale yellow hygroscopic compounds by passing chlorine over tetaethyl- or tetramethylammonium chlorides.[18] The first crystal structure of a $[Cl_3]^-$ anion was observed in 1981 by Bogaard et al.[58] $[AsPh_4][Cl_3]$ has an almost linear asymmetric structure, similar to the other known trichloride anions[59–62]. For $M[Cl_3]$ (M = Na, K, Rb, Cs, K) two bands are observed in the Raman spectrum between 225–276 and 326–375 $cm^{-1}$ in argon matrices.[63] In addition to $M^+[Cl_3^-]$ free, uncoordinated $[Cl_3]^-$ was observed for the first time in matrix-isolation experiments by co-deposition of laser ablated alkali metal chlorides (CsCl, RbCl and KCl) with chlorine. Irrespective of the matrix gases (Ne, Ar) and the used metals free $[Cl_3]^-$ shows one single band at 252 $cm^{-1}$ in the far-IR spectrum. Quantum-chemical calculations at the CCSD(T)/def2-TZVPP level confirmed this result showing that the $[Cl_3]^-$ anion becomes asymmetric once interacting with an alkali cation.[64] Structures of higher polychlorides are known from literature for $[Cl_3^- \cdot Cl_2]$ showing a hockey-stick like structure that consists of a $[Cl_3]^-$ anion coordinating a slightly elongated $Cl_2$ molecule at a distance of 317.1(2) pm,[65] $[Cl_8]^{2-}$, that was crystallized from the ionic liquid [BMP][OTf] (*N*-butyl-*N*-methylpyrrolidinium triflate)[66], the network $[(Cl_3)_2 \cdot Cl_2]^{2-}$[67], $[Cl_{11}]^-$, $[Cl_{12}]^{2-}$ and $[Cl_{13}]^-$.[68] Comparing the last four mentioned structures with known polybromide anions, in the previous section, only $[PPN][Cl_{11} \cdot Cl_2]$ shows a similar structure to the undecabromide $[PPN][Br_{11} \cdot Br_2]$[43]. However, $[AsPh_4][Cl_{11}]$ and $[PPh_4][Cl_{11}]$ feature distorted square pyramidal structures building one-dimensional chains in the solid state. The $[Cl_{12}]^{2-}$ dianions are formed by two $[Cl_5]^-$ units that are bridged by a $Cl_2$ molecule. $[Cl_{13}]^-$ shows a distorted octahedral structure, with a distance of 328.7(1) pm between the single anions which are very loosely connected to chains.[68] Evidence for a

$[Cl_9]^-$ is obtained by Raman spectroscopy measurements of $[NEt_4][Cl_9]$ at –196 °C in comparison with quantum-chemical calculations.[69]

In contrast to the polybromides and -chlorides, polyfluorides are only obtainable under matrix-isolation conditions. Although, theoretical investigations showed that $CsF_3$ should be stable at pressures between 15–30 GPa and $CsF_5$ at 50 GPa none of these compounds exist so far in preparative amounts.[70,71] Experiments, like for example the reaction of $[NMe_4]F$ with fluorine in $CH_3CN$ or $CHF_3$ at –31 and –142 °C respectively were unsuccessful.[72] So far, only two polyfluoride anions are known. The first prooven $[F_3]^-$ anion was found in 1976 by Ault and Andrews reacting alkali fluoride salts with elemental fluorine under cryogenic conditions in argon matrices. The observed $MF_3$ (M = K, Rb and Cs) were characterized by IR and Raman spectroscopy indicating a $D_{\infty h}$ symmetry for the anion.[73,74] In 2015 this results were extended to $KF_3$ and $CsF_3$ in neon that show in IR experiments absorption bands at 557 and 561 $cm^{-1}$.[75] Free $[F_3]^-$ anions were observed in the gas phase by electron capture mass spectrometry on the one hand[76], on the other hand they were formed under cryogenic conditions in argon and neon matrices during laser-ablation experiments of transition metals under access of fluorine.[77–79] Besides further laser-ablation experiments of metals and neat fluorine[78,79] $MF_3$ (M = K, Rb, Cs) as well as isolated $[F_3]^-$ anions were formed during the reaction of laser ablated alkali metal fluorides with fluorine in solid neon, argon, krypton and nitrogen.[80] The first speculation of a $[F_5]^-$ anion was based on a weak signal in the flowing afterglow of a mass spectrometry experiment.[81] Free $[F_5]^-$ was isolated after the reaction of IR-laser ablated metal atoms with neat fluorine in neon matrices.[75,82] The IR spectra suggest a V-shaped structure, that contrasts with quantum-chemical calculations at the CCSD(T)/aug-cc-pVTZ level showing that the hockey-stick like structure is energetically favored by 6.2 $kJ \cdot mol^{-1}$.[77]

This section is part of a review manuscript. Therefore, contents of chapter 3.2 with *syn*- and *anti*- $[NMe_4][I_4Br_5]$ are anticipated. Results from chapter 4, namely $[NEt_4][I_5Br_2]$, $[CoCp_2][I_2Cl_3]$, $[PPh_4][I_2Cl_3]$, $[PPh_4][I_3Cl_4]$, $[CoCp_2]_2[I_3Br_4]_2 \cdot CH_2Cl_2$, $[\{(C_6H_2F_3)_3P\}_2N]_2[I_4Cl_4] \cdot 4\ CH_3CN$ and $[PPh_4]_2[I_6Cl_6]$ are marked with an asterisk [*].

## 1.2 Polyinterhalides

As previously stated several polyhalogen anions have been prepared and characterized over the last decades. However, only homonuclear polyhalogens of fluorine, chlorine, and bromine have been summarized so far. The possible variety of polyinterhalogen anions increases dramatically compared to the homonuclear variety. Before the discussion of such polyinterhalide anions, a very important differentiation has to be made. In principle two kinds of polyinterhalide compounds are known, namely the classical and non-classical polyinterhalides. The former are built of an electropositive central atom surrounded by more electronegative halogen atoms such as $[ICl_4]^-$[83] or $[IF_6]^-$[84]. Many of these compounds are experimentally known and well characterized, see e.g. reviews[85,86] and articles for the higher classical interhalides.[18,84,87–112] For the latter non-classical polyinterhalides the central halide is more electronegative than the coordinating dihalogen or interhalogen molecules, see Figure 1-10.[4]

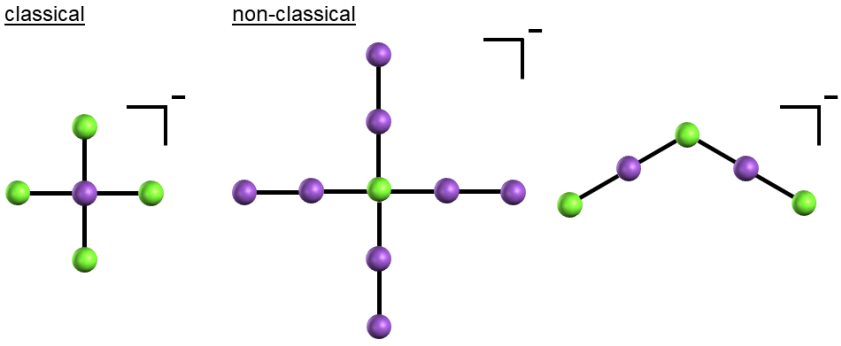


Figure 1-10: Classical (left) and non-classical polyinterhalides with coordinated dihalogen (middle) or interhalogen molecules (right) in comparison. The electropositive atoms are violet while the electronegative are green. All species are known for example for iodine (electropositive, violet) and chlorine (electronegative, green).

Herein, the focus is on non-classical polyinterhalide anions, starting with compounds that are formed by either a central halide ($X^-$) or three atomic interhalide which is in each case coordinated by dihalogen molecules ($Y_2$).

Three atomic interhalides of this design were already investigated in 1923 by Chattaway and Hoyle.[18] The stability of trihalide anions $[X_2Y]^-$ (X, Y = Cl, Br, I) was examined by

quantum-chemical calculations. It was shown by molecular orbital studies in the gas phase and in solution that in the case where Y is heavier than X the $[Y{-}Y{-}X]^-$ structure is preferred to the $[Y{-}X{-}X]^-$ structure.[113] This outcome explains why no structures of the type $[Y{-}X{-}X]^-$ have been found in a CCDC database search. Hoffmann et al. investigated the bonding situation of mixed trihalide anions based on quantum-chemical calculations. They showed that the structure of $[Y{-}Y{-}X]^-$ is also favored over $[Y{-}X{-}Y]^-$.[8]

All trihalide anions of the type $[Y{-}Y{-}X]^-$ with known crystal structure are summarized in Table 1-1.

Table 1-1: Literature known crystal structures of trihalides $[YYX]^-$.

| | |
|---|---|
| $[Br_2Cl]^-$[119] | $[I_2Cl]^-$[116,118–121] |
| | $[I_2Br]^-$[120,124–127] |

They are described in more detail in the following sections. Reactions of CsF or RbF with $Cl_2$ in argon matrices at 15 K show an infrared absorption around 410 $cm^{-1}$, which can be possibly assigned to $[Cl_2F]^-$.[74] This assignment agrees well with the 424 $cm^{-1}$ calculated at the CCSD(T)/aug-cc-pVTZ level.[114] $[Br_2F]^-$ and $[I_2F]^-$ could not be experimentally detected so far. However, the formation of $[Br_2F]^-$ was supposed during the procedure of indirect anodic fluorination with a $Br^+/Br^-$ redox mediator.[115]

Polyinterhalides of $Cl^-$ and $I_2$: $[C_{12}H_9N_2]_2[I_2Cl][ICl_2]$ ($[C_{12}H_9N_2]$ = 1,10-phenanthrolin-1-ium; $phenH^+$) contains the three atomic $[I_2Cl]^-$ anion.[116] Interestingly, in addition to the non-classical $[I{-}I{-}Cl]^-$ this compound also contains the classical polyinterhalide $[ICl_2]^-$. The $[I_2Cl]^-$ anions form infinite chains. With 273.7(1) pm the I–I bond is very close to that of elemental iodine (271.5(6) pm[117]) while the distances of I–Cl with 304.0(1) and 315.8(1) pm suggest covalent bonding. The crystal packing is influenced by hydrogen bonds between N–H groups of the cation and chlorine atoms of $[I_2Cl]^-$ as well as many weak C–H···Hal interactions. However, $[I_2Cl]^-$ is also structurally known with further counterions.[118–121] Beyond this mono-coordinated $Cl^-$ anion in $[I_2Cl]^-$ it is possible to extend the coordination sphere by four $I_2$ molecules as it can be seen in $[Cl(I_2)_4]^-$ which forms a square-planar structure.[122,123] Surprisingly, the anion in the experimentally determined structure of $[(H_5O_2)(I_2b_{15}c_5)_2][Cl(I_2)_4]$ ($I_2b_{15}c_5$ = diiodobenzo-15-crown-5) does not represent the expected tetrahedral coordination of the ligands as it was found e.g. in $[Br_9]^-$, see above. The presence of a planar instead of a tetrahedral orientation in the solid state can be explained by quantum-chemical calculations which show that halogen-halogen bonding

between the $[Cl(I_2)_4]^-$ anions stabilizes this structural motif. The coordinated iodine units show a higher electrostatic potential in the peripheral region than on the lateral site, the resulting $\sigma$-hole can therefore interact with the adjacent ion, which leads to these anion-anion interactions, see Figure 1-11.

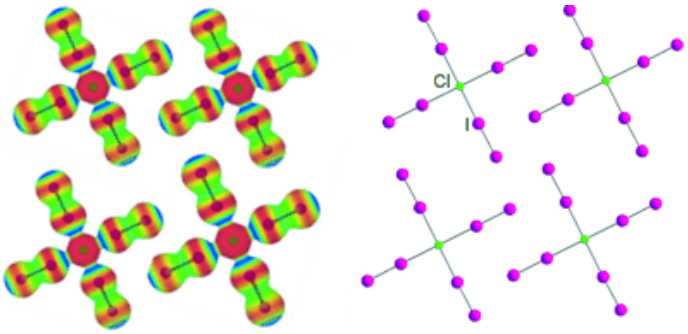


Figure 1-11: Interactions between $[Cl(I_2)_4]^-$ anions based on the electrostatic potential (red – blue: decreasing potential) and in the crystal structure.[122] *(Copyright Wiley-VCH Verlag GmbH & Co. KGaA. Reproduced with permission)*

In this example the I-I distances with 269.9(1) and 270.5(2) pm are also close to the corresponding distance in elemental iodine, and the Cl–I bonds with 299.6(1) and 302.9(1) pm are even a bit shorter than in the above described $[I_2Cl]^-$ anion. The first three-dimensional network containing iodine and chlorine was observed by Feldmann et al. in $[(Ph)_3PCl]_2[Cl_2I_{14}]$ out of the ionic liquid $[C_4MPyr][OTf]$ ($[C_4MPyr]$ = *N*-butyl-*N*-methyl-pyrrolidinium).[27] The square pyramidal structure is built of a central $Cl^-$ which coordinates five $I_2$ units, whose not exactly planar basis forms a two-dimensional network by a direct connection to the next central chloride atoms. The fifth diiodine is disordered and connects as well as a further $I_2$ molecule two layers to a polyinterhalide network, see Figure 1-12.

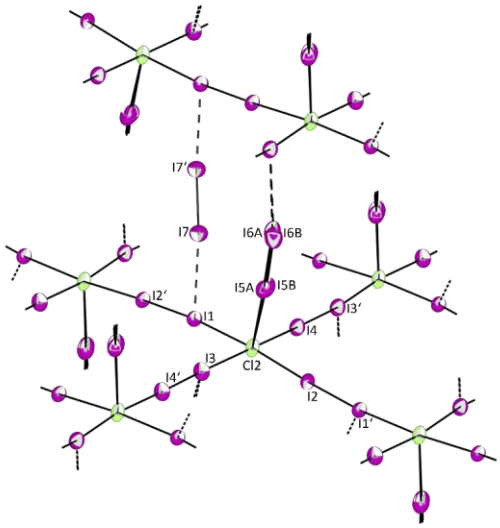


Figure 1-12: Network of the $[(Cl)_2(I_2)_7]^{2-}$ anions in $[(Ph)_3PCl]_2[Cl_2I_{14}]$.[27]

Polyinterhalides of $Br^-$ and $I_2$: For $[I_2Br]^-$ many examples are literature known. The first mentioned polyinterhalide of this kind $[BEDT\text{-}TTF]_2[I_2Br]$ (BEDT-TTF = bis(ethylenedithio)tetrathiofulvalene) was published in 1985.[124–125] Here, the $[I_2Br]^-$ anions are crystallographically disordered with $[I_3]^-$, as is apparent from the bond lengths. Further reported examples of an $[I_2Br]^-$ anion, without disorder, are $[(C_5H_5N)C_{16}H_{33}][I_2Br]$[120] and $[(C_6H_5)_3P(CH_2)_3COOH][I_2Br]$[127]. The latter shows dimeric associates of $[I_2Br]^-$ with a rather long Br–Br' distance of 386.8(3) pm. The bond length of I–I with 283.1(2) pm is elongated in comparison to elemental iodine, the I–Br distance with 280.7(2) pm is much smaller than the sum of the van der Waals radii. The crystal structure of $[Br(I_2)_2]^-$ is so far still missing. Only far IR and Raman spectra suggesting the formation of this anion have been published. Note, the recorded spectra show very similar frequencies to those of the well-known $[I_5]^-$ anion, and therefore need further investigation.[128]

Polyinterhalide of $Cl^-$ and $Br_2$: The first crystal structure of $[Br_2Cl]^-$ was obtained by reaction of hexamethonium chloride dihydrate with a stoichiometric amount of $Br_2$ vapors.[119] Two adjacent $[Br_2Cl]^-$ units form a hexaatomic system, that is controlled by Br···Br contacts between the trihalide anions, with chlorine atoms at both ends. This structural behavior is also observed for $[I_2Cl]^-$ using the same counter ion. Both trihalides are stable at room temperature and at ambient pressure.

Polyinterhalide of $[IICl]^-$ (disordered: $[ClICl]^-$) and $I_2$: The interhalide in $[H_5O_2(I_4DB_{24}K_8)]_2(I_{1.74}Cl_{1.16})_2(I_2)_4$ ($DB_{24}K_8$ = dibenzo-24-crown-8) consists of an $[I_2Cl]^-$ anion in which the terminal iodine atom is occupied with 26% chlorine, coordinating two iodine molecules to form a Z-shaped heptahalide. These are combined to form dimers, which leads to the formation of ten-membered rings out of two $[I_2Cl]^-$ ($[ICl_2]^-$) anions and two iodine molecules. The second $I_2$ of each heptahalide, that is not part of the ring shows a weak contact (390.2(2) pm) to the central iodine atom of an $[I_2Cl]^-$ ($[ICl_2]^-$) in the next ring.[129]

Polyinterhalides of $[BrIBr]^-$ and $I_2$: Parlow and Hartl reported the structure of $[BPH][I_5Br_2]$ ($BPH^+$ = 2,2´-bipyridylium).[130] One of the bromine atoms (Br1) of the almost linear $[IBr_2]^-$ anions with interatomic distances of 267.3(9) and 277(1) pm forms together with an $I_2$ molecule slightly bent Br–I–I–Br–I–I– chains. These chains are connected to curled net-like layers by additional iodine molecules (I2–I3), that connect Br2 of the first chain with Br1 of the second one, see Figure 1-13.

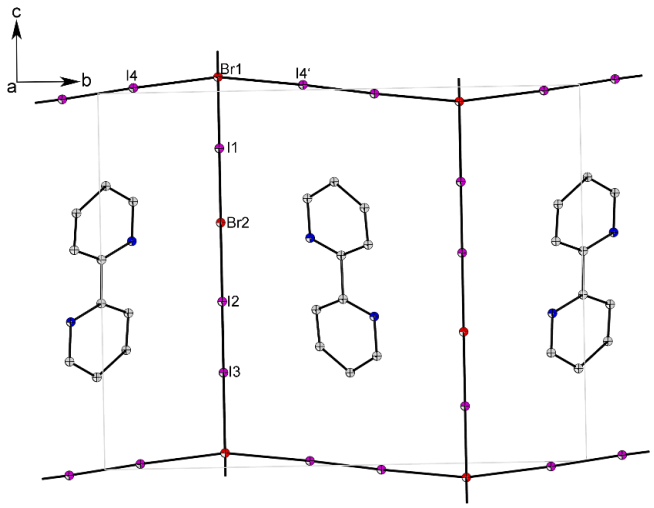


Figure 1-13: Unit cell of the molecular structure of [BPH][$I_5Br_2$]. (CSD: 51132)[130]

The column-shaped cavities are occupied by $[BPH]^+$ cations. With 270.3(8) and 270.5(6) pm the I–I distances correspond to those in solid iodine while the I-Br distances between $[IBr_2]^-$ and $I_2$ with distances between 316(2) and 340(1) pm are much weaker but shorter than the sum of the van der Waals radii. For this reason, the assignment to the non-classical polyinterhalides should be critically questioned. An $[I_5Br_2]^-$ anion is also obtained by the reaction of tetraethylammonium bromide with different amounts of IBr in the ionic liquid [HMIM][Br] (HMIM = 1-hexyl-3-methyl-imidazolium).[*] Here, symmetrical $[IBr_2]^-$ anions are formed that are connected with two neighboring $I_2$ molecules at each bromine atom. This again leads to the formation of Br–I–I–Br–I–I– zig-zag chains which are connected to those in front and behind by the iodine atoms in the middle of the $[IBr_2]^-$ anions (I1) to build double layers, see Figure 1-14. The $[NEt_4]^+$ cations exist in the middle of the double layers and lie on gaps to the I1 atoms of the $[IBr_2]^-$ anions.

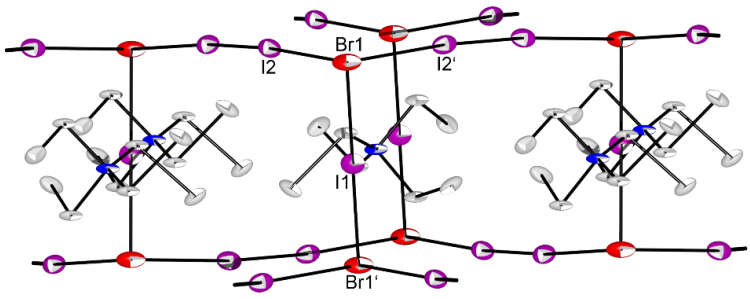


Figure 1-14: Solid state structure of $[NEt_4][I_5Br_2]$.[*]

Polyinterhalide of $[BrIBr]^-$ and $Br_2$: Rajasekharan et al.[26] reported with $[IBr_4]^-$ in $[Cu(dafone)_3](IBr_4)(I_2Br_6)_{0.5} \cdot CH_3CN$ a further example of a polyinterhalide coordinating a dihalogen molecule. The second polyinterhalide in this compound, $[I_2Br_6]^{2-}$, is described in

the dianion section. The $[IBr_4]^-$ anion consists of two building blocks $[IBr_2]^-$ and $Br_2$. The unsymmetrical V-shaped structure can be compared with the other discussed pentahalide ions. As it can be seen in Figure 1-15 these interhalides form weakly linked zig-zag chains.

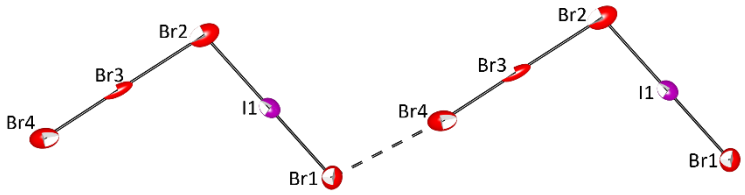


Figure 1-15: Zig-zag chains of $[IBr_4]^-$ in the solid state structure of $[Cu(dafone)_3](IBr_4)(I_2Br_6)_{0.5} \cdot CH_3CN$. (CCDC: 1051676)[26]

The following parts are focused on non-classical polyinterhalide anions that consist of an electronegative halide $X^-$ coordinating interhalogen molecules XY or YZ. For three atomic polyinterhalide anions, for example $[Cl{-}I{-}Cl]^-$ or $[Br{-}I{-}Br]^-$, it is questionable of which kind of polyinterhalide it consists (classical or non-classical). As symmetrical anions, they feature a three-electron four-center bond and clearly should be classified as classical polyinterhalides, for example the case in $KIBr_2$.[131] But if the cation changes to $Cs^+$, the anion becomes more asymmetric with bond lengths of 278 and 262 pm.[132] Is the electropositive central iodine surrounded by more electronegative bromine atoms or the bromide coordinated by an IBr unit? Based on potentially present crystal packing effects, no clear assignment can be made so far. All literature known structures of $[XYX]^-$ and $[XYZ]^-$ will be discussed below, Table 1-2 summarizes all experimentally known trihalides.

Table 1-2: Experimentally known trihalides $[XYX]^-$ and $[XYZ]^-$. (black: known crystal structure)

| | | | |
|---|---|---|---|
| $[ClF_2]^-$[133–135] | | | |
| $[BrF_2]^-$[136–138] | $[BrCl_2]^-$[155–158] | | |
| $[IF_2]^-$[89,139,140] | $[ICl_2]^-$[141–144] | $[IBr_2]^-$[131,132] | $[BrICl]^-$[160–165] |

The $[ClF_2]^-$ anion was first prepared in 1965 by Christe and Guertin.[133] In further reactions beside $[NO][ClF_2]$ the $[ClF_2]^-$ salts of potassium, rubidium, and cesium were synthesized and characterized by vibrational spectroscopy.[134] The infrared spectra of solid $Rb[ClF_2]$ and $Cs[ClF_2]$ showed a band associated to the symmetric Cl–F stretching vibration that was explained by a distortion of $[ClF_2]^-$ or crystal field effects.[135] After Raman[136] and IR measurements in solid argon[137] showing an asymmetric $[BrF_2]^-$, the first clearly

centrosymmetric $[BrF_2]^-$ anion, confirmed by IR and Raman spectroscopy was obtained for $[NMe_4][BrF_2]$.[138] For both anions no crystal structure is known so far. For further combination possibilities, such as $[BrIF]^-$, $[ClBrF]^-$ or $[ClIF]^-$ no experimental data exist.

Polyinterhalide of $F^-$ and IF: For $[IF_2]^-$ only one crystal structure is known in the literature. The anion in $[Pip][IF_2]$ shows quasi identical bond lengths of 208.2(3) and 207.5(3) pm.[89] A linear centrosymmetric structure was also confirmed for $[NEt_4][IF_2]$ by vibrational spectroscopy with a band at 445 $cm^{-1}$ in the Raman and 462 $cm^{-1}$ in the IR spectrum.[139] Christe et al. obtained bands at 446 and 397 $cm^{-1}$ for $[NMe_4][IF_2]$, from which the latter contrasts to the prior reported value but can be confirmed by *ab initio* calculations.[140]

Polyinterhalides of $Cl^-$ and ICl: Many crystal structures of $[ICl_2]^-$ are known, therefore only the first symmetric and asymmetric examples will be mentioned. The first crystal structure containing an $[ICl_2]^-$ anion was reported in 1920 by Wyckoff.[141] But the I–Cl bond lengths are not discussed there. In 1939 Mooney presented the crystal structure of $[NMe_4][ICl_2]$ with an I–Cl bond length of 234 pm[142] while Visser and Vos obtained a value of 255(2) pm.[143] The first asymmetric $[ICl_2]^-$ was reported for piperazinium di-dichloroiodide with I–Cl distances of 269 and 247 pm.[144] The higher non-classical polyinterhalide $[I_2Cl_3]^-$ was first mentioned in 1942.[145] Yogi and Popov investigated reactions of ICl with dichloroiodate salts of large organic cations and discovered yellow microcrystalline powders of $[ICl_2 \cdot ICl]^-$[146,147] that are stable at room temperature. The characterization of these substances was achieved by elemental analysis and IR spectroscopy. In solution the complexes seem to dissociate to the $[ICl_2]^-$ anion and ICl. In 1979, $[I_2Cl_3]^-$ was structurally characterized by Parlow and Hartl in the compound $[C_{18}H_{13}N_2][Cl(ICl)_2]$ ($C_{18}H_{13}N_2$ = 2,2`-bichinolinium).[148] The $[I_2Cl_3]^-$ anion is V-shaped, similar to pentahalide anions, and shows a bonding angle of 101.5(1)°. I–Cl distances between the central $Cl^-$ and the coordinating ICl units are 271.8(2) pm, the terminal ICl shows a bond length of 241.7(2) pm. Further crystal structures of the $[I_2Cl_3]^-$ anion are obtained in $[CoCp_2][I_2Cl_3]$, that shows two crystallographically independent interhalides and $[PPh_4][I_2Cl_3]$ with I–Cl–I angles of 130.8(2), 131.7(2) and 97.5(1)°.[*] $[BnMe_3N]_2[I_2Cl_3][ICl_4]$ shows the non-classical interhalide $[I_2Cl_3]^-$ next to the classical interhalide $[ICl_4]^-$. With a distance of 376.2(1) pm between the terminal chlorine atoms of $[I_2Cl_3]^-$ and the iodine atoms in the middle of $[ICl_4]^-$ the connection in this chain-like arrangement is slightly above the sum of the van der Waals radii of iodine and chlorine

(360 pm).[149] $[PPh_4][I_3Cl_4]$ was obtained once in a trigonal pyramidal structure with a central $Cl^-$ anion coordinating three ICl units[150] as well as a chain-like structure, that consists of a central asymmetric $[ICl_2]^-$ anion and two additional ICl units that are coordinated via their iodine atoms.[*]

Polyinterhalides of $Br^-$ and IBr: Examples for a symmetric and asymmetric $[IBr_2]^-$ anion are already mentioned above. The pentahalide $[Br(IBr)_2]^-$ shows a V-shaped structure, but the central I–Br–I angle is more rectangular with 94.8(1)[130] or 94.5(1)°[151] and therefore smaller than in all known $[I_2Cl_3]^-$ anions. In 2000 Minkwitz et al. reported the synthesis of $[PPh_4][I_3Br_4]$, which can be prepared by the reactions of $[PPh_4]Br$ and $[PPh_4]Cl$ with IBr,[152] due to halogen exchange reactions.[152] Like other known heptahalides, $[Br(IBr)_3]^-$ displays a distorted trigonal pyramidal structure. The salt was characterized by X-ray structure determination, compared with quantum-mechanical calculations at the B3LYP/LANL2DZ level as well as IR and Raman spectroscopy. Eight years later Aragoni et al. synthesized a planar $[I_3Br_4]^-$ anion in $[H_3tptz][I_3Br_4][IBr_2]_2$.[154] An interlaced structure of two $[I_3Br_4]^-$ anions was obtained in $[CoCp_2]_2[I_3Br_4]_2 \cdot CH_2Cl_2$, see Figure 1-16.[*]

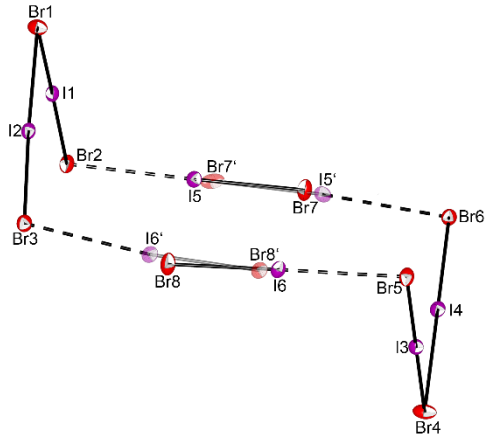


Figure 1-16: Two interlaced $[I_3Br_4]^-$ anions in the solid state structure of $[CoCp_2]_2[I_3Br_4]_2 \cdot CH_2Cl_2$ (transparent: disordered IBr unit with 14.5%)[*]

In contrast to the other two known $[I_3Br_4]^-$ anions with a central $Br^-$ coordinating three IBr molecules, this $[I_3Br_4]^-$ is formed of a slightly asymmetric $[IBr_2]^-$ coordinating two IBr units. One of these IBr units is disordered, therefore the structure seems to consist of two interlaced *syn*-$[I_4Br_5]^-$ anions, which will be described next. $[NMe_4][I_4Br_5]$ was obtained with identical stoichiometries in either the ionic liquid [HMIM]Br or in dichloromethane.[151] In both structures the central V-shaped $[I_2Br_3]^-$ unit binds at each outer bromine atom an additional IBr molecule. This further coordination is based on halogen-halogen interactions as it was shown by quantum-chemical calculations. It is interesting to note, that depending

on the solvent two different structures have been observed. The *syn*-conformation is built in the ionic liquid and an *anti*-arrangement in $CH_2Cl_2$, see Figure 1-17. The obtained structures differ significantly if compared to other known nonahalides.

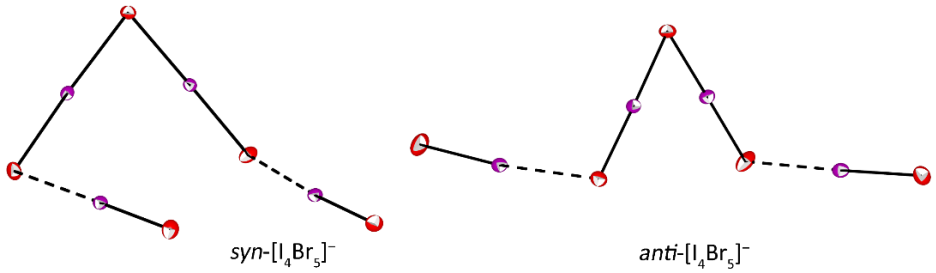


Figure 1-17: *Syn*- and *anti*-$[I_4Br_5]^-$ in the solid state structures of $[NMe_4][I_4Br_5]$ crystallized from [HMIM]Br and $CH_2Cl_2$. (CCDC: 1496857 and 1496858)[151]

Polyinterhalides of $Cl^-$ and BrCl: In the CCDC-database are so far four entries with a $[BrCl_2]^-$ anion incorporated.[155–158] Larger anions with a central $Cl^-$ coordinating BrCl molecules were recently obtained. $[Cl(BrCl)_3]^-$ is synthesized from tetraphenylarsonium chloride with an excess of BrCl in acetonitrile. $[AsPh_4][Cl(BrCl)_3]$ shows two crystallographically independent anions. Both $[Br_3Cl_4]^-$ have a distorted pyramidal structure though one shows a more planar character. The polyinterhalide in $[CCl(NMe_2)_2][Cl(BrCl)_5]$ forms a square pyramidal rather than trigonal bipyramidal arrangement, although the latter was favored by a value of 18.1 $kJ \cdot mol^{-1}$ in DFT calculations. The largest known polyinterhalide monoanion was observed in $[PPN][Cl(BrCl)_6]$ (PPN = bis(triphenylphosphoranylidene)iminium). $[Br_6Cl_7]^-$ is the first polyinterhalide anion crystallized in a slightly distorted octahedral structure. In the solid state structure $[Br_6Cl_7]^-$ anions form chains due to halogen bonding interactions, see Figure 1-18.[159]

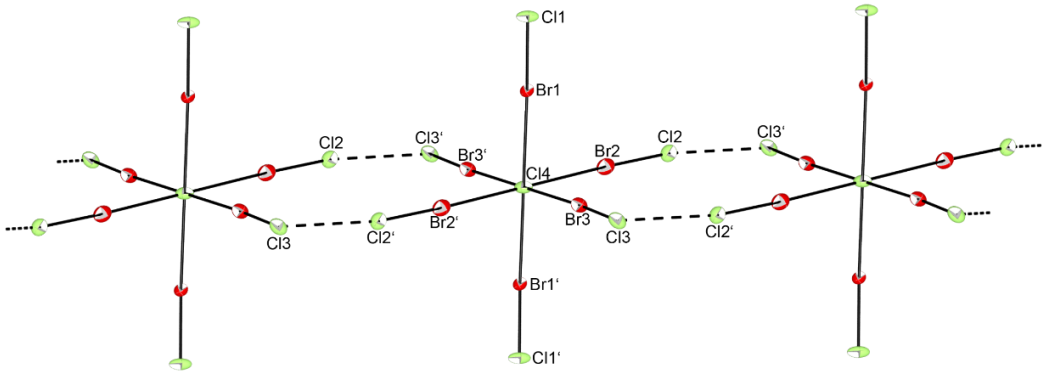


Figure 1-18: Interactions between the $[Br_6Cl_7]^-$ anions forming chains in the solid state structure of $[PPN][Cl(BrCl)_6]$. (CCDC: 1827157)[159]

Polyinterhalides of Cl, Br and I: $[BrICl]^-$ is the only crystallographic established trihalogen anion with three different atoms. It was reported for the first time in 1938 as $[NH_4][BrICl]$.[160] Other examples of this anion are only obtained in low dimensional organic conductors of bis(ethylenedithio)tetrathiofulvalene (BEDT-TTF) salts with trihalide counterions and are therefore disordered or rather a combination of different anions.[161–165] The anion $[ICl_2 \cdot IBr]^-$ was obtained by reacting both $[NMe_4][IClBr]$ with ICl and $[NMe_4][ICl_2]$ with IBr. $[NMe_4][I_2Cl_2Br]$ was investigated by IR spectroscopy.[146]

Polyinterhalides of $F^-$ and $BrF_3$: A special case, that extends the definition above, can be formulated if the central atom acts as a bridging ligand between several tetratomic interhalogen compounds, namely in $[Br_2F_7]^-$ or $[Br_3F_{10}]^-$. $[Br_2F_7]^-$ was first described in 1976 by Sukhoverkhov et al.[167] who studied the $BrF_3$-CsF-HF ternary system and reported therefore the IR spectrum of the $CsBr_2F_7$ phase. The crystal structure of $CsBr_2F_7$ was reported in 2013 by Kraus et al.[99] The central fluorine bridges the two bromine atoms of the $BrF_3$ units which show together an almost square pyramidal structure. But in contrast to previous Raman spectroscopic investigations of Stein et al.[168] the structure neither shows a planar anion, nor a linear Br-μF-Br unit. Stein et al. also reported the Raman and IR spectra of $MBr_3F_{10}$ (M = Cs, Rb) which were both crystallized in 2016 by Kraus et al.[169] as well as the structure of $RbBr_2F_7$. An analog crystal structure with $[I_2Cl_7]^-$ does not exist yet. However, Krossing et al. investigated the mixtures of [HMIM]Cl, [BMP]Cl or $[NEt_4]Cl$ with different amounts of $I_2Cl_6$. The measured Raman spectra of [BMP]Cl and $[NEt_4]Cl$ with 1.0 eq of $I_2Cl_6$ are in agreement with quantum-chemical calculations at RI-MP2/def2-TZVPP level and support the assignment of $[Cl_2I_7]^-$. There is also no clear evidence for an $[I_3Cl_{10}]^-$ anion.[112]

Polyinterhalide Dianions: For the description of polyinterhalide dianions we need to extend the definition of a non-classical polyinterhalide, too. The dianions can be built by several halides or interhalides that coordinate the same dihalogen or interhalogen molecule.

$[Cl–I–I–Cl]^{2-}$ was obtained by the reaction of 2-pyrimidone hydrochloride with elemental iodine in a solution of dichloromethane and methanol followed by the evaporation of the filtrate for crystal growing.[170] The I–I distance in the almost linear $[I_2Cl_2]^-$ anion is with 272.6(2) pm only 1.2 pm longer than in elemental iodine. The bond lengths of I–Cl are much shorter than the sum of the van der Waals radii. The complex is thermally stable up to 50 °C against the loss of $I_2$. With bands at 202 and 217 $cm^{-1}$ in the FIR-region and in the Raman spectra the I–Cl vibrations can be detected. A second $[Cl–I–I–Cl]^{2-}$ as well as

$[Br–I–I–Br]^{2–}$ were obtained by thermal treatment of $[HMET][I_2Cl]_2$ and $[HMET][I_2Br]_2$ (HMET = 1,6-bis(trimethylammonium)hexane), respectively. The crystal structures were directly determined from the powder XRD data. Interestingly, these dianions cannot be obtained from solution.[121]

In the reaction of $[PPN\text{-}3^F]Cl$ ($PPN\text{-}3^F$ = bis[tris(3,4,5-trifluorophenyl)phosphoranylidene]iminium) with ICl crystals with the stoichiometric formula $[\{(C_6H_2F_3)_3P\}_2N]_2[I_4Cl_4] \cdot 4\ CH_3CN$ were obtained from acetonitrile. The dianion $[I_4Cl_4]^{2–}$ forms a Z-shaped structure out of two slightly unsymmetrical $[ICl_2]^–$ anions that are interconnected via their chlorine atoms by an iodine molecule.[*] Therefore, the structure can be compared with the known octahalide dianions $[X_8]^{2–}$ (first reported with X = I [171], Br[49], Cl[66]). Another octainterhalide dianion is found in $[Cu(dafone)_3][(IBr_4)(I_2Br_6)_{0.5}] \cdot CH_3CN$ (dafone = 4,5-diazafluoren-9-one), that was obtained from a mixture of $CuBr_2$, dafone, iodine, and bromine in acetonitrile.[26] In addition to the already mentioned $[IBr_4]^–$, the compound also contains the Z-shaped dianion $[I_2Br_6]^{2–}$ which is built of two nearly symmetric $[Br–I–Br]^–$ anions that are linked by a central bromine molecule. Further mentioned octainterhalides, that however show a disorder are $[I_{3.77}Cl_{4.23}]^–$ with two $[ICl_2]^–$ anions connected by an iodine or chlorine molecule $[I_{4.24}Br_{3.76}]^–$ and $[I_{6.67}Br_{1.33}]^–$. The latter two show an iodine in the middle bridging in the first case two $[I–I–Br]^–$ or $[Br–I–Br]^–$ anions and in the second case two $[I_3]^–$ or $[I–I–Br]^–$ anions, wherein in the former combination a polyiodide is formed.[129]

The largest known polyiodinechloride and -bromide dianions are $[PPh_4]_2[I_6Cl_6]$ (disordered: $[PPh_4]_2[I_4Cl_8]$)[*] and $[PBr_4]_2[I_5Br_7]$, see Figure 1-19.[172]

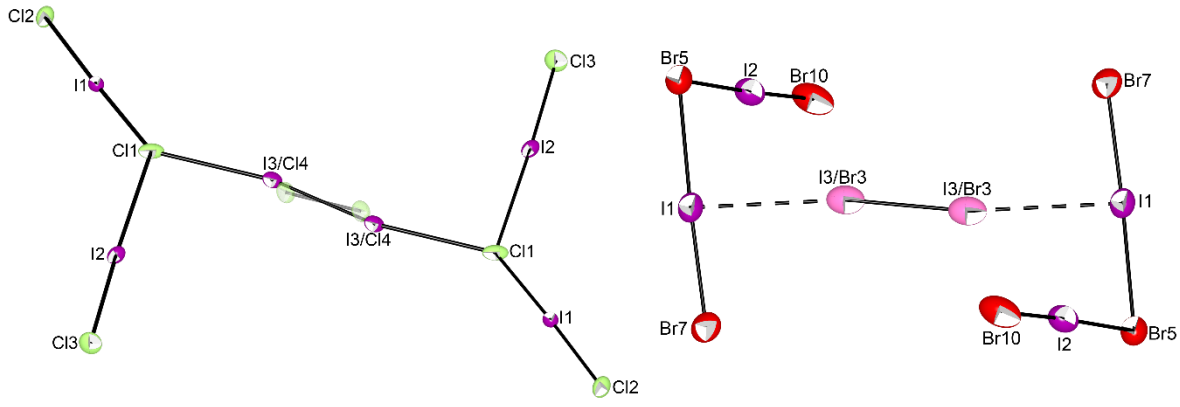


Figure 1-19: $[I_6Cl_6]^{2–}$ (transparent: disordered $Cl_2$ unit with 28.5%: $[I_4Cl_8]^{2–}$) and $[I_5Br_7]^{2–}$ in the solid state structures of $[PPh_4]_2[I_6Cl_6]$ (disordered: $[PPh_4]_2[I_4Cl_8]$) and $[PBr_4]_2[I_5Br_7]$.[*][172]

The former was obtained in the reaction of $[PPh_4]Cl$ with three equivalents of ICl. The V-shaped $[I_2Cl_3]^–$ anions are bridged over the central chlorine atoms by an iodine molecule that is disordered with 28.5% chlorine.[*] The latter was synthesized from $PBr_5$ and an

excess of IBr in the ionic liquid [(*n*-Bu)$_3$MeN][N(Tf)$_2$] (N(Tf)$_2$ = bis(trifluoromethylsulfonyl)amide). It consists of two V-shaped $[I_2Br_3]^-$ anions that are bridged by a central IBr unit, but in contrast to the compound above via two iodine atoms. The central IBr is disordered with an occupation of 50.4% of iodine and 49.6% of bromine for both positions. The absorptions at 223, 213, and 187 cm$^{-1}$ in the Raman spectrum can be assigned to I-Br stretching vibrations and therefore exclude the existence of $Br_2$ or $I_2$ instead of the disordered IBr unit. In comparison to solid IBr this bridging IBr is significantly elongated by 12 pm which can be explained by the additional bonds to the two $[I_2Br_3]^-$ units.[172]

## 1.3 Bis(triphenylphosphoranylidene)iminium Cations

The first synthesis of a bis(triphenylphosphoranylidene)iminium cation, abbreviated [PPN]$^+$, was reported in 1961 by Appel and Hauss.[173] They studied the reaction behavior of triphenylphosphine imine. Substitution of the hydrogen by bromine led to triphenylphosphine bromoimine, that reacted with triphenylphosphine in benzene to [PPN]Br (Eq. 1 and 2).

$$2\ Ph_3PNH + Br_2 \longrightarrow Ph_3PNBr + [Ph_3PNH_2]Br \qquad \text{Eq. 1}$$

$$Ph_3PNBr + PPh_3 \longrightarrow [Ph_3PNPPh_3]Br \qquad \text{Eq. 2}$$

The proposed mesomeric structures for the [PPN]$^+$ cation are shown in Figure 1-20.

$$[Ph_3P{=}N{-}\overset{\oplus}{P}Ph_3]^+ \longleftrightarrow [Ph_3P{=}\overset{\oplus}{N}{=}PPh_3]^+ \longleftrightarrow [Ph_3\overset{\oplus}{P}{-}N{=}PPh_3]^+ \longleftrightarrow [Ph_3\overset{\oplus}{P}{-}\overset{\ominus}{N}{-}\overset{\oplus}{P}Ph_3]^+$$

Figure 1-20: Mesomeric resonance structures of [PPN]$^+$.

Another synthesis route described in this context, was the reaction of triphenylphosphine dibromine with triphenylphosphine imine (Eq. 3).

$$Ph_3PBr_2 + 2\ Ph_3PNH \longrightarrow [Ph_3PNPPh_3]Br + [Ph_3PNH_2]Br \qquad \text{Eq. 3}$$

The side product aminotriphenylphosphonium bromide was separated by recrystallization from hot water. [PPN]Br is stable against acids in boiling water and only partially destroyed by concentrated bases.[173]

Ruff and Schlientz simplified this synthesis by reacting triphenyldichlorophosphorane with further triphenylphosphine and hydroxylamine hydrochloride in $C_2H_2Cl_4$ (Eq. 4 and 5).[174]

$$2\ PPh_3 + 2\ Cl_2 \longrightarrow 2\ Ph_3PCl_2 \qquad \text{Eq. 4}$$

$$2\ PPh_3Cl_2 + PPh_3 + NH_2OH \cdot HCl \longrightarrow [Ph_3PNPPh_3]Cl + Ph_3PO + 4\ HCl \qquad \text{Eq. 5}$$

Using this synthesis [PPN]Cl is readily obtained in high yield. It is described as an air-stable, non-hygroscopic salt that is soluble in ethanol, dichloromethane, and the common polar aprotic solvents. Thus, it proves to be, in comparison to tetraalkylammonium salts, a clear advantage in terms of solubility and preparation of anhydrous salts.[175] Knapp et al. used this synthesis to obtain [PPN]Cl and crystallized a solvent free form of [PPN]Cl in a $CH_3CN/Et_2O$ solution with a P–N distance of 159.8(2) pm and a P–N–P angle of 133.0(3)° (Figure 1-21).[176]

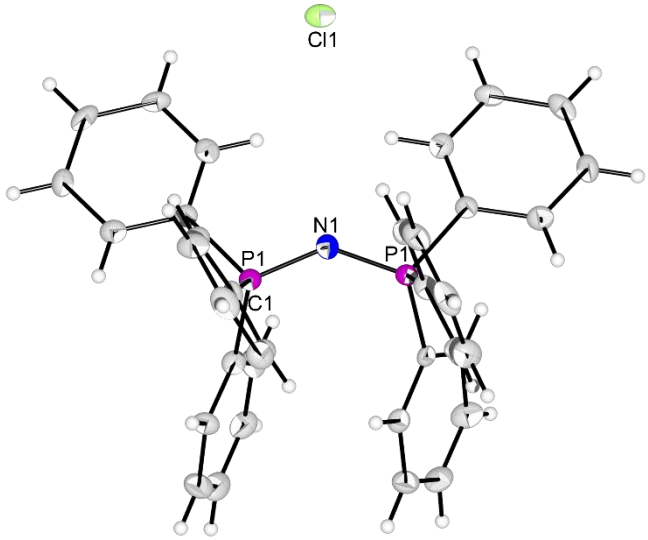


Figure 1-21: Solid state structure of [PPN]Cl. (CCDC: 803187).[176]

The $Cl^-$ anion can be replaced by the desired anion via metathesis with alkali metal salts MX (X = $Br^-$, $I^-$, $CN^-$, $NO_2^-$, $NO_3^-$, $N_3^-$, $OCN^-$, $SCN^-$).[174,177] However, [PPN]F was obtained either by the reaction of [PPN]I with silver fluoride in methanol[177] or when [PPN][$BF_4$] is treated with KF in dry methanol.[178] $[PPN]^+$ is like $[NMe_4]^+$, $[PMe_4]^+$, $[P(NMe_2)_4]^+$, $[S(NMe_2)_3]^+$ or 1,3,5-hexamethylpiperidinium a weakly coordinating cation (WCC). Due to its hydrophobic nature, the bulkiness and good distribution of the positive charge, it is an appropriate counter-ion that allows the isolation of very labile, highly basic, and nucleophilic anions which readily crystallize as stable salts.[177,179] Examples include the heavy metal carbonyl ions $[Co(CO)_4]^-$[174], $[M_2(CO)_{10}]^{2-}$ (M = Cr, Mo, W)[174,180,181] as well as mixed-metal derivatives like $[FeMn(CO)_9]^-$, $[MCo(CO)_9]^-$ and $[MMn(CO)_{10}]^-$ (M = Cr,

W)[182] or $[M_2(CO)_{10}L]^-$ (M = Cr, W; L = H, I, Br, Cl, SCN, CN).[183] As already mentioned in previous sections $[PPN]^+$ was used as counterion in the synthesis of polyhalides and polyinterhalides. $[PPN][Br_{11}] \cdot Br_2$[43], $[PPN][Cl_{13}]$[68], and $[PPN][Br_6Cl_7]$[159] are in each case the largest representatives known to date. It is also known for trifluorometyltellurates like for example $[(TeCF_3)_2X]^-$ (X = Cl, Br, I) and $[(TeCF_3)_3]^-$. The latter shows a considerably higher stability in terms of thermal resistance and decomposition on air compared to its $[NMe_4]^+$ analog.[184,185] [PPN]Cl was reported as solubility mediator in halogen exchange reactions for the synthesis of fluoroarenes. The preparation with potassium fluoride as fluorinating agent in DMSO showed nearly 100% yield after 8 hours using mild reaction conditions with 150 °C in the case of 4-fluoronitrobenzene. Here, the synthesis of [PPN]Cl was carried out as described in equation 6–9.[186]

$$\mathrm{PPh_3} \xrightarrow[-\,\mathrm{C_2Cl_4}\;-\,\mathrm{HCl}]{+\,\mathrm{C_2Cl_6}\;+\,\mathrm{NH_3}} [\mathrm{Ph_3PNH_2}]\mathrm{Cl} \qquad \text{Eq. 6}$$

$$[\mathrm{Ph_3PNH_2}]\mathrm{Cl} \xrightarrow[-\,2\ n\text{-BuH}\;-\,\mathrm{LiCl}]{+\,2\ n\text{-BuLi}} \mathrm{Ph_3PNLi}$$

$$\mathrm{Ph_3PNLi} + \mathrm{Ph_3PCl_2} \xrightarrow{-\,\mathrm{LiCl}} [\mathrm{Ph_3PNPPh_3}]\mathrm{Cl} \qquad \text{Eq. 7–9}$$

$$\mathrm{PPh_3} \xrightarrow[-\,\mathrm{C_2Cl_4}]{+\,\mathrm{C_2Cl_6}} \mathrm{Ph_3PCl_2}$$

In the first step triphenylphosphine was treated with hexachloroethane in tetrahydrofuran followed by a reaction with gaseous ammonia to form triphenylaminophosphonium chloride. This purified product was reacted with *n*BuLi in order to obtain $Ph_3PNLi$ that formed together with freshly prepared $PPh_3Cl_2$ the product [PPN]Cl. Lacour et al. also reported the reaction for [PPN]Br using bromine instead of $C_2Cl_6$.[186]

Examples containing substituents at the phenyl rings of $[PPN]^+$ are very rare. Only $[\{(4\text{-MePh})_3P\}_2N]Cl$ with a methyl-group in *para*-position of the phenyl ring was reported in the literature. It was used as counterion for the hexanuclear ruthenium carbidocarbonyl cluster $[Ru_6C(CO)_{16}(\mu\text{-Br})]^-$.[187] Studies on the conductivity of $[\{(4\text{-MePh})_3P\}_2N]Cl$ confirmed the building of larger aggregates in dilute aqueous solutions[188] as known from [PPN]Cl.[189]

Further representatives of the bisphosphineiminium salts, where at least one phenyl ring was replaced by another group are $[Ph_3PNPPh_2E]X$ (EX = $CH_3I$, $Ph_2PCl$, $Ph_2PBr$, $PhPCl_2$, $Br_2$)[190], $[Ph_3PNPPh_2NHR]Cl$ (R = H, Bn, *t*-Bu)[191] and $[MePh_2PNPPh_2Me]X$ (X = I, Cl). The latter was first prepared by Schmitz-DuMont and Klieber in 1968 who reacted two equivalents of $CH_3I$ with $Ph_2PNHK$.[192] 14 years later Ellermann et al. obtained $[MePh_2PNPPh_2Me]I$ in the reaction of lithium-bis(diphenylphosphino)amid with two equivalents of MeI (Eq. 10).

$$LiN(PPh_2)_2 + 2\ MeI \longrightarrow [MePh_2PNPPh_2Me]I + LiI \qquad \text{Eq. 10}$$

In addition, they reported the exchange reaction of iodide by $[PF_6]^-$ and $[BPh_4]^-$ and a full characterization of all products by NMR and vibrational spectroscopy.[193,194]

$[Ph_3PNPPh_2E]X$ (EX = $CH_3I$, $Ph_2PCl$, $Ph_2PBr$, $PhPCl_2$, $Br_2$) was synthesized by direct reaction of $Ph_3PNPPh_2$ with EX.[190] $[Ph_3PNPPh_2NHR]Cl$ (R = H, Bn, *t*-Bu) was reported as precursor for strong non-ionic bases which were obtained by deprotonation with sodium hydride in DMSO.[191]

Schwesinger et al. investigated organic phosphazenium cations. Thereof one series showed the $(R_2N)_3PNP(NR_2)_3$ bonding motif with $NR_2$ (R = Me; R,R = -$(CH_2)_4$-, -$(CH_2)_5$-, *cis*-CHMe-$(CH_2)_3$CHMe-) instead of the phenyl rings. They distinguished the stability of the compounds towards aqueous base and the improved anion reactivities which can be explained by a very good anion-cation separation due to the cation shape. A further advantage was the weak cation-anion interaction based on negligible hydrogen bridges. Comparing these compounds, the pyrrolidinium systems are for example more stable than the methylated ones while piperidinyl substituents did not improve the stability. $[(R_2N)_3PNP(NR_2)_3]BF_4$ was synthesized starting from $[Cl_3PNPCl_3]PCl_6$ that was treated with $R_2NH$ and $NaBF_4$.[195] Moreover, $[(Me_2N)_3PNP(NMe_2)_3]F$ is described as a convenient fluoride source among the phosphazenium fluorides and showed in E2 elimination reactions an extreme reactivity and selectivity.[196]

$[Cl_3PNPCl_3]PCl_6$ was first synthesized and characterized by Becke-Goehring et al. who reacted $PCl_5$ with $NH_4Cl$.[197] Further treating with $PCl_5$ and $NH_4Cl$ resulted in $[Cl_3P{=}N{-}PCl_2{=}N{-}PCl_3]PCl_6$, higher chains, or with $NH_4^+$ in rings like $[NPCl_2]_3$ or $[NPCl_2]_4$.[198]

Interionic C–H···$A^-$ hydrogen bonds between $[PPN]^+$ and $[PPh_4]^+$ cations and anions show longer distances for $[PPN]^+$ than for $[PPh_4]^+$ and therefore weaker interactions. The reduced polarization of the C–H system in $[PPN]^+$ cations is due to the better delocalization of the positive charge.[199] In order to stabilize less disturbed polyhalides hydrogen bridges can be

further avoided by replacing hydrogen atoms of the phenyl substituents with fluorine atoms. The influence of such an exchange on the charge distribution is discussed on the well-known example of benzene and hexafluorobenzene (Figure 1-22).

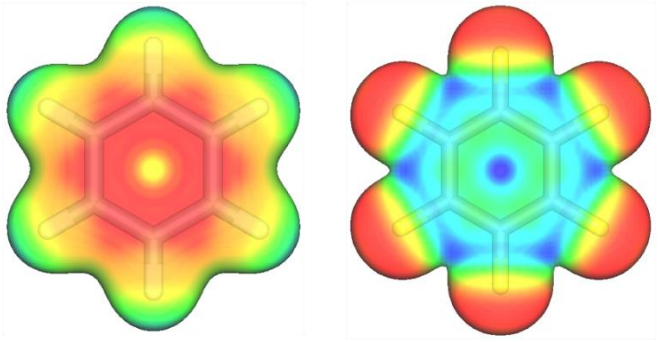

Figure 1-22: Electrostatic potential of benzene (left) and hexafluorobenzene (right) in the range from 0 a.u. (red) to 0.1 a.u. (blue) calculated at the B3LYP-D3/def2-TZVPP level (isosurface 0.01).

Benzene shows a higher electrostatic potential in the periphery. Thus, for an interaction with an anion, the motif C–H···A$^-$ is preferred over an anion-π interaction. Hexafluorobenzene features an opposite behavior, the electrostatic potential of the periphery is less positive and the center of the π-system is more electrophilic.[200] These positive regions above and below the aromatic ring, however, favor electrostatic anion-π interactions, while benzene is able to interact with positively charged groups with its π-system, as shown in quantum-chemical calculations.[201–205]

## 1.4 References


[1] W. A. Tilden, *J. Chem. Soc.* 1866, *19*, 145–147.

[2] K.-F. Tebbe, R. Buchem, *Z. Anorg. Allg. Chem.* 1998, *624*, 671–678.

[3] P. H. Svensson, L. Kloo, *Chem. Rev.* 2003, *103*, 1649–1684.

[4] H. Haller, S. Riedel, *Z. Anorg. Allg. Chem.* 2014, *640*, 1281–1291.

[5] R. J. Hach, R. E. Rundle, *J. Am. Chem. Soc.* 1951, *73*, 4321–4324.

[6] G. C. Pimentel, *J. Chem. Phys.* 1951, *19*, 446–448.

[7] M. C. Aragoni, M. Arca, F. A. Devillanova, A. Garau, F. Isaia, V. Lippolis, A. Mancini, *Bioinorg. Chem. Appl.* 2007, *2007*, 1–46.

[8] G. A. Landrum, N. Goldberg, R. Hoffmann, *J. Chem. Soc., Dalton Trans.* 1997, 3605–3613.

[9] G. R. Desiraju, P. S. Ho, L. Kloo, A. C. Legon, R. Marquardt, P. Metrangolo, P. Politzer, G. Resnati, K. Rissanen, *Pure Appl. Chem.* 2013, *85*, 1711–1713.

[10] L. C. Gilday, S. W. Robinson, T. A. Barendt, M. J. Langton, B. R. Mullaney, P. D. Beer, *Chem. Rev.* 2015, *115*, 7118–7195.

[11] T. Clark, M. Hennemann, J. S. Murray, P. Politzer, *J. Mol. Model* 2007, *13*, 291–296.

[12] P. Metrangolo, G. Resnati, *Halogen bonding*, Springer, 2008.

[13] P. Politzer, J. S. Murray, *ChemPhysChem* 2013, *14*, 278–294.

[14] P. Politzer, J. S. Murray, T. Clark, *Phys. Chem. Chem. Phys.* 2013, *15*, 11178–11189.

[15] P. Politzer, J. S. Murray, T. Clark, *Phys. Chem. Chem. Phys.* 2010, *12*, 7748–7757.

[16] M. H. Kolář, P. Hobza, *Chem. Rev.* 2016, *116*, 5155–5187.

[17] G. Cavallo, P. Metrangolo, R. Milani, T. Pilati, A. Priimägi, G. Resnati, G. Terraneo, *Chem. Rev.* 2016, *116*, 2478–2601.

[18] F. D. Chattaway, G. Hoyle, *J. Chem. Soc. Trans.* 1923, *123*, 654–662.

[19] F. Pichierri, *Chem. Phys. Lett.* 2011, *515*, 116–121.

[20] H. Slebocka-Tilk, R. G. Ball, R. S. Brown, *J. Am. Chem. Soc.* 1985, *107*, 4504–4508.

[21] J. J. Novoa, F. Mota, S. Alvarez, *J. Phys. Chem.* 1988, *92*, 6561–6566.

[22] G. Bellucci, R. Bianchini, C. Chiappe, R. Ambrosetti, *J. Am. Chem. Soc.* 1989, *111*, 199–202.

[23] J. C. Evans, G. Y.-S. Lo, *Inorg. Chem.* 1967, *6*, 1483–1486.

[24] V. Vitske, H. Herrmann, M. Enders, E. Kaifer, H.-J. Himmel, *Chem. Eur. J.* 2012, *18*, 14108–14116.

[25] V. Nemec, K. Lisac, V. Stilinović, D. Cinčić, *J. Mol. Struct.* 2017, *1128*, 400–409.

[26] R. Babu, G. Bhargavi, M. V. Rajasekharan, *Eur. J. Inorg. Chem.* 2015, *2015*, 4689–4698.

[27] M. Wolff, A. Okrut, C. Feldmann, *Inorg. Chem.* 2011, *50*, 11683–11694.

[28] I. D. Gorokh, S. A. Adonin, M. N. Sokolov, P. A. Abramov, I. V. Korolkov, E. Y. Semitut, V. P. Fedin, *Inorg. Chim. Acta* 2018, *469*, 583–587.

[29] F. B. Alhanash, N. A. Barnes, S. M. Godfrey, R. Z. Khan, R. G. Pritchard, *Polyhedron* 2013, *65*, 102–109.

[30] X. Chen, M. A. Rickard, J. W. Hull, C. Zheng, A. Leugers, P. Simoncic, *Inorg. Chem.* 2010, *49*, 8684–8689.

[31] H. Haller, M. Ellwanger, A. Higelin, S. Riedel, *Angew. Chem. Int. Ed.* 2011, *50*, 11528–11532; *Angew. Chem.* 2011, *123*, 11732–11736.

[32] H. Haller, M. Ellwanger, A. Higelin, S. Riedel, *Z. Anorg. Allg. Chem.* 2012, *638*, 553–558.

[33] H. Haller, M. Hog, F. Scholz, H. Scherer, I. Krossing, S. Riedel, *Z. Naturforsch.* 2013, *68b*, 1103–1107.

[34] I. Rubinstein, M. Bixon, E. Gileadi, *J. Phys. Chem.* 1980, *84*, 715–721.

[35] D. J. Eustace, *Electrochem. Soc.* 1980, *127*, 528-532.

[36] M. Hog, B. Burgenmeister, K. Bromberger, M. Schuster, S. Riedel, I. Krossing, *ChemElectroChem* 2017, *4*, 2934–2942.

[37] K. Kakiage, T. Tokutome, S. Iwamoto, T. Kyomen, M. Hanaya, *Chem. Commun.* 2013, *49*, 179–180.

[38] Z.-S. Wang, K. Sayama, H. Sugihara, *J. Phys. Chem. B* 2005, *109*, 22449–22455.

[39] S. P. Borikar, T. Daniel, V. Paul, *Tetrahedron Lett.* 2009, *50*, 1007–1009.

[40] V. Kavala, S. Naik, B. K. Patel, *J. Org. Chem.* 2005, *70*, 4267–4271.

[41] J. Salazar, R. Dorta, *Synlett* 2004, *2004*, 1318–1320.

[42] T. M. Beck, H. Haller, J. Streuff, S. Riedel, *Synthesis* 2014, *46*, 740–747.

[43] H. Haller, J. Schröder, S. Riedel, *Angew. Chem. Int. Ed.* 2013, *52*, 4937–4940; *Angew. Chem.* 2013, *125*, 5037–5040.

[44] K. O. Strømme, *Acta Chem. Scand.* 1959, *13*, 2089–2100.

[45] R. Siepmann, H. G. von Schnering, *Z. Anorg. Allg. Chem.* 1968, *357*, 289–298.

[46] G. B. M. Vaughan, A. J. Mora, A. N. Fitch, P. N. Gates, A. S. Muir, *J. Chem. Soc., Dalton Trans.* 1999, 79–84.

[47] M. C. Aragoni, M. Arca, F. A. Devillanova, M. B. Hursthouse, S. L. Huth, F. Isaia, V. Lippolis, A. Mancini, H. Ogilvie, *Inorg. Chem. Commun.* 2005, *8*, 79–82.

[48] K. Sonnenberg, P. Pröhm, C. Müller, H. Beckers, S. Steinhauer, D. Lentz, S. Riedel, *Chem. Eur. J.* 2018, *24*, 1072–1075.

[49] K. N. Robertson, P. K. Bakshi, T. S. Cameron, O. Knop, *Z. Anorg. Allg. Chem.* 1997, *623*, 104–114.

[50] K. M. Fromm, R. D. Bergougnant, A. Y. Robin, *Z. Anorg. Allg. Chem.* 2006, *632*, 828–836.

[51] K. Sonnenberg, P. Pröhm, S. Steinhauer, A. Wiesner, C. Müller, S. Riedel, *Z. Anorg. Allg. Chem.* 2017, *643*, 101–105.

[52] L. Silaghi-Dumitrescu, A. A. A. Attia, R. Silaghi-Dumitrescu, A. J. Blake, D. B. Sowerby, *Inorg. Chim. Acta* 2018, *475*, 120–126.

[53] N. Bricklebank, P. J. Skabara, D. E. Hibbs, M. B. Hursthouse, K. M. A. Malik, *J. Chem. Soc., Dalton Trans.* 1999, 3007–3014.

[54] C. W. Cunningham, G. R. Burns, V. McKee, *Inorg. Chim. Acta* 1990, *167*, 135–137.

[55] H. Haller, *Dissertation*, Albert-Ludwigs-Universität Freiburg, Freiburg (Breisgau), 2014.

[56] M. Wolff, J. Meyer, C. Feldmann, *Angew. Chem. Int. Ed.* 2011, *50*, 4970–4973; *Angew. Chem.* 2011, *123*, 5073–5077.

[57] M. E. Easton, A. J. Ward, T. Hudson, P. Turner, A. F. Masters, T. Maschmeyer, *Chem. Eur. J.* 2015, *21*, 2961–2965.

[58] M. P. Bogaard, J. Peterson, A. D. Rae, *Acta Crystallogr. B* 1981, *37*, 1357–1359.

[59] R. T. Boeré, A. W. Cordes, S. L. Craig, R. T. Oakley, R. W. Reed, *J. Am. Chem. Soc.* 1987, *109*, 868–874.

[60] R. T. Boeré, A. W. Cordes, R. T. Oakley, R. W. Reed, *J. Chem. Soc. Chem. Commun.* 1985, 655–656.

[61] T. Chivers, J. F. Richardson, N. R. M. Smith, *Inorg. Chem.* 1985, *24*, 2453–2458.

[62] M. Jansen, S. Strojek, *Z. Naturforsch.* 1995, *50b*, 1171–1174.

[63] B. S. Ault, L. Andrews, *J. Chem. Phys.* 1976, *64*, 4853–4859.

[64] F. A. Redeker, H. Beckers, S. Riedel, *Chem. Commun.* 2017, *53*, 12958–12961.

[65] J. Taraba, Z. Zak, *Inorg. Chem.* 2003, *42*, 3591–3594.

[66] R. Brückner, P. Pröhm, A. Wiesner, S. Steinhauer, C. Müller, S. Riedel, *Angew. Chem. Int. Ed.* 2016, *55*, 10904–10908; *Angew. Chem.* 2016, *128*, 11064–11068.

[67] R. Brückner, H. Haller, S. Steinhauer, C. Müller, S. Riedel, *Angew. Chem. Int. Ed.* 2015, *54*, 15579–15583; *Angew. Chem.* 2015, *127*, 15800–15804.

[68] K. Sonnenberg, P. Pröhm, N. Schwarze, C. Müller, H. Beckers, S. Riedel, *Angew. Chem. Int. Ed.* 10.1002/anie.201803486; *Angew. Chem.* 10.1002/ange.201803486.

[69] R. Brückner, H. Haller, M. Ellwanger, S. Riedel, *Chem. Eur. J.* 2012, *18*, 5741–5747.

[70] M.-s. Miao, *Nature Chemistry* 2013, *5*, 846–852.

[71] S. Riedel, P. Schwerdtfeger, *Nature Chemistry* 2013, *5*, 815–816.

[72] K. O. Christe, *J. Fluorine Chem.* 1995, *71*, 149–150.

[73] B. S. Ault, L. Andrews, *J. Am. Chem. Soc.* 1976, *98*, 1591–1593.

[74] B. S. Ault, L. Andrews, *Inorg. Chem.* 1977, *16*, 2024–2028.

[75] T. Vent-Schmidt, F. Brosi, J. Metzger, T. Schlöder, X. Wang, L. Andrews, C. Müller, H. Beckers, S. Riedel, *Angew. Chem. Int. Ed.* 2015, *54*, 8279–8283; *Angew. Chem.* 2015, *127*, 8397–8401.

[76] A. A. Tuinman, A. A. Gakh, R. J. Hinde, R. N. Compton, *J. Am. Chem. Soc.* 1999, *121*, 8397–8398.

[77] S. Riedel, T. Köchner, X. Wang, L. Andrews, *Inorg. Chem.* 2010, *49*, 7156–7164.

[78] X. Wang, L. Andrews, F. Brosi, S. Riedel, *Chem. Eur. J.* 2013, *19*, 1397–1409.

[79] T. Schlöder, T. Vent-Schmidt, S. Riedel, *Angew. Chem. Int. Ed.* 2012, *51*, 12063–12067; *Angew. Chem.* 2012, *124*, 12229–12233.

[80] F. A. Redeker, H. Beckers, S. Riedel, *RSC Adv* 2015, *5*, 106568–106573.

[81] A. Artau, K. E. Nizzi, B. T. Hill, L. S. Sunderlin, P. G. Wenthold, *J. Am. Chem. Soc.* 2000, *122*, 10667–10670.

[82] F. Brosi, T. Vent-Schmidt, S. Kieninger, T. Schlöder, H. Beckers, S. Riedel, *Chem. Eur. J.* 2015, *21*, 16455–16462.

[83] R. J. Elema, J. L. de Boer, A. Vos, *Acta Crystallogr. A* 1963, *16*, 243–247.

[84] A. R. Mahjoub, K. Seppelt, *Angew. Chem. Int. Ed.* 1991, *30*, 323–324; *Angew. Chem.* 1991, *103*, 309–311.

[85] A. G. Sharpe, *Q. Rev., Chem. Soc.* 1950, *4*, 115–130.

[86] E. H. Wiebenga, E. E. Havinga, K. H. Boswijk, *Adv. Inorg. Chem. Radiochem.* 1961, *3*, 133–169.

[87] K. O. Christe, J. P. Guertin, *Inorg. Chem.* 1966, *5*, 473–476.

[88] K. O. Christe, W. Sawodny, *Z. Anorg. Allg. Chem.* 1968, *357*, 125–133.

[89] X. Zhang, K. Seppelt, *Z. Anorg. Allg. Chem.* 1997, *623*, 491–500.

[90] K. O. Christe, W. W. Wilson, R. V. Chirakal, J. C. P. Sanders, G. J. Schrobilgen, *Inorg. Chem.* 1990, *29*, 3506–3511.

[91] K. O. Christe, C. J. Schack, *Inorg. Chem.* 1970, *9*, 1852–1858.

[92] S. Siegel, *Acta Cryst* 1956, *9*, 493–495.

[93] W. G. Sly, R. E. Marsh, *Acta Cryst* 1957, *10*, 378–379.

[94] S. Siegel, *Acta Cryst* 1957, *10*, 380.

[95] A. J. Edwards, G. R. Jones, *J. Chem. Soc. A* 1969, 1936.

[96] A. I. Popov, Y. M. Kiselev, V. F. Sukhoverkhov, N. A. Chumaevsky, O. A. Krasnyanskaya, A. T. Sadikova, *Russ. J. Inorg. Chem.* 1987, *32*, 619–622.

[97] S. I. Ivlev, R. V. Ostvald, F. Kraus, *Monatsh. Chem.* 2016, *147*, 1661–1668.

[98] S. I. Ivlev, A. J. Karttunen, R. Ostvald, F. Kraus, *Z. Anorg. Allg. Chem.* 2015, *641*, 2593–2598.

[99] S. Ivlev, P. Woidy, V. Sobolev, I. Gerin, R. Ostvald, F. Kraus, *Z. Anorg. Allg. Chem.* 2013, *639*, 2846–2850.

[100] K. O. Christe, W. W. Wilson, *Inorg. Chem.* 1989, *28*, 3275–3277.

[101] A. R. Mahjoub, A. Hoser, J. Fuchs, K. Seppelt, *Angew. Chem. Int. Ed.* 1989, *28*, 1526–1527; *Angew. Chem.* 1989, *101*, 1528–1529.

[102] A. R. Mahjoub, X. Zhang, K. Seppelt, *Chem. Eur. J.* 1995, *1*, 261–265.

[103] K. O. Christe, D. Naumann, *Inorg. Chem.* 1973, *12*, 59–62.

[104] J. Shamir, I. Yaroslavsky, *Isr. J. Chem.* 1969, *7*, 495–497.

[105] K. Seppelt, *Acc. Chem. Res.* 2003, *36*, 147–153.

[106] K. O. Christe, J. P. Guertin, W. Sawodny, *Inorg. Chem.* 1968, *7*, 626–628.

[107] C. J. Adams, *Inorg. Nucl. Chem. Lett.* 1974, *10*, 831–835.

[108] K. O. Christe, J. C. P. Sanders, G. J. Schrobilgen, W. W. Wilson, *J. Chem. Soc. Chem. Commun.* 1991, *28*, 837–840.

[109] K. O. Christe, W. W. Wilson, G. W. Drake, D. A. Dixon, J. A. Boatz, R. Z. Gnann, *J. Am. Chem. Soc.* 1998, *120*, 4711–4716.

[110] T. M. Greene, A. J. Downs, A. P. Wilkinson, *J. Fluorine Chem.* 1991, *54*, 416.

[111] K. O. Christe, *Inorg. Chem.* 1972, *11*, 1215–1219.

[112] B. Burgenmeister, K. Sonnenberg, S. Riedel, I. Krossing, *Chem. Eur. J.* 2017, *23*, 11312–11322.

[113] Y. Ogawa, O. Takahashi, O. Kikuchi, *J. Mol. Struct. (Theochem)* 1998, *429*, 187–196.

[114] F. A. Redeker, *Personal Communication* 2018.

[115] T. Fuchigami, M. Sano, *J. Electroanal. Chem.* 1996, *414*, 81–84.

[116] Y.-Q. Wang, Z.-M. Wang, C.-S. Liao, C.-H. Yan, *Acta Cryst.* 1999, *C55*, 1503–1506.

[117] F. van Bolhuis, P. B. Koster, T. Migchelsen, *Acta Cryst.* 1967, *23*, 90–91.

[118] A. S. Romanov, M. Bochmann, *Organometallics* 2015, *34*, 2439–2454.

[119] L. Meazza, J. Martí-Rujas, G. Terraneo, C. Castiglioni, A. Milani, T. Pilati, P. Metrangolo, G. Resnati, *CrystEngComm* 2011, *13*, 4427.

[120] G. V. Shilov, O. N. Kazheva, O. A. D`yachenko, M. S. Chernov`yants, S. S. Simonyan, V. E. Gol`eva, A. I. Pyshchev, *Russ. J. Phys. Chem.* 2002, *76*, 1295–1301.

[121] J. Martí-Rujas, L. Meazza, G. K. Lim, G. Terraneo, T. Pilati, Harris, Kenneth D. M., P. Metrangolo, G. Resnati, *Angew. Chem.* 2013, *125*, 13686–13690.

[122] C. Walbaum, M. Richter, U. Sachs, I. Pantenburg, S. Riedel, A.-V. Mudring, G. Meyer, *Angew. Chem. Int. Ed.* 2013, *52*, 12732–12735; *Angew. Chem.* 2013, *125*, 12965–12968.

[123] C. Walbaum, M. Richter, U. Sachs, I. Pantenburg, S. Riedel, A.-V. Mudring, G. Meyer, *Angew. Chem. Int. Ed.* 2014, *53*, 5233.

[124] T. J. Emge, H. H. Wang, M. A. Beno, P. C. W. Leung, M. A. Firestone, H. C. Jenkins, J. D. Cook, J. M. Williams, E. L. Venturini, J. E. Schirber, *Inorg. Chem.* 1985, *24*, 1736–1738.

[125] H. Kobayashi, R. Kato, A. Kobayashi, G. Saito, M. Tokumot, H. Anzai, T. Ishigur, *Chem. Lett.* 1985, *14*, 1293–1296.

[126] H. Endres, M. Hiller, H. J. Keller, *Z. Naturforsch.* 1985, *40b*, 1664–1671.

[127] O. N. Kazheva, G. G. Aleksandrov, O. A. D'yachenko, M. S. Chernov'yants, S. S. Simonyan, E. O. Lykova, *Russ. J. Coord. Chem.* 2003, *29*, 819–827.

[128] E. M. Nour, L. H. Chen, J. Laane, *J. Phys. Chem.* 1986, *90*, 2841–2846.

[129] C. Walbaum, *Dissertation*, Universität zu Köln, Köln, 2009.

[130] A. Parlow, H. Hartl, *Z. Naturforsch.* 1985, *40b*, 45–52.

[131] S. Soled, G. B. Carpenter, *Acta Cryst.* 1973, *B29*, 2556–2559.

[132] J. E. Davies, E. K. Nunn, *J. Chem. Soc. D* 1969, *23*, 1374.

[133] K. O. Christe, J. P. Guertin, *Inorg. Chem.* 1965, *4*, 905–908.

[134] K. O. Christe, J. P. Guertin, *Inorg. Chem.* 1965, *4*, 1785–1787.

[135] K. O. Christe, W. Sawodny, J. P. Guertin, *Inorg. Chem.* 1967, *6*, 1159–1162.

[136] T. Surles, L. A. Quarterman, H. H. Hyman, *J. Inorg. Nucl. Chem.* 1973, *35*, 668–670.

[137] J. H. Miller, L. Andrews, *Inorg. Chem.* 1979, *18*, 988–992.

[138] R. Minkwitz, R. Broechler, R. Ludwig, *Inorg. Chem.* 1997, *36*, 4280–4283.

[139] D. Naumann, A. Meurer, *J. Fluorine Chem.* 1995, *70*, 83–84.

[140] K. O. Christe, W. W. Wilson, G. W. Drake, M. A.Petrie, J. A. Boatz, *J. Fluorine Chem.* 1998, *88*, 185–189.

[141] R. W. G. Wyckoff, *J. Am. Chem. Soc.* 1920, *42*, 1100–1116.

[142] R. C. L. Mooney, *Z. Kristallogr.* 1939, *100*, 519–529.

[143] G. J. Visser, A. Vos, *Acta Cryst.* 1964, *17*, 1336–1337.

[144] C. Rømming, *Acta Chem. Scand.* 1958, *12*, 668–677.

[145] J. Cornog, E. E. Bauer, *J. Am. Chem. Soc.* 1942, *64*, 2620–2624.

[146] Y. Yagi, A. I. Popov, *J. Inorg. Nucl. Chem.* 1967, *29*, 2223–2230.

[147] Y. Yagi, A. I. Popov, *Inorg. Nucl. Chem. Lett.* 1965, *1*, 21–24.

[148] A. Parlow, H. Hartl, *Acta Cryst.* 1979, *B35*, 1930–1933.

[149] D. Hausmann, A. Eich, C. Feldmann, *J. Mol. Struct.* 2018, *1166*, 159-163.

[150] L. Mann, *Master thesis*, Albert-Ludwigs-Universität Freiburg, Freiburg (Breisgau), 2013.

[151] L. Mann, P. Voßnacker, C. Müller, S. Riedel, *Chem. Eur. J.* 2017, *23*, 244–249.

[152] R. Minkwitz, M. Berkei, R. Ludwig, *Inorg. Chem.* 2001, *40*, 25–28.

[153] L. F. Olsson, *Inorg. Chem.* 1985, *24*, 1398–1405.

[154] M. C. Aragoni, M. Arca, F. A. Devillanova, M. B. Hursthouse, S. L. Huth, F. Isaia, V. Lippolis, A. Mancini, *Eur. J. Inorg. Chem.* 2008, *2008*, 3921–3928.

[155] G. L. Breneman, R. D. Willett, *Acta Cryst.* 1967, *23*, 334.

[156] F. Zobi, O. Blacque, G. Steyl, B. Spingler, R. Alberto, *Inorg. Chem.* 2009, *48*, 4963–4970.

[157] W. Gabes, K. Olie, *Cryst. Struct. Comm.* 1974, *3*, 753–755.

[158] CCDC: 790138 in The Cambridge Structural Database, C. R. Groom, I. J. Bruno, M. P. Lightfoot, S. C. Ward, *Acta Cryst.* 2016, *B72*, 171–179.

[159] B. Schmidt, K. Sonnenberg, H. Beckers, S. Steinhauer, S. Riedel, *Angew. Chem. Int. Ed.* 10.1002/anie.201803705; *Angew. Chem.* 10.1002/ange.201803705.

[160] R. C. L. Mooney, *Z. Kristallogr.* 1938, *38*, 324–333.

[161] H. Kobayashi, R. Kato, A. Kobayashi, G. Saito, M. Tokumoto, H. Anzai, T. Ishiguro, *Chem. Lett.* 1986, *15*, 89–92.

[162] T. J. Emge, H. H. Wang, P. C. W. Leung, P. R. Rust, J. D. Cook, P. L. Jackson, K. D. Carlson, J. M. Williams, M. H. Whangbo, E. L. Venturini et al., *J. Am. Chem. Soc.* 1986, *108*, 695–702.

[163] P. C. W. Leung, T. J. Emge, A. J. Schultz, M. A. Beno, K. D. Carlson, H. H. Wang, M. A. Firestone, J. M. Williams, *Solid State Comm.* 1986, *57*, 93–97.

[164] E. Laukhina, J. Vidal-Gancedo, S. Khasanov, V. Tkacheva, L. Zorina, R. Shibaeva, J. Singleton, R. Wojciechowski, J. Ulanski, V. Laukhin et al., *Adv. Mater.* 2000, *12*, 1205–1210.

[165] E. Laukhina, J. Vidal-Gancedo, V. Laukhin, J. Veciana, I. Chuev, V. Tkacheva, K. Wurst, C. Rovira, *J. Am. Chem. Soc.* 2003, *125*, 3948–3953.

[166] M. Watanabe, Y. Noda, H. Taniguchi, *J. Low Temp. Phys.* 2006, *142*, 163–166.

[167] N. D. Takanova, A. A. Uskova, *Russ. J. Inorg. Chem.* 1976, *21*, 2250–2253.

[168] L. Stein, *J. Fluorine Chem.* 1985, *27*, 249–256.

[169] S. I. Ivlev, A. J. Karttunen, R. V. Ostvald, F. Kraus, *Chem. Commun.* 2016, *52*, 12040–12043.

[170] I.-E. Parigoridi, G. J. Corban, S. K. Hadjikakou, N. Hadjiliadis, N. Kourkoumelis, G. Kostakis, V. Psycharis, C. P. Raptopoulou, M. Kubicki, *Dalton Trans.* 2008, 5159–5165.

[171] E. E. Havinga, K. H. Boswijk, E. H. Wiebenga, *Acta Crystallogr. A* 1954, *7*, 487–490.

[172] D. Hausmann, R. Köppe, S. Wolf, P. W. Roesky, C. Feldmann, *Dalton Trans.* 2016, *45*, 16526–16532.

[173] R. Appel, A. Hauss, *Z. Anorg. Allg. Chem.* 1961, *311*, 290–301.

[174] J. K. Ruff, W. J. Schlientz, *Inorg. Synth.* 1974, *15*, 84–90.

[175] M. Makosza, E. Bialecka, *Synth. Commun.* 1976, *6*, 313–318.

[176] C. Knapp, R. Uzun, *Acta Crystallogr. E* 2010, *66*, o3185.

[177] A. Martinsen, J. Songstad, *Acta Chem. Scand. A* 1977, *31*, 645–650.

[178] C. Bolli, J. Gellhaar, C. Jenne, M. Keßler, H. Scherer, H. Seeger, R. Uzun, *Dalton Trans.* 2014, *43*, 4326–4334.

[179] A. F. Hollemann, N. Wiberg, *Lehrbuch der Anorganischen Chemie*, Walter de Gruyter, Berlin New York, 2007, p. 257.

[180] L. B. Handy, J. K. Ruff, L. F. Dahl, *J. Am. Chem. Soc.* 1970, *92*, 7312–7326.

[181] I. Lee, S. J. Geib, N. J. Cooper, *Acta Crystallogr. C* 1996, *52*, 292–294.

[182] J. K. Ruff, *Inorg. Chem.* 1968, *7*, 1818–1821.

[183] J. K. Ruff, R. B. King, *Inorg. Chem.* 1969, *8*, 180–181.

[184] H. T. M. Fischer, *Dissertation*, Universität zu Köln, Köln, 2007.

[185] H. T. M. Fischer, D. Naumann, W. Tyrra, *Z. Anorg. Allg. Chem.* 2007, *633*, 127–131.

[186] M.-A. Lacour, M. Zablocka, C. Duhayon, J.-P. Majoral, M. Taillefer, *Adv. Synth. Catal.* 2008, *350*, 2677–2682.

[187] T. Chihara, H. Yamazaki, *J. Chem. Soc., Dalton Trans.* 1995, *30*, 1369–1377.

[188] T. Palmesen, J. Songstad, *Acta Chem. Scand.* 1989, *43*, 763–770.

[189] T. Palmesen, H. Høiland, J. Songstad, *Acta Chem. Scand.* 1981, *35a*, 599–605.

[190] H. G. Mardersteig, H. Nöth, *Z. Anorg. Allg. Chem.* 1970, *375*, 272–280.

[191] M. Taillefer, N. Rahier, A. Hameau, J.-N. Volle, *Chem. Commun.* 2006, 3238–3239.

[192] O. Schmitz-DuMont, H. Klieber, *Z. Naturforsch.* 1968, *23b*, 1604.

[193] J. Ellermann, M. Lietz, K. Geibel, *Z. Anorg. Allg. Chem.* 1982, *492*, 122–134.

[194] A. Winkler, F. W. Heinemann, M. Moll, J. Ellermann, *Inorg. Chim. Acta* 1999, *284*, 288–291.

[195] R. Schwesinger, R. Link, P. Wenzl, S. Kossek, M. Keller, *Chem. Eur. J.* 2005, *12*, 429–437.

[196] R. Schwesinger, R. Link, P. Wenzl, S. Kossek, *Chem. Eur. J.* 2005, *12*, 438–445.

[197] M. Becke-Goehring, W. Lehr, *Chem. Ber.* 1961, *94*, 1591–1594.

[198] M. Becke-Goehring, E. Fluck, *Angew. Chem. Int. Ed.* 1962, *1*, 281–285; *Angew. Chem.* 1962, *74*, 382–386.

[199] D. Braga, F. Grepioni, *New J. Chem.* 1998, *22*, 1159–1161.

[200] P. Kirsch, *Modern Fluoroorganic Chemistry*, Wiley-VCH, Weinheim, Germany, 2013, p. 48.

[201] I. Alkorta, J. Elguero, *J. Phys. Chem. A* 2003, *107*, 9428–9433.

[202] M. Aschi, F. Mazza, A. D. Nola, *J. Mol. Struct. (Theochem)* 2002, *587*, 177–188.

[203] C. Garau, A. Frontera, D. Quiñonero, P. Ballester, A. Costa, P. M. Deyà, *Chem. Phys. Lett.* 2004, *392*, 85–89.

[204] Y. Mo, G. Subramanian, J. Gao, D. M. Ferguson, *J. Am. Chem. Soc.* 2002, *124*, 4832–4837.

[205] J. Thirman, M. Head-Gordon, *J. Phys. Chem. A* 2017, *121*, 717–728.

[*] see chapter 4

# 2 Aims and Objectives

Although the number of known polyhalides and polyinterhalides steadily increases, many of the influences that contribute to the formation and structure of this class of compounds remains poorly understood. The amount of halogen used in the reaction reflects the formed anion. However, the contributions of the solvent and cation influences on polyhalide or polyinterhalide formation are largely unanswered.

The aim of this work is the synthesis and characterization of novel polybromides and polyinterhalides based on ICl and IBr. For the polybromides, the effect of a stepwise fluorination of the counter cation and the used amount of bromine on the obtained compounds is to be investigated. Polybromides of the unfluorinated and perfluorinated triarylbromophosphonium cation are already known. The series of compounds are to be extended and completed by the use of partially fluorinated triphenylphosphanes.

Starting from iodine monochloride and iodine monobromide new polyinterhalides are to be synthesized. In the case of iodobromides, possible influences on the resulting molecular structure in the solid state will be emphasized. For this purpose, the reaction of $[NMe_4]Br$ with iodine monobromide in an ionic liquid shall be compared to that in organic solvents. In addition to X-ray structure determination and Raman spectroscopy, supported by quantum-chemical calculations, the obtained iodobromides are to be investigated by conductivity measurements and thermogravimetric analysis.

Until now, only cobaltocenium cation based trihalides were known. The suitability of cobaltocenium as a counterion for larger polybromides and polyinterhalides is to be tested in reactions with bromine, iodine monochloride and -monobromide.

Due to its weakly coordinating properties and large volume, the bis(triphenyl-phosphoranylidene)iminium cation is particularly suitable for the synthesis of large polyhalides and polyinterhalides. Appropriate synthesis conditions for novel $[PPN]^+$ salts are to be developed. Of interest here are halogen substituents on the phenyl rings, especially fluorine atoms and their influence on the weakly coordinating properties of the new cations.

# 3 Publications

## 3.1 Polybromide Dianions and Networks Stabilized by Fluorinated Bromo(triaryl)phosphonium Cations

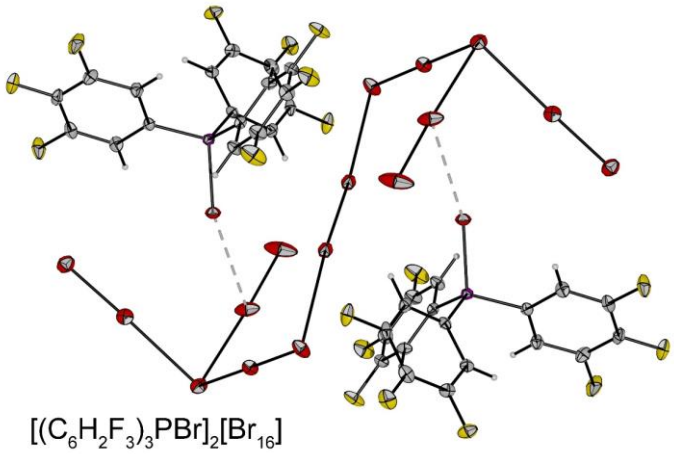


Figure 3-1: Graphical abstract.

*Accepted Manuscript*

Lisa Mann, Gene Senges, Karsten Sonnenberg, Heike Haller, and Sebastian Riedel*

*Eur. J. Inorg. Chem.* 10.1002/ejic.201800404

http://dx.doi.org/10.1002/ejic.201800404



### Author Contribution

Lisa Mann contributed to the project design, performed experiments, the product characterization, quantum-chemical calculations and wrote the manuscript. Gene Senges did some of the experiments during his bachelor thesis, which was supervised by Heike Haller and Lisa Mann. Karsten Sonnenberg performed experiments for the additional $[Br_{20}]^{2-}$ anions. Heike Haller contributed to the project design; she and Sebastian Riedel supervised the project. Simon Steinhauer, Helmut Beckers and Sebastian Riedel provided scientific guidelines and suggestions and corrected the manuscript.

## 3.2 $[NMe_4][I_4Br_5]$: A new Iodobromide from an Ionic Liquid with Halogen–Halogen Interactions

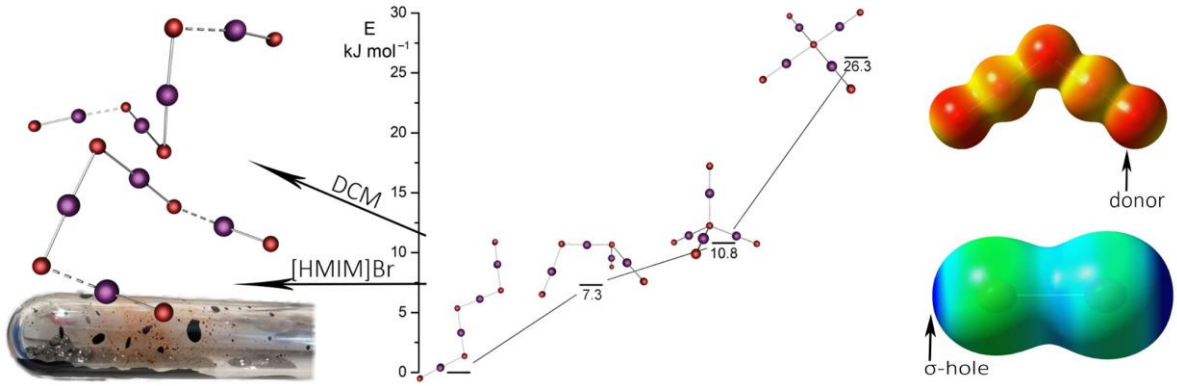


Figure 3-2. Graphical abstract.

Lisa Mann, Patrick Voßnacker, Carsten Müller, and Sebastian Riedel*

*Chem. Eur. J.* 2017, *23*, 244–249.

https://doi.org/10.1002/chem.201604392



### Author Contribution

Lisa Mann designed the project and wrote the paper. Patrick Voßnacker did some of the experiments and calculations for the molecules during his bachelor thesis, which was supervised by Lisa Mann. Lisa Mann completed the syntheses and calculations and performed the characterization. All further quantum-chemical calculations were performed by Carsten Müller. Sebastian Riedel supervised the project and provided scientific guidelines and suggestions. Carsten Müller and Sebastian Riedel corrected the manuscript.

## 3.3 Further Development of Weakly Coordinating Cations: Fluorinated Bis(triarylphosphoranylidene)iminium Salts

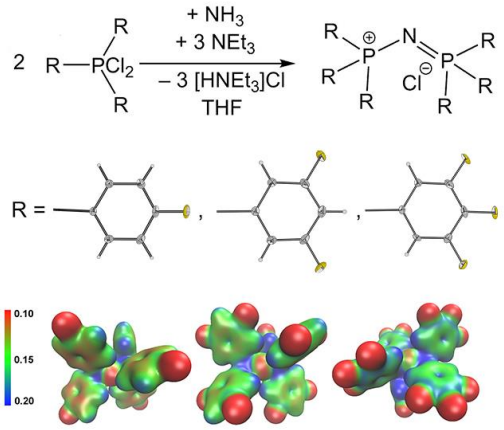


Figure 3-3: Graphical abstract.

Lisa Mann, Elisabeth Hornberger, Simon Steinhauer, and Sebastian Riedel*

*Chem. Eur. J.* 2018, *24*, 3902–3908.

https://doi.org/10.1002/chem.201705992



### Author Contribution

Lisa Mann designed the project, performed the main experiments, the product characterization, quantum-chemical calculations and wrote the paper. Elisabeth Hornberger did first experiments on the project during her research internship, that was supervised by Lisa Mann. Simon Steinhauer and Sebastian Riedel supervised the project, provided scientific guidelines and suggestions and corrected the manuscript.

# 4 Further Investigations on Polyhalides and Polyinterhalides

Parts of the experimental work described in this chapter include results from the bachelor theses of Maxim Gawrilow[1] and Patrick Voßnacker[2] carried out under my supervision.

## 4.1 Investigation of Polyhalides and Polyinterhalides of the Cobaltocenium Cation

Previous work has shown that for the synthesis of large polyhalides especially ammonium[3–7], phosphonium[8,9] and other bulky cations[10,11], for example $[PPN]^{+}$[12,13] or $[Fe(phen)_3]^{2+}$[14] are suitable. We wanted to study the cobaltocenium cation as an alternative counterion. With 18 valence electrons, it should be stable towards the oxidation of bromine or interhalogens. Substituents at the cyclopentadienyl rings result in a further increased size and stability.[15] Until now only cobaltocenium triiodide and tribromide are known.[16,17]

When cobaltocenium bromide was treated with an excess of neat bromine crystals of $[CoCp_2][Br_{11}]$ were obtained (Figure 4-1). The compound crystallizes in the orthorhombic space group *Pnma*.

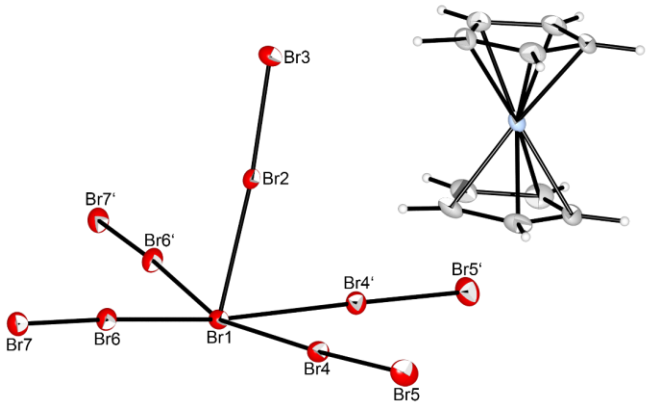


Figure 4-1: Solid state structure of $[CoCp_2][Br_{11}]$. Ellipsoids are set at the 50% probability level. Selected bond lengths (pm) and angles (°): Br1–Br2: 278.4(2), Br2–Br3: 238.9(2), Br1–Br4: 303.6(1), Br4–Br5: 231.7(1), Br1–Br6: 304.0(1), Br6–Br7: 232.9(1); Br4–Br1–Br4': 84.5(1), Br4–Br1–Br6: 82.4(1), Br2–Br1–Br4: 81.6(1), Br2–Br1–Br6: 88.0(1).

The $[Br_{11}]^{-}$ anion is built of a central $Br^{-}$ (Br1) that acts as Lewis base and donates electron density in the LUMOs of the five coordinating bromine molecules resulting in an elongation of the Br–Br bond length in comparison to solid elemental bromine (228.1 pm[18]). The anion shows a distorted square pyramidal structure. So far, an undecabromide was described only once in the structure of $[PPN][Br_{11} \cdot Br_2]$[12]. The $[Br_{11} \cdot Br_2]^{-}$ anion features

an additional embedded $Br_2$ molecule next to the also rather square pyramidal $[Br_{11}]^-$ anion, that does not interact with the central $Br^-$, but the closest intermolecular distance to a terminal $Br_2$ unit still lies below twice the van der Waals radius of bromine (370 pm). Considering the value of 370 pm there are further interactions between the bromine atoms of $[PPN][Br_{11} \cdot Br_2]$, that result in a chain like structure. Interactions below a distance of 370 pm are also found between the $[Br_{11}]^-$ anions in $[CoCp_2][Br_{11}]$ (Figure 4-2, left).

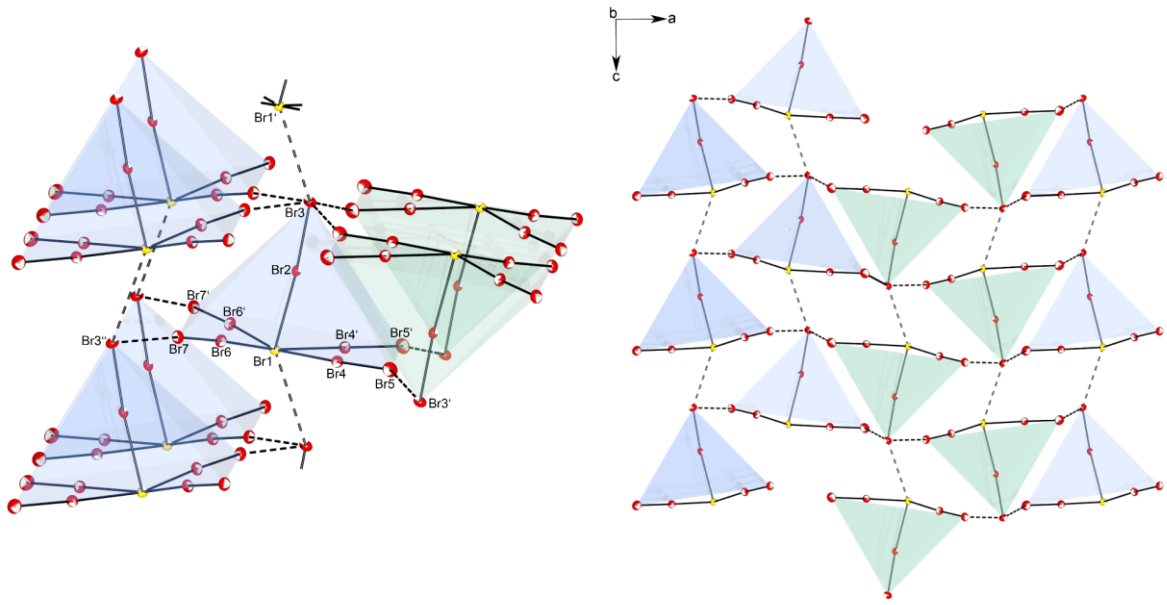


Figure 4-2: Three dimensional arrangement of $[Br_{11}]^-$ anions in the solid state structure of $[CoCp_2][Br_{11}]$. The central $Br^-$ (Br1) is yellow colored. Ellipsoids are set at the 50% probability level. *Left:* Selected bond lengths (pm) between the distorted pyramids: Br3–Br1': 341.8(2), Br5–Br3': 366.4(1), Br7–Br3'': 320.2(1). *Right*: Excerpt from the $[Br_{11}]^-$ network along *b*-axis.

The $[Br_{11}]^-$ anions are linked via the top of the distorted pyramid (Br3) to the bottom center (Br1) of the next one, resulting in long zig-zag chains along the *c*-axis (Figure 4-2, right). These are associated in pairs where the pyramids show the same orientation (Figure 4-2, left). The pyramids are only slightly tilted (blue colored). The adjacent pair of chains are upside down oriented (green colored). Neighboring pairs of mutually twisted pyramids are at the same height and linked together by their bases and tops. Adjacent chains featuring pyramids of the same orientation are shifted along the *c*-axis. Therefore, the interchain interactions occur with two successive pyramids of the neighboring chain.

Furthermore, the reaction of cobaltocenium bromide with different amounts of iodine monobromide ratios (1:3, 1:5, 1:7, 1:9) was studied. For the 1:3 and 1:7 approach single crystals were formed and examined by X-ray crystallography. They show in both cases the same compound with the stoichiometric formula $[CoCp_2]_2[I_3Br_4]_2 \cdot CH_2Cl_2$ in the monoclinic space group *Cc* (Figure 4-3). $[I_3Br_4]^-$ was already described. In a trigonal pyramidal as well

as a trigonal planar structure a central $Br^-$ is coordinated by three IBr molecules.[19,20] In contrast to both literature known anions the structure obtained here is more reminiscent of two interlaced *syn*-$[I_4Br_5]^-$ anions, which were presented in chapter 3.2.

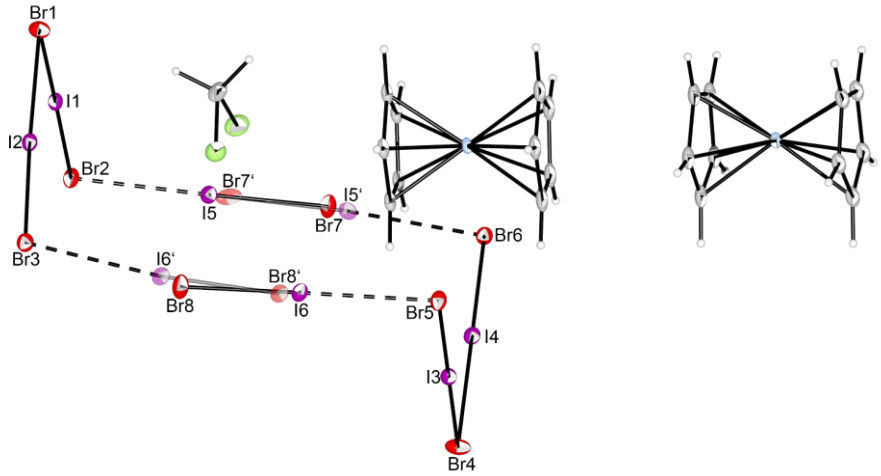


Figure 4-3: Solid state structure of $[CoCp_2]_2[I_3Br_4]_2 \cdot CH_2Cl_2$. Ellipsoids are set at the 50% probability level. The IBr units I5–I7 and I6–I8 are disordered (major domains (85.5%): I5, I6, Br7, Br8; minor domains (14.5%): I5', I6', Br7', Br8'). Selected bond lengths (pm) and angles (°): Br1–I1: 272.9(1), I1–Br2: 271.6(1), Br1–I2: 295.6(1), I2–Br3: 257.6(1), Br4–I3: 271.9(1), I3–Br5: 270.5(1), Br4–I4: 292.6(1), I4–Br6: 258.3(1), Br2–I5: 295.2(2), I5–Br7: 256.7(2), Br5–I6: 296.9(2), I6–Br8: 256.1(2), Br2–Br7': 338.1(2), Br7'–I5': 259.5(2), I5'–Br6: 304.3(7), Br5–Br8': 340.2(1), Br8'–I6': 258.1(9), I6'–Br3: 303.5(7), Br6–Br7: 351.0(2), Br3–Br8: 350.3(2); I1–Br1–I2: 91.9(1), Br1–I1–Br2: 177.4(1), Br1–I2–Br3: 177.5(1), I3–Br4–I4: 92.6(1), Br4–I3–Br5: 176.7(1), Br4–I4–Br6: 178.7(1), I1–Br2–I5: 100.6(1), I3–Br5–I6: 93.6(1), I2–Br3–I6': 105.6(2), I4–Br6–I5': 100.1(2).

The $[I_3Br_4]^-$ anions are built of a V-shaped $[I_2Br_3]^-$ and a further IBr molecule that interacts via halogen bonding with one of the terminal bromine atoms. Due to the disorder of the terminal connected IBr molecule interactions between two opposing $[I_3Br_4]^-$ anions occur. The IBr of the minor domain, which is turned, interacts with the still free terminal bromine atom resulting in a *syn*-$[I_4Br_5]^-$, which indeed only has the occupancy of an $[I_3Br_4]^-$. To have a closer look on the remaining parts of the anion we investigated the bonding situation of the V-shaped $[I_2Br_3]^-$. Salts of $[I_2Br_3]^-$ anions with $[BPH]^+$ (BPH = 2,2'-bipyridylium)[21] and $[NMe_4]^+$ (chapter 3.2) are known. They exist of a central $Br^-$ coordinated by two IBr molecules via the more electropositive iodine atoms with I–Br distances to the central $Br^-$ of 285.7(2)–295.9(2) pm and outer IBr distances of 255.9(2)–260.7(2) pm. The $[I_2Br_3]^-$ in $[CoCp_2]_2[I_3Br_4]_2 \cdot CH_2Cl_2$ shows instead slightly asymmetric $[IBr_2]^-$ anions (Br1–I1–Br2: 272.9(1) pm, 271.6(1) pm; Br4–I3–Br5: 271.9(1) pm, 270.5(1) pm) that coordinate an IBr molecule, respectively. The IBr molecules of the major domain connect on the $[IBr_2]^-$ side of the V-shaped $[I_2Br_3]^-$ (Br2–I5: 295.2(2) pm, Br5–I6: 296.9(2) pm). They show shorter distances than the IBr units of the minor domain that interact with the other side (Br3–I6': 303.5(7) pm, Br6–I5': 304.3(7) pm). However, the $[I_2Br_3]^-$ anion in *syn*-$[NMe_4][I_4Br_5]$

(see chapter 3.2) also shows the known bonding situation where the angles only slightly deviate by < 8°.

For a reaction with iodine monochloride $[CoCp_2]Cl$ was synthesized based on the procedure described by Hartley and Ware.[22] When the salt was treated with seven equivalents of ICl crystals of $[CoCp_2][I_2Cl_3]$ were isolated. $[CoCp_2][I_2Cl_3]$ crystallizes in the monoclinic space group $P2_1$.

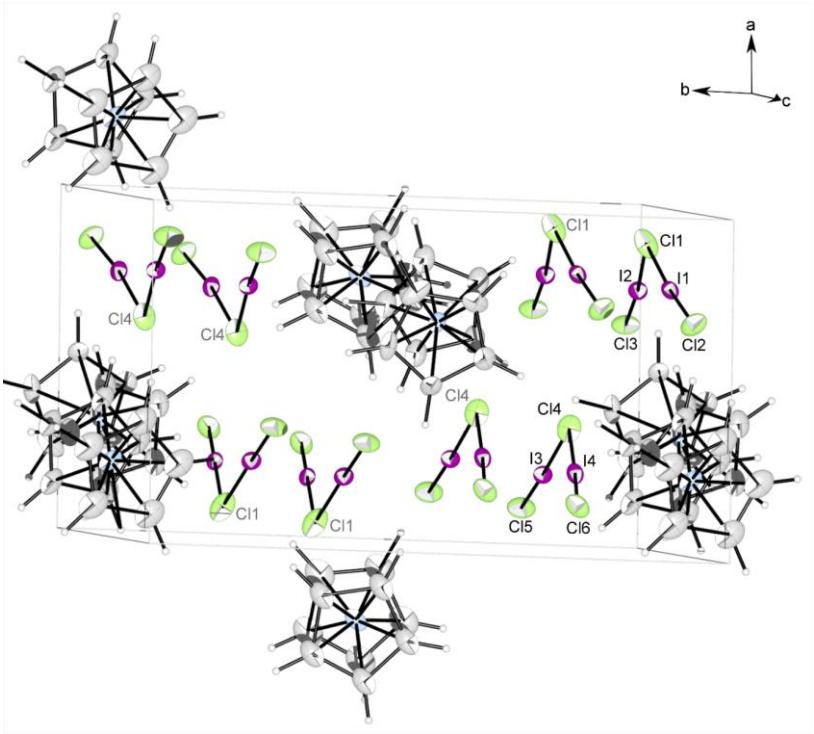


Figure 4-4: Unit cell of the solid state structure of $[CoCp_2][I_2Cl_3]$. Ellipsoids are set at the 50% probability level. Selected bond lengths (pm) and angles (°): Cl1–I1: 271.7(4), I1–Cl2: 243.5(4), Cl1–I2: 268.5(3), I2–Cl3: 245.3(3), Cl4–I3: 271.0(2), I3–Cl5: 243.1(1), Cl4–I4: 271.1(3), I4–Cl6: 244.4(3); I1–Cl1–I2: 130.8(2), Cl1–I1–Cl2: 175.6(2) , Cl1–I2–Cl3: 174.3(2), I3–Cl4–I4: 131.7(2), Cl4–I3–Cl5: 174.7(1), Cl4–I4–Cl6: 174.9(2).

Figure 4-4 shows the unit cell of $[CoCp_2][I_2Cl_3]$. The two different $[I_2Cl_3]^-$ anions are built of a central $Cl^-$ coordinated by two ICl molecules via the iodine atoms. The V-shaped structures show I–Cl–I angles of 130.8(2) (I1–Cl1–I2) and 131.7(2)° (I3–Cl4–I4), the Cl–I–Cl bonds are nearly linear with angles between 174.3(2) and 175.6(2)°. The anions seemed to build chains along the *c*-axis, but the distances of the adjacent chlorine atoms are with 378.3(4) (Cl3–Cl2') and 376.7(4) pm (Cl5–Cl6'), respectively above twice the van der Waals radius of chlorine (350 pm). So far, only two crystal structures of an $[I_2Cl_3]^-$ anion are known. The central I–Cl–I angles in $[BHP][I_2Cl_3]$ with 101.5(1)° and in $[BnMe_3N]_2[I_2Cl_3][ICl_4]$ with 99.5(1)° are clearly smaller than in the obtained structure of $[CoCp_2][I_2Cl_3]$. Furthermore, both groups reported $C_{2v}$ symmetric $[I_2Cl_3]^-$ anions with inner I–Cl bond lengths of 271.8(2) and 269.8(1) pm and an outer bond lengths of 241.7(2) and

243.0(1) pm, respectively.[23,24] These values only show a small variance to the I–Cl distances in $[CoCp_2][I_2Cl_3]$ which lie between 268.5(3) – 271.7(4) pm and 243.1(1) – 245.3(3) pm.

In addition to single crystal X-ray analysis both interhalides and the polybromide of the cobaltocenium cation were investigated by vibrational spectroscopy. Especially Raman spectra of the stretching region of the investigated poly- and interhalide anions are revealing. Beginning with $[CoCp_2][Br_{11}]$ the room temperature Raman spectrum as well as the spectrum at –150 °C are shown in Figure 4-5 in comparison to the Raman spectrum of $[PPN][Br_{11} \cdot Br_2]$ at –196 °C[12].

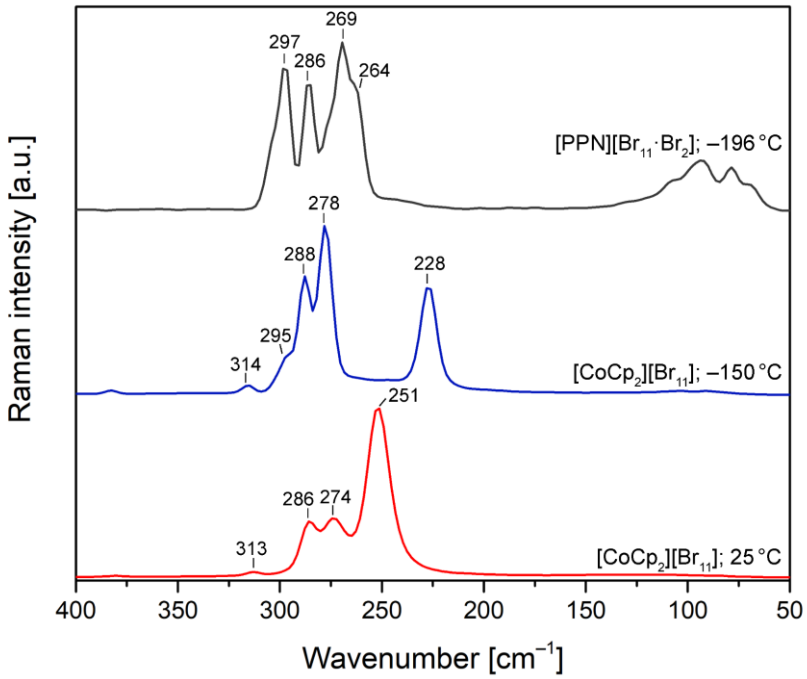


Figure 4-5: Raman spectra of $[CoCp_2][Br_{11}]$ at 25 °C (red line) and –150 °C (blue line) in comparison to the Raman spectrum of $[PPN][Br_{11} \cdot Br_2]$ at –196 °C[12].

The room temperature Raman spectrum of $[CoCp_2][Br_{11}]$ shows a weak band at 313 $cm^{-1}$ (–150 °C: 314 (w), 295 (sh) $cm^{-1}$), two medium bands at 286 and 274 $cm^{-1}$ (–150 °C: 288 (s) and 278 (vs) $cm^{-1}$) and a very strong band at 251 $cm^{-1}$. The latter reveals a large temperature-dependent shift of 23 $cm^{-1}$ (–150°C: 228 (s) $cm^{-1}$). In the case of $[PPN][Br_{11} \cdot Br_2]$ the Raman spectrum features bands at 286, 269 and 264 $cm^{-1}$ for $[Br_{11}]^-$ and 297 $cm^{-1}$ for the additional embedded $Br_2$.[12] Also the band at 313 $cm^{-1}$ at 25 °C and the bands at 314 and 295 $cm^{-1}$ obtained at lower temperatures can be assigned to non-coordinated or very weakly coordinated bromine in the solid state, respectively (gaseous bromine: 325 $cm^{-1}$[18]). The $[Br_{11}]^-$ anion of the $[PPN]^+$ salt shows bands between 286 and 264 $cm^{-1}$ while for the $[CoCp_2]^+$ salts analog bands between 288 and 278 $cm^{-1}$ are obtained at lower temperatures. The observed differences in the band positions for the $[Br_{11}]^-$ anions

can in part be explained by different Br–Br bond lengths. While in [PPN][$Br_{11} \cdot Br_2$] the distances of the central $Br^-$ and the coordinating $Br_2$ units lie between 232.0(1) and 233.5(1) pm[12] [$CoCp_2$][$Br_{11}$] exhibits slightly shorter equatorial bond lengths of 231.7(1) and 232.9(1) pm. [$CoCp_2$][$Br_{11}$] also shows one strongly polarized Br–Br unit with a longer bond distance of 238.9(2) pm that reveals a large shift to smaller wavenumbers at the transition from solution to solid. This is due to interactions with adjacent pyramids followed by an elongation of the axial Br–Br bond length. In addition, between 400 and 290 $cm^{-1}$ the cobaltocenium cation shows bands at 395, 383, 328, and 295 $cm^{-1}$. The reaction series of cobaltocenium bromide with elemental bromine from 1:1.3 to 1:120 is described elsewhere.[1] Already the use of a ratio > 1:3.8 as well as the direct reaction of cobaltocene with an excess of elemental bromine lead to spectra similar to those shown in Figure 4-5 for [$CoCp_2$][$Br_{11}$].

Crystals obtained by the reaction of [$CoCp_2$]Br with different amounts of IBr were investigated by Raman microscope measurements. Regardless of the amount of IBr used, they all show the same bands. Figure 4-6 presents theses spectra in comparison to that of *syn*-[$NMe_4$][$I_4Br_5$], see chapter 3.2.

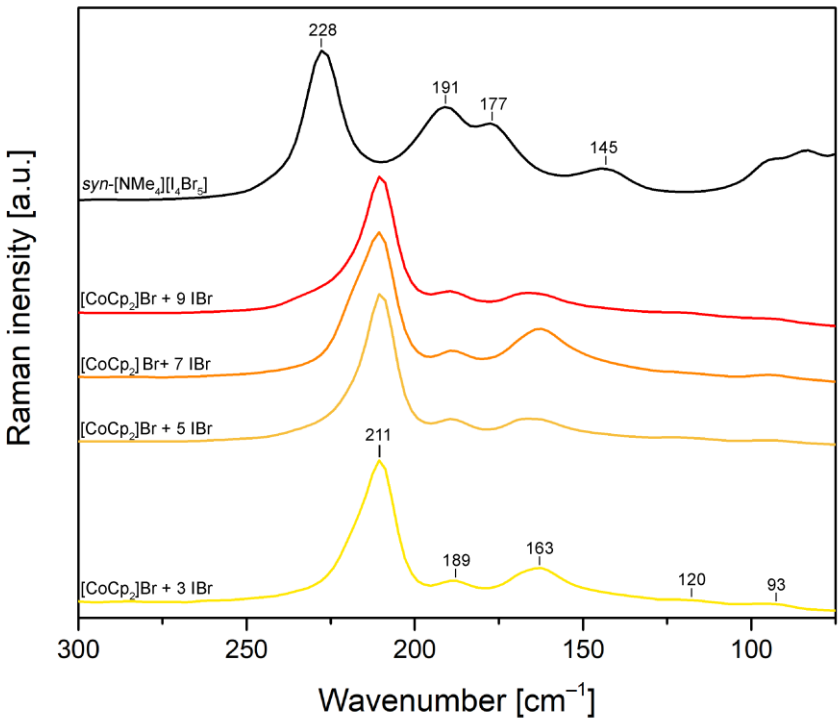


Figure 4-6: Raman spectra (Raman microscope) of [$CoCp_2$]Br + x IBr (x = 3, 5, 7, 9) or rather [$CoCp_2$][$I_3Br_4$] (disordered, see above) in comparison to the spectrum (Raman microscope) of [$NMe_4$][$I_4Br_5$] (see chapter 3.2).

[$CoCp_2$][$I_3Br_4$] shows in Raman microscope measurements of crystals, vibrational bands at 211 (s), 189 (w), 163 (m) $cm^{-1}$, and two very weak ones at 120 and 93 $cm^{-1}$. In comparison

to *syn*-[$NMe_4$][$I_4Br_5$] with bands at 228 (s), 191 (m), 177 (m), and 145 (w) $cm^{-1}$ the strong to medium bands are shifted to lower frequencies due to a different bonding situation. The band at 163 $cm^{-1}$ is assigned to both central $[IBr_2]^-$ anions (Br1–I1–Br2 and Br4–I3–Br5) that are almost symmetric with bond lengths between 270.5(1) and 272.9(1) pm. This value is comparable to the symmetric I–Br stretching vibration of [$NMe_4$][$IBr_2$] with 160 $cm^{-1}$.[25] In the case of an asymmetric $[IBr_2]^-$ anion, like in [$NBu_4$][$IBr_2$] two bands at 162 and 176 (w) $cm^{-1}$ for the symmetric and asymmetric stretching mode in $CH_2Cl_2$ solution are obtained.[26] In comparison to this, the band at 189 $cm^{-1}$ in Figure 4-6 could probably be attributed to residual iodine (compare the following chapters). The strong and slightly asymmetric broad band at 211 $cm^{-1}$ is associated with the IBr units that are coordinated to the central $[IBr_2]^-$ anion (I2–Br3, I4–Br6, I5–Br7, I6–Br8, I5'–Br7', I6'–Br8'). With bond lengths between 256.1(2) and 259.5(14) pm they are shifted to lower wavenumbers compared to the 228 $cm^{-1}$ obtained for the IBr units, that are involved in the V-shaped $[I_2Br_3]^-$ anion of *syn*-[$NMe_4$][$I_4Br_5$] with bond lengths of 253.7(1) and 254.5(1) pm. The distances between the building blocks are larger than 292.6(1) pm. The very weak bands at 120 and 93 $cm^{-1}$ could tentatively be assigned to bending modes of the anion.

Solid [$CoCp_2$][$I_2Cl_3$] was investigated by FIR and Raman spectroscopy. Whereas Yagi and Popov[27,28] described the IR spectrum of [$NMe_4$][$ICl_2 \cdot ICl$] with bands at 312.6 and 294.5 $cm^{-1}$ to the best of our knowledge no Raman spectrum of an $[I_2Cl_3]^-$ anion is known in literature. Therefore, we compare in Figure 4-7 both vibrational spectra of [$CoCp_2$][$I_2Cl_3$] with calculated spectra of the $[I_2Cl_3]^-$ anion at the SCS-MP2/def-SV(P) level. The far-IR spectrum with a weak band at 318 and a strong, asymmetric band around 291 $cm^{-1}$ is similar to that described in the literature for [$NMe_4$][$ICl_2 \cdot ICl$].[27,28] The additional very strong calculated band at 204 $cm^{-1}$, attributed to a bond deformation, is not well observed in the experimental spectrum. The experimental Raman spectrum shows bands at 386 (w), 324 (m), 306 (s), 191 (sh), 182 (vs), 95 (m), and 72 (m) $cm^{-1}$. Bands at 386 and 324 $cm^{-1}$ were already recorded in the spectrum of the educt [$CoCp_2$]Cl. The latter is likely superimposed by the symmetric stretching vibration. The antisymmetric I–Cl stretching vibration appeared at 306 $cm^{-1}$, which fit well with the calculated value at 304 $cm^{-1}$. The bands at 191 and 182 $cm^{-1}$ are attributed to iodine. Both band positions and intensities are comparable to the stretching vibrations of crystalline iodine at 188 and 180 $cm^{-1}$.[29]

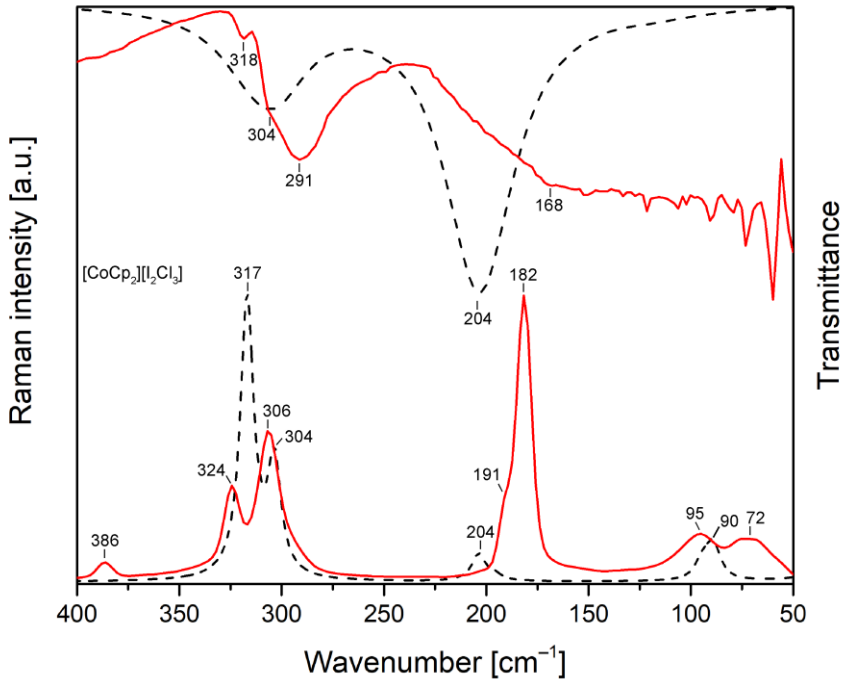


Figure 4-7: Experimental Raman (bottom) and FIR spectrum (top) of $[CoCp_2][I_2Cl_3]$ (red) in comparison to calculated spectra for the $[I_2Cl_3]^-$ anion at SCS-MP2/def-SV(P) level (black, dashed).

Further reactions of the cobaltocenium salts, especially with substituted cobaltocenium cations are described elsewhere.[1,30]

## 4.2 Iodobromide Synthesized from Tetraethylammonium Bromide in an Ionic Liquid

As already presented, tetramethylammonium tetraiodopentabromide $[NMe_4][I_4Br_5]$ crystallizes in two different structures depending on the solvent used. In the case of the ionic liquid [HMIM]Br the anion is built of a V-shaped $[I_2Br_3]^-$ and two further IBr molecules connecting the terminal bromine atoms in a *syn*-orientation due to halogen-halogen interactions. In contrast to the *syn* structure *anti*-$[NMe_4][I_4Br_5]$ was formed in the organic solvent dichloromethane. Here, the two IBr units coordinate from opposite directions on the central $[I_2Br_3]^-$ (see chapter 3.2).

To investigate the influence of the alkyl chain length of the cation on the forming anion the experiments in [HMIM]Br were repeated treating $[NEt_4]$Br with 3 and 5 equivalents of IBr, respectively. In both approaches crystals of the stoichiometric formula $[NEt_4][I_5Br_2]$ were obtained (Figure 4-8).

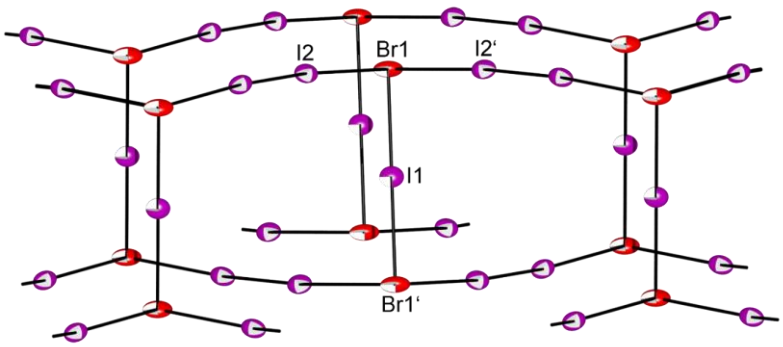


Figure 4-8: Solid state structure of the connected anions in $[NEt_4][I_5Br_2]$. Ellipsoids are set at the 50% probability level. Selected bond lengths (pm) and angles (°): Br1–I1: 273.2(2), Br1–I2: 331.5(2), I2–I2': 268.5(2); Br1–I1–Br1': 180.0°, I1–Br1–I2: 82.9(1), I2–Br1–I2': 84.8(1), Br1–I2–I2': 175.9(1).

The crystal structure shows the orthorhombic space group *Cmce*. $[I_5Br_2]^-$ consists of an $[IBr_2]^-$ anion and two iodine molecules. The bromine atoms of $[IBr_2]^-$ are connected with each other over $I_2$ molecules to form curled chains. This Br–I–I–Br–I–I– chains are linked via the $[IBr_2]^-$ iodine atoms with those in front and behind to build double layers. The $[IBr_2]^-$ anions are symmetric and show a Br1–I1 bond length of 273.2(2) pm which is comparable to those in $[NEt_4][IBr_2]$ (274.2(2) pm)[31]. The bond length of the $I_2$ molecules (268.5(2) pm) is only slightly elongated compared to molecular iodine (266 pm) while the Br1–I2 distance (331.5(2) pm) lies underneath the sum of the van der Waals radii of IBr (383 pm).

An interhalide anion with the same formula $[I_5Br_2]^-$ is already known for the substance $[BPH][I_5Br_2]$ (BPH = 2,2'-bipyridylium).[21] The unit cells of both compounds are pictured in Figure 4-9.

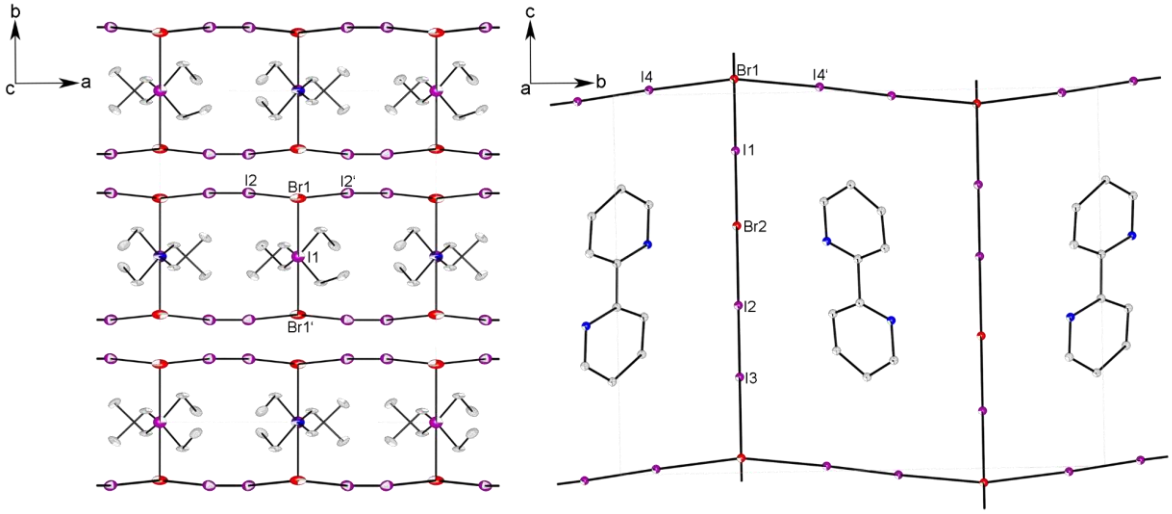


Figure 4-9: *Left:* Unit cell of the solid state structure of $[NEt_4][I_5Br_2]$ along *c*-axis. The $[NEt_4]^+$ cations are disordered. *Right:* Unit cell of the solid state structure of $[BPH][I_5Br_2]$ along *a*-axis.[21] In both structures the ellipsoids are drawn at 50% probability and the hydrogen atoms are omitted for clarity.

[BHP][$I_5Br_2$] is also build of an [$IBr_2$]$^-$ anion and two iodine molecules. The [$IBr_2$]$^-$ anion shows two different bond lengths (I1–Br1: 267.3(9) pm, I1–Br2: 277(1) pm) and the unequal iodine molecules (I2–I3: 270.3(8) pm, I4–I4': 270.5(6) pm) are elongated around 2 pm compared to [$NEt_4$][$I_5Br_2$]. Furthermore, they are connected in a different way. While one of the bromine atoms (Br1) also forms Br–I–I–Br–I–I– chains, the other bromine atom (Br2) of [$IBr_2$]$^-$ is connected via the second $I_2$ molecule (I2–I3) to Br1. Hence, curled netlike layers with a distance of 435.1(2) pm are formed. The [BHP]$^+$ cations lie in the cavities between the polyinterhalides.[21]

In [$NEt_4$][$I_5Br_2$] (Figure 4-9, left) the cations are in the middle of the double layers, that are parallel to the *a*-*c*-plane. The positions of the [$NEt_4$]$^+$ nitrogen atoms and the [$IBr_2$]$^-$ iodine atoms are reminiscent of the NaCl structure. The double layers have a high of 575 pm, the distance to the next one is only 176 pm. However, since the double layers show ABAB stacking, the shortest atom to atom distance is 571.1(1) pm (I2–$I2_{next\ layer}$).

A layered structure, even if less pronounced, can also be found in *syn*-[$NMe_4$][$I_4Br_5$] (see chapter 3.2) along the *a*-axis. The distance is with 244 pm clearly larger than in [$NEt_4$][$I_5Br_2$]. Furthermore, the [$NMe_4$]$^+$ cations extend into the interspace. But in contrast to both [$NMe_4$][$I_4Br_5$] compounds the ratio of iodine to bromine in [$NEt_4$][$I_5Br_2$] does not correspond to that of the starting materials used. This fact can be explained by halogen exchange reactions. Furthermore, at room temperature 8% of iodine monobromide are dissociated into the elements.[32] For the synthesis of [BPH][$I_5Br_2$] the [BPH]Br, IBr, and $I_2$ were used in a ratio of 5:5:2.[21] Again, the product contains a larger percentage of iodine than used.

For the Raman microscope measurement crystals of [$NEt_4$][$I_5Br_2$] have been used, see Figure 4-10. The Raman spectrum shows a strong band at 191 cm$^{-1}$ and two medium bands at 224 and 160 cm$^{-1}$. The latter is assigned to the symmetric [$IBr_2$]$^-$ anion in the network. The I–Br bond is with 273.2(2) pm only slightly elongated in comparison to the above described [$IBr_2$]$^-$ units in [$CoCp_2$]$_2$[$I_3Br_4$]$_2$ · $CH_2Cl_2$ with bond lengths of 270.5(1) – 272.9(1) pm that show a band at 163 cm$^{-1}$ in the Raman spectrum. The band obtained at 191 cm$^{-1}$ is in the frequency range for crystalline iodine with 180 and 188 cm$^{-1}$.[29] Presumably, the band at 224 cm$^{-1}$ belongs to some remaining IBr. Solid IBr shows a broad band between 200 and 250 cm$^{-1}$ with a maximum at 218 cm$^{-1}$.[33,34]

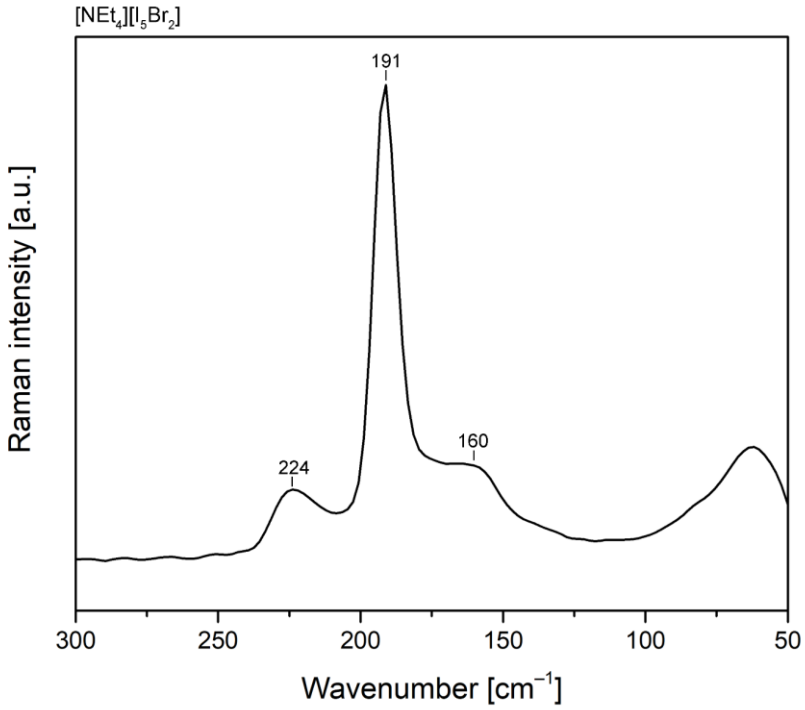


Figure 4-10: Raman microscope measurement of $[NEt_4][I_5Br_2]$.

Further details, such as Raman spectra of the reaction mixtures and further reactions of ICl and IBr in ionic liquids are described elsewhere.[2]

## 4.3 Investigation of [PPN-3$^F$]Cl in the Synthesis of a Polyhalide and a Polyinterhalide

In first attempts partially fluorinated bis(triarylphosphoranylidene)iminium cations $[PPN\text{-}3^F]^+$ were used for the preparation of polyhalides and polyinterhalides. However, the reaction of [PPN-3$^F$]Cl with an excess of chlorine (112 eq.) and some drops of acetonitrile resulted in the formation of the side product 2,4,6-tris(trichlorometyl)-1,3,5 triazine and the evolution of HCl. The product was characterized by Raman spectra of the solid[35] as well as single crystal X-ray structure determination. $^{31}P$ and $^{19}F$ NMR spectra show that $[PPN\text{-}3^F]^+$ does not react in this mixture. Furthermore, by repeating the reaction without $[PPN\text{-}3^F]^+$ or after its replacement by $[PPN]^+$ 2,4,6-tris(trichlorometyl)-1,3,5 triazine was formed again. Due to the fact that the reaction did not occur in the dark the chlorination of $CH_3CN$ is photochemically induced. Further work of K. Sonnenberg confirmed this result for the preparation of $[PPN][Cl_{13}]$ where the chlorinated triazine derivative was obtained after a few days, too.[13]

If [PPN-3$^F$]Cl was treated with iodine monochloride crystals were obtained from an acetonitrile solution with the formula $[\{(C_6H_2F_3)_3P\}_2N]_2[I_4Cl_4]\cdot 4\ CH_3CN$. The compound crystallizes in the monoclinic space group $P2_1/c$. The discrete polyinterhalide can be described by two slightly unsymmetrical $[ICl_2]^-$ anions (Cl1–I1: 253.5(1) pm; I1–Cl2: 255.5(2) pm) that are linked by an iodine molecule to a Z-shaped polyinterhalide, see Figure 4-11. This $I_2$ shows a bond length of 271.6(1) pm, that is comparable with crystalline iodine (271.5(6) pm).[36] The distance to the chlorine atom of each $[ICl_2]^-$ anion lies with 311.2(2) pm clearly below the sum of the van der Waals radii of iodine and chlorine (373 pm).

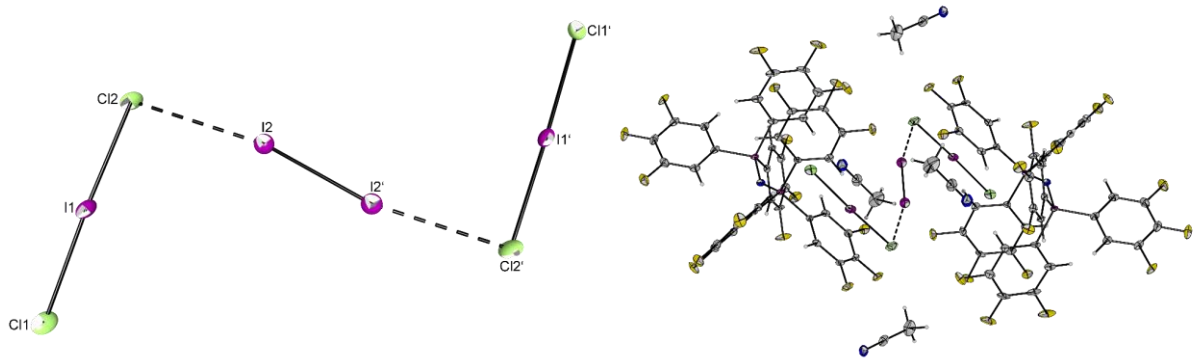


Figure 4-11: *Left:* Molecular structure of $2[ICl_2]^-\cdot I_2$ in $[PPN\text{-}3^F]_2[I_4Cl_4]\cdot 4\ CH_3CN$. Ellipsoids are shown at the 50% probability level. Selected bond lengths (pm) and angles (°): Cl1–I1: 253.5(1), I1–Cl2: 255.5(2), Cl2–I2: 311.2(2) pm, I2–I2': 271.6(1); Cl1–I1–Cl2: 177.5(1), I1–Cl2–I2: 92.4(1), Cl2–I2–I2': 166.1(1). *Right:* Cutout of the solid state structure of $[PPN\text{-}3^F]_2[I_4Cl_4]\cdot 4\ CH_3CN$.

Z-shaped structures are already known from other polyhalide dianions. $[I_8]^{2-}$ was first mentioned in literature in 1954, $[Br_8]^{2-}$ in 1997.[37,38] $[Cl_8]^{2-}$ was recently reported to be prepared in the ionic liquid [BMP][OTf] (*N*-butyl-*N*-methylpyrrolidinium triflate) and shows a more linear structure.[39] A mixed octahalide dianion is known for $[I_2Br_6]^{2-}$ in $[Cu(dafone)_3][IBr_4][I_2Br_6]_{0.5}\cdot CH_3CN$ (dafone = 4,5-diazafluoren-9-one). For this compound, Rajasekharan et al. added iodine and an excess of bromine to a mixture of $CuBr_2$ and dafone in acetonitrile.[40] The structure motif of the here prepared $[I_4Cl_4]^{2-}$ is compared to $[I_2Br_6]^{2-}$, $[Cl_8]^{2-}$ and one of the numerous known $[I_8]^{2-}$ dianions in Figure 4-12.[39–41]

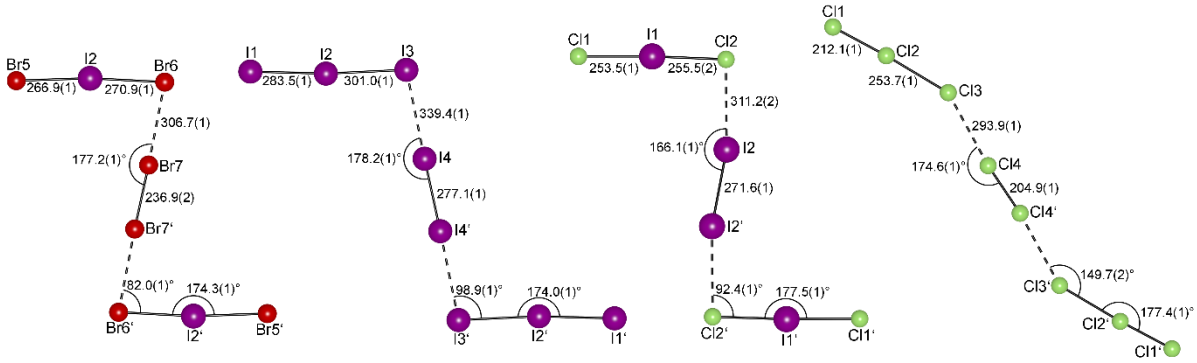


Figure 4-12: Comparison of the octahalide anions $[I_2Br_6]^{2-}$[40] (CCDC: 1051676), $[I_8]^{2-}$[41] (CSD: 58639), $[I_4Cl_4]^{2-}$ and $[Cl_8]^{2-}$[39] (CCDC: 1456573).

An overview of some octaiodides is given by Svensson and Kloo.[10] Whereas the $[I_8]^{2-}$ shown in Figure 4-12 has an elongated bond length I4–I4' and an I2–I3–I4 angle of 98.9(1)° the corresponding values obtained in $[Cu(phen)_2I]_2[I_8]$[10,42] are with 272.3 pm and 95.7° more closer to those obtained in our $[I_4Cl_4]^{2-}$: 271.6(1) pm for I2–I2' and an I1–Cl2–I2 angle of 92.4(1)°. The Br7–Br7' contact (236.9(2) pm) in $[I_2Br_6]^{2-}$ and the Cl4–Cl4' contact (204.9(1) pm) in $[Cl_8]^{2-}$ are elongated in comparison to, respectively, crystalline bromine (229.4(2) pm at 80 K) and chlorine (198.5(2) pm at 100 K).[43] This again illustrates weak if any interactions between the two $[ICl_2]^-$ units and the bridging $I_2$. Furthermore, the $[X_2Y]^-$ anions as part of the octainterhalides show nearly equal bond lengths (X–Y difference: 2–4 pm) while the $[X_3]^-$ units are clearly asymmetric (X–X difference: 18–42 pm). At this point a reference to further Z-shaped disordered interhalides should be made. Among them is $[Sr(B_{15}K_5)_2][I_{3.77}Cl_{4.23}]$ ($B_{15}K_5$ = benzo-15-crown-5) which consists like the $[I_4Cl_4]^{2-}$ dianion described here of two $[ICl_2]^-$ units that are connected by a dihalogen with a statistic occupancy of 12% chlorine and 88% iodine.[44]

Raman microscope measurements of a single crystal of $[PPN\text{-}3^F]_2[I_4Cl_4]\cdot 4\ CH_3CN$ show two strong bands at 268 and 195 $cm^{-1}$ for the $[ICl_2]^-$ and $I_2$ units. With values between 254 and 278 $cm^{-1}$ for $[ICl_2]^-$, depending on the used cation,[45–47] 207 $cm^{-1}$ for iodine (in $CHCl_3$ solution),[48] and 168 $cm^{-1}$ for the central $I_2$ molecule in $[Mn(Ur)_6][I_8]$,[49] respectively, the obtained bands are in good agreement with the literature. For further bands due to the $[PPN\text{-}3^F]^+$ cation, see Figure 4-13.

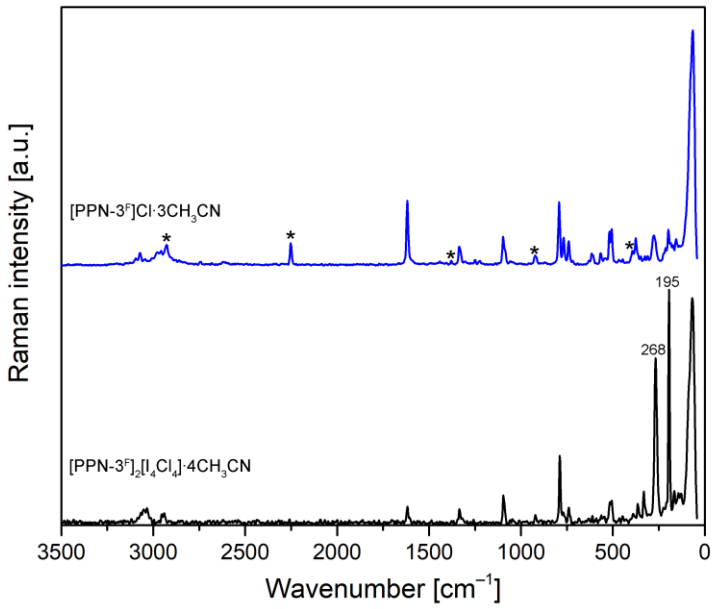


Figure 4-13: Raman microscope spectra (single crystal, 0 °C) of $[PPN\text{-}3^F]_2[I_4Cl_4] \cdot 4\ CH_3CN$ (black) with marked bands at 286 ($ICl_2^-$) and 195 $cm^{-1}$ ($I_2$) in comparison to $[PPN\text{-}3^F]Cl \cdot 3\ CH_3CN$. Bands of $CH_3CN$ are indicated by an asterisk.

Although iodine monochloride is only dissociated to 0.4% at room temperature[32] the obtained compound contains an iodine molecule. The presence of $I_2$ is confirmed by a very weak band at 198 $cm^{-1}$ (molten $I_2$: 194 $cm^{-1}$)[50] obtained in the Raman spectrum of the starting material ICl at room temperature.

## 4.4 Reaction of $[PPh_4]Cl$ with ICl

In an earlier work the reaction of $[PPh_4]Cl$ with ICl (ratio 1:3) was described to led between –30 and –40 °C to crystals of $[PPh_4][I_3Cl_4]$, that show a distorted trigonal pyramidal structure.[51] In order to learn more about the system of $[PPh_4]Cl$ and ICl a reaction series was started with ratios from 1:1 to 1:7. Like in the synthesis of $[PPh_4][I_3Cl_4]$ the volatile materials were removed under reduced pressure while cooling. Figure 4-14 shows the compounds prepared for Raman measurements before they were resolved in dichloromethane for crystallization experiments again. The 1:3 mixture was additionally performed without using $CH_2Cl_2$ to solve the educts.

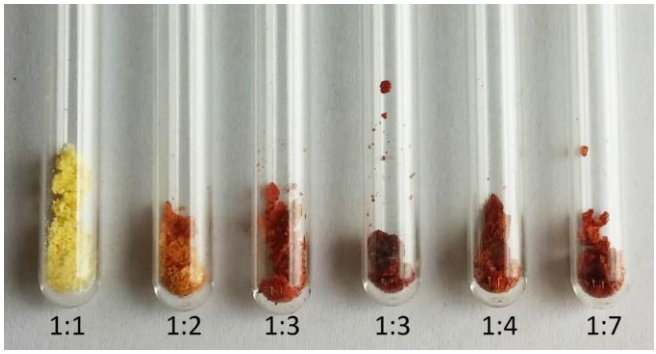


Figure 4-14: Reactions of $[PPh_4]Cl$ with ICl in the ratios 1:1, 1:2, 1:3, 1:3 (prepared without the solvent $CH_2Cl_2$), 1:4 and 1:5.

But in contrast to previous results the reaction of $[PPh_4]Cl$ with 3 equivalents of ICl shows at –30 °C crystals of $[PPh_4]_2[I_6Cl_6]$ (Figure 4-15). The compound crystallizes in the triclinic space group $P\bar{1}$ The $[I_6Cl_6]^{2-}$ anions consist of two V-shaped $[I_2Cl_3]^-$ anions bridged by an $I_2$ molecule over the central $Cl^-$. The bridging iodine molecule is disordered and therefore substituted by 28.5% chlorine.

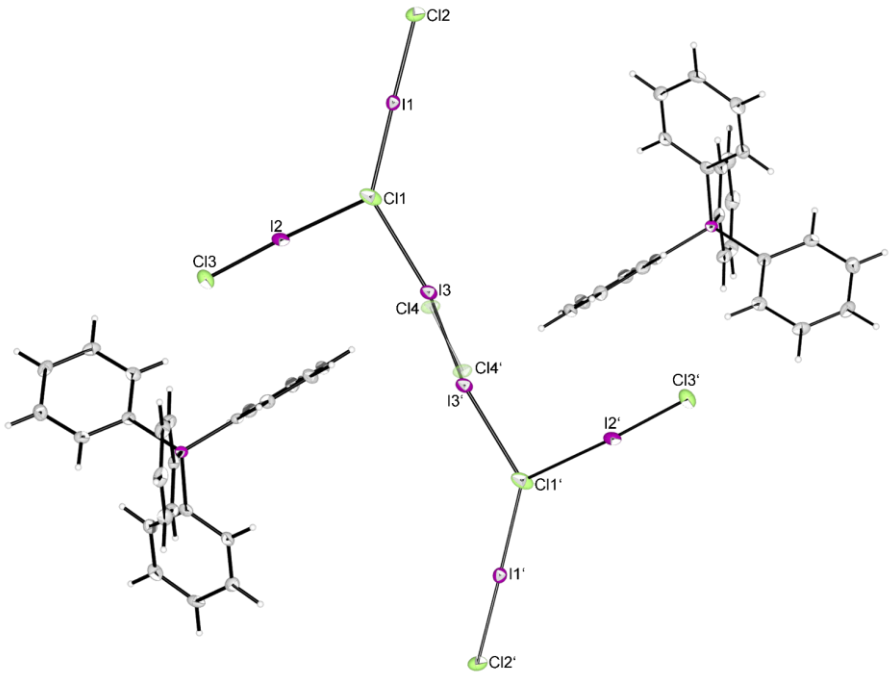


Figure 4-15: Solid state structure of $[PPh_4]_2[I_6Cl_6]$. The central bridging position occupied with an $I_2$ unit is disordered, being substituted with 28.5% $Cl_2$. Ellipsoids are set at the 50% probability level. Selected bond lengths (pm) and angles (°): Cl1–I1: 263.5(1), I1–Cl2: 247.0(1), Cl1–I2: 281.9(1), I2–Cl3: 238.8(1), Cl1–I3: 306.5(2), I3–I3': 275.2(2), Cl1–Cl4: 345.9(7), Cl4–Cl4': 194.9(15); Cl1–I1–Cl2: 176.4(1), Cl1–I2–Cl3: 177.0(1), I1–Cl1–I2: 125.7(1), Cl1–I3–I3': 169.4(1), I1–Cl1–I3: 134.1(1), I2–Cl1–I3: 93.4(1), Cl1–Cl4–Cl4': 171.1(8), I1–Cl1–Cl4: 136.1(2), I2–Cl1–Cl4: 90.0(2).

Repeating this reaction with educts from alternative suppliers ([$PPh_4$]Cl: Sigma-Aldrich instead of Riedel-de Haën, ICl: Alfa Aesar instead of Merck) crystals of [$PPh_4$][$I_2Cl_3$] were obtained (Figure 4-16).

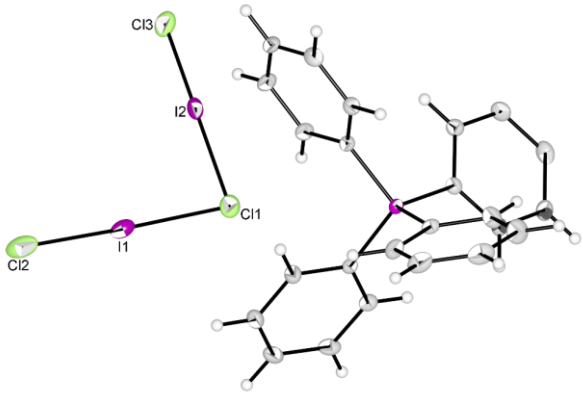


Figure 4-16: Solid state structure of [$PPh_4$][$I_2Cl_3$]. Ellipsoids are set at the 50% probability level. Selected bond lengths (pm) and angles (°): Cl1–I1: 270.5(1), I1–Cl2: 243.0(1), Cl1–I2: 272.1(1), I2–Cl3: 243.1(1); Cl1–I1–Cl2: 174.9(1), Cl1–I2–Cl3: 177.1(1), I1–Cl1–I2: 97.5(1).

[$PPh_4$][$I_2Cl_3$] crystallizes in the monoclinic space group $P2_1/c$. In contrast to the literature known [BHP][$I_2Cl_3$] with an I–Cl–I angle of 101.5(1)°[23], [$BnMe_3N$]$_2$[$I_2Cl_3$][$ICl_4$] with 99.5(1)°[24] and the above described [$CoCp_2$][$I_2Cl_3$] with 130.8(2) or 131.7(2)° [$PPh_4$][$I_2Cl_3$] shows the smallest I–Cl–I angle with 97.5(1)°. The bond lengths with 243.0(1) (I1–Cl2) and 243.1(1) pm (I2–Cl3) for the outer I–Cl units and 270.5(1) (Cl1–I1) and 272.1(1) pm (Cl1–I2) to the central $Cl^-$ are in the same range as those in the other three $[I_2Cl_3]^-$ anions: 241.7(2) – 245.3(3) pm, and 268.5(3) – 271.8(2) pm.

In a further 1:3 approach [$PPh_4$]Cl (Sigma-Aldrich) was purified from contaminations of [$PPh_4$]Br before treated with 3 equivalents of ICl (Merck). The orange solid crystallized at room temperature before it was resolved in dichloromethane again. The sample shows two different types of crystals. Orange crystals of [$PPh_4$]$_2$[$I_6Cl_6$] (disordered with [$PPh_4$]$_2$[$I_4Cl_8$]) were found next to colorless crystals of [$PPh_4$][$ICl_2$]. The latter are already described by Minkwitz and Berkei.[52]

Since the obtained crystals always show a smaller ratio of [$PPh_4$]Cl and ICl than the used 1:3 we tested a 1:5 ratio in order to get larger iodochlorides. In this reaction mixture crystals of [$PPh_4$][$I_3Cl_4$] were obtained at –30 °C. But in contrast to the known distorted trigonal pyramidal structure[51] the $[I_3Cl_4]^-$ anions show a chain-like structure (Figure 4-17).

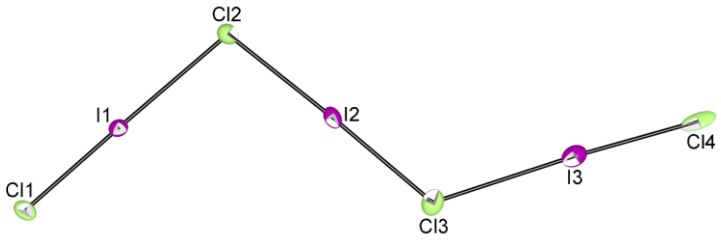


Figure 4-17: $[I_3Cl_4]^-$ in the solid state structure of $[PPh_4][I_3Cl_4]$. Ellipsoids are set at the 50% probability level. Selected bond lengths (pm) and angles (°): Cl1–I1: 240.3(2), I1–Cl2: 278.9(2), Cl2–I2: 258.2(2), I2–Cl3: 253.0(2), Cl3–I3: 288.1(2), I3–Cl4: 249.0(2); Cl1–I1–Cl2: 179.1(1), I1–Cl2–I2: 100.8(1), Cl2–I2–Cl3: 178.2(1), I2–Cl3–I3: 121.4(1), Cl3–I3–Cl4: 177.6(1).

In quantum-chemical calculations at the SCS-MP2/def2-TZVPP level the chain-like structure in $C_{2h}$ symmetry is 5.1 $kJ \cdot mol^{-1}$ energetically less favorable than the $C_{3v}$ structure.[51] This small energy difference can be overcome by crystal packing effects. In summary, it becomes apparent that in addition to the used $Cl^-$: ICl ratio the crystallization conditions may play an important role for the formation of the here shown samples, too.

$[PPh_4][I_3Cl_4]$ crystallizes in the tetragonal space group $P\bar{4}$. It is built of a central asymmetric $[ICl_2]^-$ anion with bond lengths of 258.2(2) (Cl2–I2) and 253.0(2) pm (I2–Cl3), that is coordinated by two ICl molecules. The $[PPh_4]^+$ cations and $[I_3Cl_4]^-$ anions are both stacked along the *c*-axis (Figure 4-18).

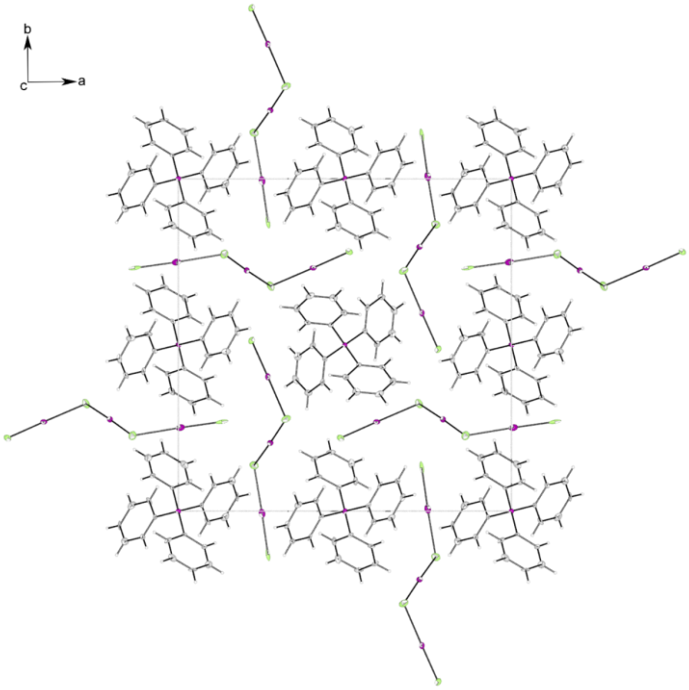


Figure 4-18: Unit cell of the solid state structure of $[PPh_4][I_3Cl_4]$ along *c*-axis. Ellipsoids are set at the 50% probability level. Both anions and cations are stacked along the *c*-axis.

Figures 4-19, 4-20 and 4-21 show the Raman spectra of the described reaction approaches and crystals. The Raman microscope measurements of $[PPh_4][ICl_2]$ and $[PPh_4]_2[I_6Cl_6]$ (disordered with $[PPh_4]_2[I_4Cl_8]$) (Figure 4-19) show a strong band at 258 $cm^{-1}$ in the yellow spectrum (bottom trace) that decreases with increasing orange color of the crystals (bright orange and orange spectrum at the middle and top traces). This band is assigned to the $[ICl_2]^-$ anion which is confirmed by literature spectra of $[ICl_2]^-$ with bands at 254 and 278 $cm^{-1}$[45–47] or the band at 268 $cm^{-1}$ for the aforementioned $[ICl_2]^-$ as part of $[PPN\text{-}3^F]_2[I_4Cl_4]\cdot 4\ CH_3CN$ (see 4.3). The yellow color can be explained by overlaying the colorless $[PPh_4][ICl_2]$ and the orange $[PPh_4]_2[I_6Cl_6]$ ($[PPh_4]_2[I_4Cl_8]$) crystals (see bottom trace). Therefore, the weak and medium strong bands in the yellow spectrum (bottom trace) belong to the $[I_6Cl_6]^{2-}$ anion.

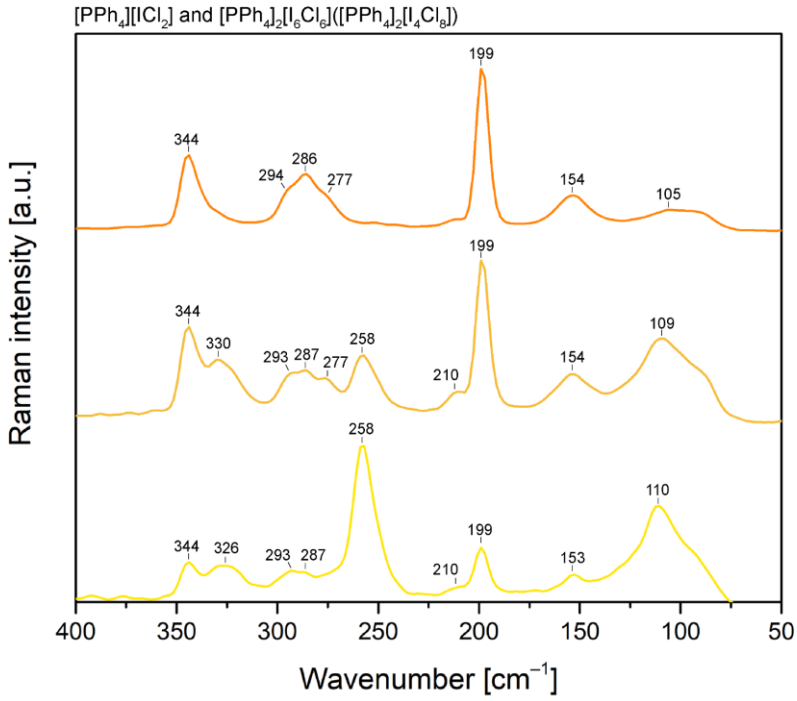


Figure 4-19: Raman microscope measurement of the crystals $[PPh_4][ICl_2]$ and $[PPh_4][I_6Cl_6]$ (disordered with $[PPh_4][I_4Cl_8]$). The color of the traces roughly match with the color of the measured crystals (*top*: yellow, *middle*: light orange, *bottom*: orange colored crystals).

The bright orange spectrum in the middle trace of Figure 4-19 also shows superimposed frequencies of both crystal types. In the orange spectrum in the top trace of Figure 4-19 the band at 258 $cm^{-1}$ is completely disappeared. It can be assumed that this is probably the pure spectrum of $[PPh_4]_2[I_6Cl_6]$ ($[PPh_4]_2[I_4Cl_8]$). However, this is a tentative assignment, any impurities cannot be ruled out. The band at 199 (vs) $cm^{-1}$ can be assigned to the bridging iodine molecule (I3–I3': 275.2(2) pm) which fits very well compared to the band

at 195 $cm^{-1}$ of the bridging $I_2$ in $[PPN\text{-}3^F]_2[I_4Cl_4]\cdot 4\ CH_3CN$ (see 4.3) that shows a shorter bond length (I2–I2': 271.6(1) pm). Frequencies of the chlorine molecule were not identified in the spectrum (stretching frequencies for crystalline $Cl_2$ at 168 K: 526.5 – 542.3 $cm^{-1}$[29,53]). Beside the band at 199$cm^{-1}$ the orange spectrum shows bands at 344 (s), 294 (sh), 286 (m), 277 (sh), 154 (m) and a band at 105 (w) $cm^{-1}$ with a shoulder at lower wavenumbers. In comparison to the above described $[CoCp_2][I_2Cl_3]$ with stretching frequencies at 324 and 306 $cm^{-1}$ (I1–Cl2: 243.5(4) pm, I2–Cl3: 245.3(3) pm) the obtained bands centered at 344 and 286 $cm^{-1}$ are consistent considering the shorter and longer I–Cl distances of the $[I_2Cl_3]^-$ units in $[PPh_4]_2[I_6Cl_6]$ of 238.8(1) and 247.0(1) pm.

Based on these results the obtained bands of the reaction series of $[PPh_4]Cl$ with different ratios of ICl are evaluated (Figure 4-20).

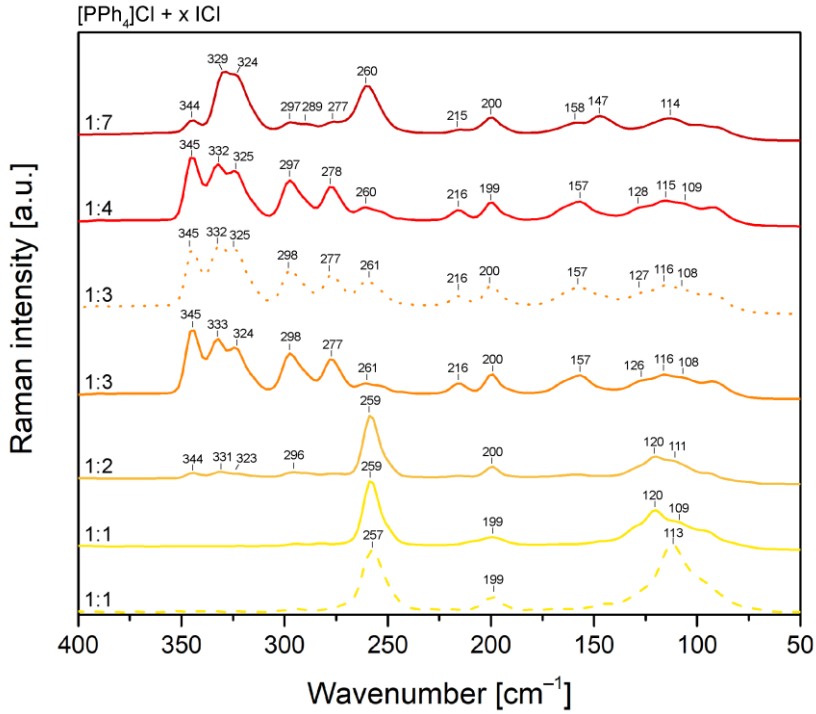


Figure 4-20: Raman spectra of the reaction series of $[PPh_4]Cl$ with ICl in the ratios 1:1 (Raman microscope measurement: dashed), 1:2, 1:3 (without prior solving in $CH_2Cl_2$: dotted), 1:4 and 1:7 at –150 °C.

The 1:1 approach shows the band at 259 and 257 $cm^{-1}$ in both the spectrum of the solid (continuous line) and the Raman microscope measurement of a crystal (dashed line) respectively, which can be assigned to the $[ICl_2]^-$ anion. The deformation vibrations at 120, 109, or 113 $cm^{-1}$, which could also be longitudinal and transversal vibrations of the solid, will not be discussed any further. All spectra show a band around 200 $cm^{-1}$ which is due to iodine. The 1:2 ratio shows in addition to the bands we know from the 1:1 approach further very weak bands, that are found in the 1:3 approach again. Spectra of the reaction

mixtures of $[PPh_4]Cl$ with 3 and 4 equivalents of ICl show the same band positions, even without solving the educts in $CH_2Cl_2$ during the reaction (dotted line) no differences can be seen. However, the 1:7 approach differs significantly. The Raman spectrum of the solid obtained for the 1:3 ratio shows a mixture of several species. In addition to $[ICl_2]^-$ (261 $cm^{-1}$) and $[I_6Cl_6]^{2-}$ (345, 298, 277, 157 $cm^{-1}$, the band at 286 $cm^{-1}$ is missing compared to Figure 4-19), that crystallizes from this sample, additional strong bands at 333 and 324 $cm^{-1}$ are obtained. Broad bands at 330 and 326 $cm^{-1}$ respectively are also found in the yellow and bright orange spectrum in Figure 4-19.

Suitable for this Figure 4-21a) (top trace) shows strong bands at 331 and 326 $cm^{-1}$ during the warm up of the compound after it had been frozen with liquid nitrogen. In comparison to the measurement of $[PPh_4][I_2Cl_3]$ crystals in a Raman cuvette at –196 °C that shows strong bands at 308 and 298 $cm^{-1}$ with the expected low-frequency shift the solid reaction mixture also consists of several compounds.

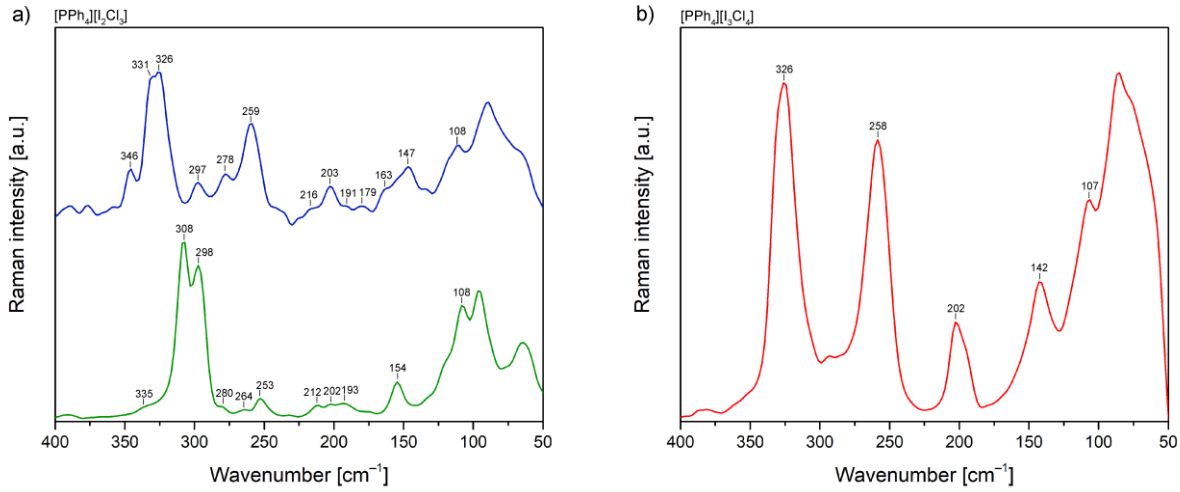


Figure 4-21: a) Raman spectra of $[PPh_4][I_2Cl_3]$ (*bottom*: measurement of the crystals in the Raman cuvette at –196 °C, *top*: low temperature measurement of the solid). b) Raman microscope measurement of chain-like $[PPh_4][I_3Cl_4]$.

Figure 4-21b) shows the Raman microscope measurement for the chain like $[I_3Cl_4]^-$ anion in $[PPh_4][I_3Cl_4]$ with bands at 326 (vs), 258 (s), 202 (m), 142 (m) and 107 (s) $cm^{-1}$. The band at 258 $cm^{-1}$ can be assigned to the central $[ICl_2]^-$ unit which is consistent with previous observations. The two coordinated ICl units are assigned to the slightly asymmetric bands at 326 $cm^{-1}$. The band at 202 $cm^{-1}$ again shows remaining iodine, and frequencies at 142 and 107 $cm^{-1}$ are in the range of the deformation vibrations or the stretching vibration of the weak bonding interaction Cl2–I1 and Cl3–I3.

## 4.5 Overview of the Stretching Vibrations of Non-Classical Iodochlorides and -bromides

Tables 4-1 and 4-2 sum up the stretching vibrations of iodochlorides and -bromides. The reported values originate from this work as well as from literature Raman spectra.

Table 4-1: Characteristic wavenumbers for the stretching vibrations of iodochlorides.

| Interhalide | Building Block | Wavenumber [$cm^{-1}$] |
|---|---|---|
| $[I_2Cl]^-$ [54] | $[I–I–Cl]^-$ | 160 (vs) |
| $[ICl_2]^-$ [47] | $[Cl–I–Cl]^-$ | 278 or 268 or 254 (depending on the cation) |
| $[ICl_2]^-$ [44] | $[Cl–I–Cl]^-$ | 264 (vs) |
| $[ICl_2]^-$ | $[Cl–I–Cl]^-$ | 258 |
| $[I_2Cl_3]^-$ | I–Cl | 324 (m), 306 (s) |
| $[I_2Cl_3]^-$ | I–Cl | 308 (vs), 298 (vs) |
| $[I_3Cl_4]^-$(trigonal pyramidal)[51] | I–Cl | 330 (vs), 320 (vs) |
| $[I_3Cl_4]^-$(chain) | I–Cl | 326 (vs) |
| | $[Cl–I–Cl]^-$ | 258 (s) |
| $[I_2Cl_7]^-$ [55] | $[I–Cl–I]^-$ | 216 (vw) |
| $[I_2Cl_2]^{2-}$[37] | $[Cl–I–I–Cl]^-$ | 217, 202 |
| $[I_4Cl_4]^{2-}$ | $[Cl–I–Cl]^-$ | 268 (s) |
| | I–I | 195 (vs) |
| $[I_6Cl_6]^{2-}$ | I–Cl | 344 (s), 294 (m), 277 (m) |
| | I–I | 199 (vs) |

Table 4-2: Characteristic wavenumbers for the stretching vibrations of iodobromides.

| Interhalide | Building Block | Wavenumber [$cm^{-1}$] |
|---|---|---|
| $[I_2Br]^-$ | $[I–I–Br]^-$ and $[I–Br–I]^-$ | 154 (s), 132(s), 111(s) |
| $[IBr_2]^-$[20] | $[Br–I–Br]^-$ | 168 |
| $[IBr_2]^-$[25] | $[Br–I–Br]^-$ | 160 (s) |
| $[I_2Br_3]^-$ (chapter 3.2) | I–Br | 230 (sh), 214 (s), 193 (m) |
| $[I_3Br_4]^-$ (trigonal | I–Br | 228 (s), 215 (vs) |
| pyramidal)[19] | $I_3$–Br | 161 (w), 101 (w) |
| $[I_3Br_4]^-$ (trigonal planar)[20] | I–Br | 228 (vs), 211 (sh), 190 (s) |
| | $I_3$–Br | 130 (w, br) |
| $[I_3Br_4]^-$ (chain) | I–Br | 211 (s) |
| | $[Br–I–Br]^-$ | 163 (m) |
| $[I_5Br_2]^-$ | I–I | 191 (s) |
| | $[Br–I–Br]^-$ | 160 (m) |
| $[I_4Br_5]^-$ (chapter 3.2) | I–Br | 228 (s, br) |
| | I–Br ($[I_2Br_3]^-$) | 191 (m), 177 (m) |
| | $IBr_2$ | 145 (w) |
| $[I_5Br_7]^-$[33] | I–Br | 223 (s), 213 (m), 187 (s) |
| $[I_2Br_6]^{2-}$[40] | Br–Br | 275 (m) |
| | $[Br–I–Br]^-$ | 187 (vs), 167 (m) |

## 4.6 Experimental Section

### 4.6.1 Methods

The far-IR spectrum was recorded on a Nicolet FT-IR Nexus spectrometer with a solid substrate beam splitter (resolution 4 $cm^{-1}$) between 50 and 600 $cm^{-1}$. The IR spectrum was measured on a Nexus 670 Nicolet FT-IR spectrometer (resolution 4 $cm^{-1}$) between 500 and 4000 $cm^{-1}$.

FT Raman spectra were recorded on a Bruker RFS 100/S or MultiRam II spectrometer with low-temperature Ge detector (1064 nm, 30–300 mW power, resolution 4 $cm^{-1}$) in a temperature range between room temperature and –196 °C. For low temperature measurements the sample was either frozen in liquid $N_2$ or measured in an additional cooling unit or a Raman cuvette. Single-crystal Raman spectra were recorded on a Raman Microscope (Bruker RamanScope III) equipped with a Linkam stage. Graphical representations were created with Origin 2016.

NMR spectra were recorded on a JEOL 400 MHz ECZ spectrometer.

Quantum-chemical calculations were performed using the SCS-MP2[56] functional together with def-SV(P) basis set as implemented in Turbomole V6.4[57].

Crystal data were collected on a Bruker D8 Venture CMOS area detector diffractometer with $MoK_\alpha$ radiation. A single crystal was coated with perfluoroether oil at –30 to 25 °C and mounted on a 0.1–0.2 mm Micromount. The structures were solved by direct methods with SHELXT[58], SHELXS[59] or SIR2004[60] and refined by least squares on weighted $F_2$ values for all reflections in SHELXL[61] using Olex2[62]. Diamond 3[63] was used to prepare the graphical representations.

## 4.6.2 Crystallographic Data

| Compound | $[CoCp_2][Br_{11}]$ | $[CoCp_2]_2[I_3Br_4]_2 \cdot CH_2Cl_2$ | $[CoCp_2][I_2Cl_3]$ | $[NEt_4][I_5Br_2]$ |
|---|---|---|---|---|
| CCDC number | 1843805 | 1843806 | 1843807 | 1843808 |
| Empirical formula | $C_{10}H_{10}Br_{11}Co$ | $C_{21}H_{22}Br_8Cl_2Co_2I_6$ | $C_{10}H_{10}Cl_3CoI_2$ | $Br_4C_{16}I_{10}N_2$ (Hs are omitted) |
| Formula weight | 1068.12 | 1863.82 | 549.26 | 1808.82 |
| Crystal system | orthorhombic | monoclinic | monoclinic | orthorhombic |
| Space group | *Pnma* | *Cc* | $P2_1$ | *Cmce* |
| *a* [Å] | 20.870(2) | 27.8213(19) | 8.2409(9) | 12.5325(13) |
| *b* [Å] | 13.5903(15) | 8.9868(5) | 13.9868(16) | 15.0196(15) |
| *c* [Å] | 8.2937(9) | 17.8049(12) | 13.2783(14) | 10.8639(10) |
| $\alpha$ [°] | 90 | 90 | 90 | 90 |
| $\beta$ [°] | 90 | 115.548(2) | 99.253(5) | 90 |
| $\gamma$ [°] | 90 | 90 | 90 | 90 |
| Volume [Å$^3$] | 2352.4(4) | 4016.4(4) | 1510.6(3) | 2044.9(3) |
| *Z* | 4 | 4 | 4 | 2 |
| $\rho_{calc}$ [g · cm$^{-3}$] | 3.016 | 3.082 | 2.415 | 2.938 |
| *F*(000) | 1928.0 | 3336.0 | 1016.0 | 1560.0 |
| Crystal size [mm$^3$] | 0.24×0.05×0.04 | 0.60×0.20×0.14 | 0.19×0.15×0.09 | 0.21×0.05×0.02 |
| Wavelength [Å] | 0.71073 | 0.71073 | 0.71073 | 0.71073 |
| Temperature [K] | 100.0 | 100 | 100.0 | 100.03 |
| $\mu$ [mm$^{-1}$] | 19.407 | 13.546 | 5.726 | 11.494 |
| Absorption correction | multi-scan | multi-scan | multi-scan | multi-scan |
| $T_{min}$ | 0.0950 | 0.3813 | 0.6272 | 0.2029 |
| $T_{max}$ | 0.2387 | 0.7461 | 0.7456 | 0.7454 |
| Reflections collected | 73859 | 126158 | 119434 | 12015 |
| Independent reflections | 2343<br>$R_{int}$ = 0.1042<br>$R_{sigma}$ = 0.0265 | 11766<br>$R_{int}$ = 0.0663<br>$R_{sigma}$ = 0.0374 | 7349<br>$R_{int}$ = 0.0936<br>$R_{sigma}$ = 0.0331 | 1113<br>$R_{int}$ = 0.0574<br>$R_{sigma}$ = 0.0315 |
| Data/restrains/parameters | 2343/0/109 | 11766/2/288 | 7349/121/218 | 1113/36/48 |
| Goodness-of-fit on $F^2$ | 1.060 | 1.022 | 1.124 | 1.159 |
| Final R indexes [I≥2σ (I)] | $R_1$ = 0.0345<br>$wR_2$ = 0.0631 | $R_1$ = 0.0275<br>$wR_2$ = 0.0432 | $R_1$ = 0.0353<br>$wR_2$ = 0.0616 | $R_1$ = 0.0511<br>$wR_2$ = 0.1374 |
| Final R indexes [all data] | $R_1$ = 0.0467<br>$wR_2$ = 0.0668 | $R_1$ = 0.0375<br>$wR_2$ = 0.0451 | $R_1$ = 0.0487<br>$wR_2$ = 0.0653 | $R_1$ = 0.0551<br>$wR_2$ = 0.1401 |

| Compound | $[PPN\text{-}3^F]_2[I_4Cl_4]\cdot 4\ CH_3CN$ | $[PPh_4]_2[I_6Cl_6]$ (disordered with $[PPh_4]_2[I_4Cl_8]$) | $[PPh_4][I_2Cl_3]$ | $[PPh_4][I_3Cl_4]$ |
|---|---|---|---|---|
| CCDC number | 1843809 | 1843810 | 1843811 | 1843812 |
| Empirical formula | $C_{40}H_{18}Cl_2F_{18}I_2N_3P_2$ | $C_{24}H_{20}Cl_{3.29}I_{2.71}P$ | $C_{24}H_{20}Cl_3I_2P$ | $C_{24}H_{20}Cl_4I_3P$ |
| Formula weight | 1269.21 | 800.36 | 699.57 | 861.87 |
| Crystal system | monoclinic | triclinic | monoclinic | tetragonal |
| Space group | $P2_1/c$ | $P\bar{1}$ | $P2_1/c$ | $P\bar{4}$ |
| *a* [Å] | 12.1504(6) | 6.9629(5) | 10.6026(6) | 19.660(3) |
| *b* [Å] | 15.9622(9) | 10.6356(7) | 13.3871(8) | 19.660(3) |
| *c* [Å] | 22.6526(13) | 18.2762(13) | 17.7973(10) | 7.4187(8) |
| $\alpha$ [°] | 90 | 97.677(2) | 90 | 90 |
| $\beta$ [°] | 92.692(2) | 95.273(2) | 95.030(2) | 90 |
| $\gamma$ [°] | 90 | 91.210(2) | 90 | 90 |
| Volume [Å$^3$] | 4388.6(4) | 1334.86(16) | 2516.4(3) | 2867.4(9) |
| *Z* | 4 | 2 | 4 | 4 |
| $\rho_{calc}$ [g · cm$^{-3}$] | 1.921 | 1.991 | 1.8464 | 1.996 |
| *F(000)* | 2444.0 | 757.0 | 1343.3 | 1624.0 |
| Crystal size [mm$^3$] | 0.27×0.15×0.04 | 0.21×0.14×0.05 | 0.68×0.42×0.08 | 0.60×0.22×0.18 |
| Wavelength [Å] | 0.71073 | 0.71073 | 0.71073 | 0.71073 |
| Temperature [K] | 100.01 | 100.13 | 100.85 | 100.04 |
| $\mu$ [mm$^{-1}$] | 1.740 | 3.583 | 2.892 | 3.711 |
| Absorption correction | multi-scan | multi-scan | multi-scan | multi-scan |
| $T_{min}$ | 0.6627 | 0.5606 | 0.3038 | 0.2222 |
| $T_{max}$ | 0.7454 | 0.7452 | 0.6478 | 0.4296 |
| Reflections collected | 76886 | 76744 | 44914 | 20164 |
| Independent reflections | 9027<br>$R_{int}$ = 0.0413<br>$R_{sigma}$ = 0.0244 | 4892<br>$R_{int}$ = 0.0463<br>$R_{sigma}$ = 0.0173 | 7720<br>$R_{int}$ = 0.0447<br>$R_{sigma}$ = 0.0293 | 5619<br>$R_{int}$ = 0.0696<br>$R_{sigma}$ = 0.0604 |
| Data/restrains/ parameters | 9027/0/606 | 4892/0/290 | 7720/0/271 | 5619/0/289 |
| Goodness-of-fit on $F^2$ | 1.043 | 1.079 | 1.048 | 1.026 |
| Final R indexes [I≥2$\sigma$ (I)] | $R_1$ = 0.0354<br>$wR_2$ = 0.0880 | $R_1$ = 0.0193<br>$wR_2$ = 0.0374 | $R_1$ = 0.0298<br>$wR_2$ = 0.0686 | $R_1$ = 0.0361<br>$wR_2$ = 0.0729 |
| Final R indexes [all data] | $R_1$ = 0.0465<br>$wR_2$ = 0.0940 | $R_1$ = 0.0259<br>$wR_2$ = 0.0389 | $R_1$ = 0.0344<br>$wR_2$ = 0.0722 | $R_1$ = 0.0471<br>$wR_2$ = 0.0767 |

### 4.6.3 Syntheses

All syntheses were performed using standard Schlenk techniques, unless mentioned otherwise. When using water sensitive chemicals bromine was additionally condensed and stored over molecular sieve. Chlorine gas was dried by passing through $CaCl_2$. [HMIM]Br was dried in vacuum ($1\times10^{-3}$ mbar) for 2 days at 80 °C.

#### 4.6.3.1 Materials

| | |
|---|---|
| Acetonitrile ($CH_3CN$) | solvent system |
| Bis(triphenylphosphoranylidene)iminium chloride ($C_{36}H_{30}ClNP_2$, [PPN]Cl) | group supply |
| Bis[tris(3,4,5-trifluorophenyl)phosphoranylidene]-iminium chloride ($C_{36}H_{12}F_{18}ClNP_2$, [PPN-3$^F$]Cl) | see chapter 3.3 |
| Bromine ($Br_2$) (99%) | Merck |
| Chlorine ($Cl_2$) | Linde |
| Cobaltocene ($C_{10}H_{10}Co$, $CoCp_2$) | see[1] |
| Cobaltocenium bromide ($C_{10}H_{10}CoBr$, [$CoCp_2$]Br) | see[1] |
| Dichloromethane ($CH_2Cl_2$) | solvent system |
| Diethyl ether ($C_4H_{10}O$, $Et_2O$) | VWR |
| 1-Hexyl-3-metylimidazolium bromide ($C_{10}H_{19}BrN_2$, [HMIM]Br) (99%) | Iolitec |
| Hydrochloric acid (HCl) (37%) | VWR |
| Iodine monobromide (IBr) (98%) | Sigma-Aldrich |
| Iodine monochloride (ICl) (98%) | Alfa Aesar; Merck |
| Tetraethylammonium bromide ($C_8H_{20}NBr$, [$NEt_4$]Br) (99%) | Merck |
| Tetraphenylphosphonium chloride ($C_{24}H_{20}PCl$, [$PPh_4$]Cl) (98%) | Riedel-de Haën; Sigma-Aldrich |

### 4.6.3.2 Reactions of $[CoCp_2]Br$ or $CoCp_2$ with $Br_2$ ($[CoCp_2][Br_{11}]$)[1]

Elemental bromine was added to ice-cooled $[CoCp_2]Br$ or $CoCp_2$ respectively in different ratios. While for $CoCp_2$ inert reaction conditions are required, $[CoCp_2]Br$ can be handled under air. The mixture was heated to 60 °C to complete the reaction. The products are stable in closed glass ware.

For suitable crystals of $[CoCp_2][Br_{11}]$ an excess of bromine (1:120) was required. The reaction mixture was stored at 5 °C to obtain orange crystals.

$[CoCp_2][Br_{11}]$: Raman (–150 °C, region: 350–150 $cm^{-1}$): 314 (w), 295 (sh), 288 (s), 278 (vs), 228 (s) $cm^{-1}$.

### 4.6.3.3 Reactions of $[CoCp_2]Br$ with IBr ($[CoCp_2]_2[I_3Br_4]_2 \cdot CH_2Cl_2$)

$[CoCp_2]Br$ was solved in $CH_2Cl_2$ (2–4 ml). IBr was added in the desired ratio (1:3, 1:5, 1:7, 1:9). The reaction mixture was stirred until everything was dissolved and afterwards stored for 19 h at room temperature. The volatile materials were removed under reduced pressure at 0 °C. The orange-brown solid was again dissolved in $CH_2Cl_2$ (7–16 ml). Light orange crystals were obtained at –27 °C.

$[CoCp_2]_2[I_3Br_4]_2 \cdot CH_2Cl_2$: Raman (RT, crystals, region: 300–100 $cm^{-1}$): 211 (s), 189 (w), 163 (m), 120 (vw) $cm^{-1}$.

### 4.6.3.4 Synthesis of $[CoCp_2]Cl$ and reaction with ICl ($[CoCp_2][I_2Cl_3]$)

The $[CoCp_2]Cl$ synthesis was based on literature.[22] HCl (5 N) was added to $CoCp_2$ (1.00 g, 5.29 mmol). The reaction mixture was stirred until the gas evolution finished. The yellow-green solid was filtered, extracted with $Et_2O$ and dried under reduced pressure (0.74 g, 3.31 mmol, 63%).

$[CoCp_2]Cl$: IR (RT, region: 3500–550 $cm^{-1}$): 3078 (m), 2009 (w), 1719 (w), 1413 (vs), 1110 (w), 1068 (w), 1006 (s), 862 (vs), 820 (w), 564 (w) $cm^{-1}$.

$[CoCp_2]Cl$: Raman (RT, region: 3500–100 $cm^{-1}$): 3113 (w), 1419 (m), 1110 (s), 1064 (w), 854 (w), 386 (m),324 (s), 308 (s), 194 (vs) $cm^{-1}$.

To obtain crystals of $[CoCp_2][I_2Cl_3]$ $CH_2Cl_2$ (5 ml) and ICl (1.26 g, 7.78 mmol) were added to $[CoCp_2]Cl$ (0.24 g, 1.06 mmol). The suspension was held at room temperature over a period of 5 days. The volatile materials were removed under reduced pressure to obtain an

orange-brown solid, that was after analysis dissolved again in $CH_2Cl_2$. Light orange crystals were obtained at –33 °C.

$[CoCp_2][I_2Cl_3]$: FIR (RT, region: 400–150 $cm^{-1}$): 318 (w), 291 (s), 168 (w) $cm^{-1}$.

$[CoCp_2][I_2Cl_3]$: Raman (RT, region: 350–100 $cm^{-1}$): 324 (m), 306 (s), 191 (sh), 182 (vs) $cm^{-1}$.

### 4.6.3.5 Reactions of $[NEt_4]Br$ with IBr in [HMIM]Br ($[NEt_4][I_5Br_2]$)[2]

$[NEt_4]Br$ was solved in [HMIM]Br (0.4–0.9 g). IBr was added in the desired ratio (1:3, 1:5). The reaction mixture was stirred for 30 min. Red crystals were obtained at –30 °C.

$[NEt_4][I_5Br_2]$: Raman (–30 °C, crystal, region: 300–100 $cm^{-1}$): 224 (m), 191 (s), 160 (m) $cm^{-1}$.

### 4.6.3.6 Reaction of $[PPN\text{-}3^F]Cl$ with $Cl_2$ (2,4,6-Tris-(trichloromethyl)-1,3,5-triazine)

$[PPN\text{-}3^F]$ (0.07 g, 0.08 mmol) was suspended in $CH_3CN$ (0.1 ml). Chlorine was condensed onto the suspension that was slowly allowed to warm to room temperature. This procedure was repeated after 6 days (total amount of chlorine: 0.56 g, 7.86 mmol). Colorless crystals were formed at room temperature. When opening the reaction vessel HCl exhausted.

Reaction mixture: Raman (RT, region: 3000–150 $cm^{-1}$): 3000 (w), 2940 (m), 1618 (m), 1351 (m), 994 (m), 810 (m), 435 (sh), 415 (vs), 390 (sh), 375 (m), 328 (w), 290 (m), 272 (m), 259 (sh), 219 (w), 186 (m), 172 (sh) $cm^{-1}$.

Reaction mixture (after removing all volatile materials under vacuum): $^{31}P$ NMR (162 MHz, $CD_3OD$, 20 °C): $\delta$ = 19.9 ppm (m); $^{19}F$ NMR (376 MHz, $CD_3OD$, 20 °C): $\delta$ = –151.3 (m, 6F, *para*-F), –130.9 ppm (m, 12 F, *meta*-F).

### 4.6.3.7 Reaction of $[PPN\text{-}3^F]Cl$ with ICl ($[PPN\text{-}3^F]_2[I_4Cl_4] \cdot 4\ CH_3CN$)

$[PPN\text{-}3^F]Cl$ (0.25 g, 0.27 mmol) was suspended in $CH_2Cl_2$ (2 ml) and ICl (0.29 g, 1.80 mmol) was added. The mixture was stirred for 30 min and stored at room temperature for 8 days. The orange-brown liquid was separated from the orange solid. After removing volatile

materials under reduced pressure, the latter was dissolved in $CH_3CN$ (1 ml). Orange-yellow crystals were obtained at 0 °C.

$[PPN\text{-}3^F]_2[I_4Cl_4] \cdot 4\ CH_3CN$: Raman (0 °C, crystal, region: 350 –150 $cm^{-1}$): 346 (w), 332 (m), 319 (sh), 307 (w), 300 (w), 268 (s), 225 (w), 209 (w), 195 (vs), 166 (m) $cm^{-1}$.

### 4.6.3.8 Reactions of $[PPh_4]Cl$ with ICl

$[PPh_4]Cl$ (Riedel-de Haën) was solved in $CH_2Cl_2$ (8–10 ml). For one 1:3 approach the synthesis was also tested without the solvent $CH_2Cl_2$. ICl (Merck) was added in the desired ratio (1:1, 1:2, 1:3, 1:4, 1:7). The reaction mixture was stirred until everything was dissolved and afterwards stored for 29 h at room temperature. The volatile materials were removed under reduced pressure at 0 °C. The obtained solid was again dissolved in $CH_2Cl_2$ (1–18 ml). Orange crystals of the 1:3 approach that were formed at –30 °C, showed in X-ray structure analysis a formula of $[PPh_4]_2[I_6Cl_6]$ (disordered with $[PPh_4]_2[I_4Cl_8]$).

1:1: Raman (RT, crystal, region: 350–100 $cm^{-1}$): 257 (s), 199 (m), 113 (s) $cm^{-1}$.

1:1: Raman (–150 °C, region: 350–100 $cm^{-1}$): 259 (s), 199 (m), 120 (m), 109 (sh) $cm^{-1}$.

1:2: Raman (–150 °C, region: 350–100 $cm^{-1}$): 344 (w), 331 (w), 323 (w), 296 (w), 259 (s), 220 (m), 120 (m), 111 (sh) $cm^{-1}$.

1:3: Raman (–150 °C, region: 350–100 $cm^{-1}$): 345 (vs), 333 (s), 324 (s), 296 (s), 277 (s), 261 (w), 216 (m), 200 (m), 157 (m), 126 (sh), 116 (m), 108 (sh) $cm^{-1}$.

1:3: Raman (–150 °C, without prior solving in $CH_2Cl_2$, region: 350–100 $cm^{-1}$): 245 (vs), 332 (vs), 325 (vs), 298 (s), 277 (s), 261 (m), 216 (m), 200 (m), 157 (m), 127 (sh), 116 (m), 108 (sh) $cm^{-1}$.

1:4: Raman (–150 °C, region: 350–100 $cm^{-1}$): 345 (vs), 332 (s), 325 (s), 297 (s), 278 (s), 260 (m), 216 (m), 199 (m), 157 (m), 128 (sh), 115 (m), 109 (sh) $cm^{-1}$.

1:7: Raman (–150 °C, region: 350–100 $cm^{-1}$): 344 (m), 329 (vs), 324 (vs), 297 (w), 289 (w), 277 (w), 260 (s), 215 (w), 200 (m), 158 (w), 147 (m), 114 (m) $cm^{-1}$.

The synthesis with a 1:3 ratio was repeated with educts from different suppliers ($PPh_4Cl$: Sigma Aldrich, ICl: Alfa Aesar). Orange crystals of $[PPh_4][I_2Cl_3]$ were obtained at –30 °C.

$[PPh_4][I_2Cl_3]$: Raman (–196 °C, crystals in Raman cuvette, region: 350–100 $cm^{-1}$): 335 (sh), 308 (vs), 298 (vs), 280 (w), 264 (w), 53 (m), 212 (w), 202 (w), 193 (w), 154 (m), 108 (s) $cm^{-1}$.

In a further reaction $[PPh_4]Cl$ (Sigma-Aldrich) was first purified from residues of $[PPh_4]Br$. Therefore, a hot saturated solution in $CH_2Cl_2$ was slowly cooled down. The precipitated solid was filtered off and disposed. $CH_2Cl_2$ was removed under reduced pressure. Then $[PPh_4]Cl$ was solved in $CH_2Cl_2$ (5 ml) and reacted with ICl (Merck) in an 1:3 approach. The reaction mixture was stored for 4 days at room temperature. The volatile materials were removed under reduced pressure at 0 °C. The obtained orange solid crystallized within one day at room temperature. Orange crystals of $[PPh_4]_2[I_6Cl_6]$ (disordered with $[PPh_4]_2[I_4Cl_8]$) and colorless crystals of $[PPh_4][ICl_2]$ were obtained.

The different crystals have not completely separated for Raman microscope measurements.

Yellow colored spot: Raman (RT, crystals, region: 350–100 $cm^{-1}$): 344 (m), 326 (m), 293 (m), 287 (m), 258 (vs), 210 (w), 199 (m), 153 (m), 110 (s) $cm^{-1}$.

Bright orange colored spot: Raman (RT, crystals, region: 350–100 $cm^{-1}$): 344 (s), 330 (m), 293 (sh), 287 (m), 277 (sh), 258 (m), 210 (sh), 199 (vs), 154 (m), 109 (s) $cm^{-1}$.

Orange colored spot: Raman (RT, crystals, region: 350–100 $cm^{-1}$): 344 (s), 294 (sh), 286 (m), 277 (sh), 199 (vs), 154 (m), 105 (w) $cm^{-1}$.

In the reaction of $[PPh_4]Cl$ (0.29 g, 0.76 mmol) with 5 equivalents of ICl (0.61 g, 3.75 mmol) in $CH_2Cl_2$ (1 ml) yellow-orange crystals of $[PPh_4][I_3Cl_4]$ were obtained at –30 °C. In contrast to all syntheses above, the removal of the volatile materials was omitted.

$[PPh_4][I_3Cl_4]$: Raman (–30 °C, crystal, region: 350–100 $cm^{-1}$): 326 (vs), 258 (s), 202 (m), 142 (m), 107 (s) $cm^{-1}$.

## 4.7 References


[1] M. Gawrilow, *Bachelor thesis*, Freie Universität Berlin, Berlin, 2014.

[2] P. Voßnacker, *Bachelor thesis*, Freie Universität Berlin, Berlin, 2015.

[3] M. Wolff, J. Meyer, C. Feldmann, *Angew. Chem. Int. Ed.* 2011, *50*, 4970–4973; *Angew. Chem.* 2011, *123*, 5073–5077.

[4] M. Wolff, A. Okrut, C. Feldmann, *Inorg. Chem.* 2011, *50*, 11683–11694.

[5] R. Brückner, H. Haller, S. Steinhauer, C. Müller, S. Riedel, *Angew. Chem. Int. Ed.* 2015, *54*, 15579–15583; *Angew. Chem.* 2015, *127*, 15800–15804.

[6] H. Haller, M. Ellwanger, A. Higelin, S. Riedel, *Angew. Chem. Int. Ed.* 2011, *50*, 11528–11532; *Angew. Chem.* 2011, *123*, 11732–11736.

[7] H. Haller, M. Ellwanger, A. Higelin, S. Riedel, *Z. Anorg. Allg. Chem.* 2012, *638*, 553–558.

[8] M. E. Easton, A. J. Ward, T. Hudson, P. Turner, A. F. Masters, T. Maschmeyer, *Chem. Eur. J.* 2015, *21*, 2961–2965.

[9] K.-F. Tebbe, T. Farida, *Z. Naturforsch.* 1995, *50b*, 1440–1444.

[10] P. H. Svensson, L. Kloo, *Chem. Rev.* 2003, *103*, 1649–1684.

[11] H. Haller, S. Riedel, *Z. Anorg. Allg. Chem.* 2014, *640*, 1281–1291.

[12] H. Haller, J. Schröder, S. Riedel, *Angew. Chem. Int. Ed.* 2013, *52*, 4937–4940; *Angew. Chem.* 2013, *125*, 5037–5040.

[13] K. Sonnenberg, P. Pröhm, N. Schwarze, C. Müller, H. Beckers, S. Riedel, *Angew. Chem. Int. Ed.* 10.1002/anie.201803486; *Angew. Chem.* 10.1002/ange.201803486.

[14] C. Horn, M. Scudder, I. Dance, *CrystEngComm* 2001, *3*, 9–14.

[15] S. Gu, J. Wang, R. B. Kaspar, Q. Fang, B. Zhang, E. B. Coughlin, Y. Yan, *Sci. Rep.* 2015, *5*, 11668.

[16] E. Diana, M. R. Chierotti, E. M. C. Marchese, G. Croce, M. Milanesio, P. L. Stanghellini, *New J. Chem.* 2012, *36*, 1099–1107.

[17] E. Diana, P. L. Stanghellini, *J. Am. Chem. Soc.* 2004, *126*, 7418–7419.

[18] K. P. Huber, G. Herzberg, *Constants of diatomic molecules*, Van Nostrand Reinhold, New York, 1979, p. 106.

[19] R. Minkwitz, M. Berkei, R. Ludwig, *Inorg. Chem.* 2001, *40*, 25–28.

[20] M. C. Aragoni, M. Arca, F. A. Devillanova, M. B. Hursthouse, S. L. Huth, F. Isaia, V. Lippolis, A. Mancini, G. Verani, *Eur. J. Inorg. Chem.* 2008, *2008*, 3921–3928.

[21] A. Parlow, H. Hartl, *Z. Naturforsch.* 1985, *40b*, 45–52.

[22] D. Hartley, M. J. Ware, *J. Chem. Soc. A* 1969, 138–142.

[23] A. Parlow, H. Hartl, *Acta Crystallogr. B* 1979, *35*, 1930–1933.

[24] D. Hausmann, A. Eich, C. Feldmann, *J. Mol. Struct.* 2018, *1166*, 159-163.

[25] G. C. Hayward, P. J. Hendra, *Spectrochim. Acta* 1967, *23A*, 2309–2314.

[26] W. Gabes, H. Gerding, *J. Mol. Struct.* 1972, *14*, 267–279.

[27] Y. Yagi, A. I. Popov, *Inorg. Nucl. Chem. Lett.* 1965, *1*, 21–24.

[28] Y. Yagi, A. I. Popov, *J. Inorg. Nucl. Chem.* 1967, *29*, 2223–2230.

[29] A. Anderson, T. S. Sun, *Chem. Phys. Lett.* 1970, *6*, 611–616.

[30] L. Hoffmann, *Bachelor thesis*, Freie Universität Berlin, Berlin, 2016.

[31] CCDC: 144861 in The Cambridge Structural Database, C R. Groom, I. J. Bruno, M. P. Lightfoot, S. C. Ward, *Acta Cryst.* 2016, *B72*, 171–179.

[32] A. F. Hollemann, *Lehrbuch der Anorganischen Chemie*, Walter de Gruyter, Berlin New York, 2007, p. 458.

[33] D. Hausmann, R. Köppe, S. Wolf, P. W. Roesky, C. Feldmann, *Dalton Trans.* 2016, *45*, 16526–16532.

[34] P. K. Stoimenov, V. Zaikovski, K. J. Klabunde, *J. Am. Chem. Soc.* 2003, *125*, 12907–12913.

[35] A. O. Diallo, *Spectrochim. Acta* 1976, *32A*, 1665–1669.

[36] F. van Bolhuis, P. B. Koster, T. Migchelsen, *Acta Crystallogr. A* 1967, *23*, 90–91.

[37] E. E. Havinga, K. H. Boswijk, E. H. Wiebenga, *Acta Crystallogr. A* 1954, *7*, 487–490.

[38] K. N. Robertson, P. K. Bakshi, T. S. Cameron, O. Knop, *Z. Anorg. Allg. Chem.* 1997, *623*, 104–114.

[39] R. Brückner, P. Pröhm, A. Wiesner, S. Steinhauer, C. Müller, S. Riedel, *Angew. Chem. Int. Ed.* 2016, *55*, 10904–10908; *Angew. Chem.* 2016, *128*, 11064–11068.

[40] R. Babu, G. Bhargavi, M. V. Rajasekharan, *Eur. J. Inorg. Chem.* 2015, *2015*, 4689–4698.

[41] K.-F. Tebbe, M. El Essawi, S. A. El Khalik, *Z. Naturforsch.* 1995, 1429–1439.

[42] B. Freckmann, K.-F. Tebbe, *Acta Cryst A* 1981, *37*, C228.

[43] B. M. Powell, K. M. Heal, B. H. Torrie, *Mol. Phys.* 1984, *53*, 929–939.

[44] C. Walbaum, *Dissertation*, Universität zu Köln, Köln, 2009.

[45] K. Sasaki, I. Kuwano, K. Aida, *J. Inorg. Nucl. Chem.* 1981, *43*, 485–489.

[46] W. Gabes, H. Gerding, *J. Mol. Struct.* 1972, *14*, 267–279.

[47] A. G. Maki, R. Forneris, *Spectrochim. Acta* 1967, *23A*, 867–880.

[48] U. Müller, K. Dehnicke, J. Weidlein, *Schwingungsfrequenzen I. Hauptgruppenelemente*, Georg Thieme, Stuttgart New York, 1981, p. 73.

[49] E. V. Savinkina, B. N. Mavrin, D. V. Al'bov, V. V. Kravchenko, M. G. Zaitseva, *Russ. J. Coord. Chem.* 2009, *35*, 96–100.

[50] J. R. Magana, J. S. Lannin, *Phys. Rev. B* 1988, *37*, 2475–2482.

[51] L. Mann, *Master thesis*, Albert-Ludwigs-Universität Freiburg, Freiburg (Breisgau), 2013.

[52] R. Minkwitz, M. Berkei, *Z. Naturforsch. B* 2001, *56*, 39–42.

[53] J. E. Cahill, G. E. Leroi, *J. Chem. Phys.* 1969, *51*, 4514–4519.

[54] L. Meazza, J. Martí-Rujas, G. Terraneo, C. Castiglioni, A. Milani, T. Pilati, P. Metrangolo, G. Resnati, *CrystEngComm* 2011, *13*, 4427.

[55] B. Burgenmeister, K. Sonnenberg, S. Riedel, I. Krossing, *Chem. Eur. J.* 2017, *23*, 11312–11322.

[56] S. Grimme, *J. Chem. Phys.* 2003, *118*, 9095–9102.

[57] Turbomole 6.4 ed., a development of University of Karlsruhe and Forschungszentrum Karlsruhe GmbH, Karlsruhe, can be found under http://www.turbomole.com, 2012.

[58] G. M. Sheldrick, *Acta Crystallogr. A* 2015, *71*, 3–8.

[59] G. M. Sheldrick, *Acta Crystallogr. A* 2008, *64*, 112–122.

[60] M. C. Burla, R. Caliandro, M. Camalli, B. Carrozzini, G. L. Cascarano, L. De Caro, C. Giacovazzo, G. Polidori, R. Spagna, *J. Appl. Cryst.* 2005, *38*, 381–388.

[61] G. M. Sheldrick, *Acta Crystallogr. C* 2015, *71*, 3–8.

[62] O. V. Dolomanov, L. J. Bourhis, R. J. Gildea, J. A. K. Howard, H. Puschmann, *J. Appl. Crystallogr.* 2009, *42*, 339–341.

[63] K. Brandenburg, *DIAMOND*, Crystal Impact GbR, Bonn, 2014.

# 5 Summary

In this work novel polyhalides and polyinterhalides were synthesized and characterized. For the first time fluorinated bis(triarylphosphoranylidene)iminium salts, new kinds of weakly coordinating cations, were prepared and fully characterized.

Polybromide dianions and networks $[(C_6H_5)_3PBr]_2[Br_{14}]$, $[(C_6H_4F)_3PBr]_2[Br_{14}]$, $[(C_6H_4F)_3PBr][Br_{11}]$ and $[(C_6H_2F_3)_3PBr]_2[Br_{16}]$ were obtained, which could be included in the series of known compounds $[(C_6H_5)_3PBr][Br_7]$ and $[(C_6F_5)_3PBr]_2[Br_{20}] \cdot Br_2$. The so far unknown polyhalide networks with the repeating units $[Br_{14}]^{2-}$ and $[Br_{16}]^{2-}$ both make a valuable contribution to the structural diversity of polybromide dianions. It could be shown that fluorination of the bromo(triphenyl)phosphonium cation resulted in an increased bromine content in the resulting polybromides. The P–Br···Br distance decreases in the series $P(C_6H_4F)_3 > P(C_6H_2F_3)_3 > P(C_6F_5)_3$. This result could be supported by quantum-chemical calculations and the evaluation of the electrostatic potential, such as the $\sigma$-hole. An excess of bromine (≥ 5 equivalents) is of minor importance in the formation of the reported polybromides. The weakly perturbed $Br_2$ units from which the polybromides are formed allow to establish a relationship between their bond lengths and their Raman shift. This correlation has been confirmed by quantum-chemical calculations, is consistent to literature reported values and therefore revealed Raman spectroscopy as an excellent characterization method for this type of polybromides. Furthermore, the $[Br_{20}]^{2-}$ dianions [BMDIM][$Br_{20}$] and $[AsPh_4]_2[Br_{20}] \cdot ½\ Br_2$ as well as $[CoCp_2][Br_{11}]$, the first undecabromide that crystallized without further embedded $Br_2$ molecules in the crystal structure, were structurally characterized.

In the field of polyinterhalides a great variety of novel compounds was synthesized as well. With $[NMe_4][I_4Br_5]$ the so far largest iodobromide monoanion was synthesized and characterized. The $[I_4Br_5]^-$ anion shows a structural motif which was previously unknown among the nonahalides. It consists of a V-shaped $[I_2Br_3]^-$ coordinating two further IBr molecules via halogen-halogen interactions, which could be supported by quantum-chemical calculations. Depending on the selected solvent one of the two following isomers was formed: *syn*-$[NMe_4][I_4Br_5]$ in the ionic liquid [HMIM]Br and *anti*-$[NMe_4][I_4Br_5]$ in dichloromethane. In further investigations the iodobromides $[NEt_4][I_5Br_2]$ and $[CoCp_2]_2[I_3Br_4]_2 \cdot CH_2Cl_2$ were obtained. From the reaction of $[PPh_4]Cl$ a series of iodochlorides, namely $[ICl_2]^-$, $[I_2Cl_3]^-$, a novel chain-like structure of $[I_3Cl_4]^-$, the dianion $[I_6Cl_6]^{2-}$ as well as $[CoCp_2][I_2Cl_3]$ were obtained. This great variety of polyinterhalides extend the existing Raman spectral library and can therefore contribute to the future characterization of this compound class.

Besides the ratio between halide and halogen the structure of the obtained polyhalide strongly depends on the employed cation. Therefore, this thesis dealt with the synthesis and full characterization of fluorinated bis(triarylphosphoranylidene)iminium cations $[PPN\text{-}1^F]^+$, $[PPN\text{-}2^F]^+$ and $[PPN\text{-}3^F]^+$. These compounds were obtained by a new-developed one-pot reaction. By calculating the electrostatic potential and the fluoride ion affinity it could be shown that within the series the $[PPN\text{-}3^F]^+$ reveals the most weakly coordinating properties. These fluorinated $[PPN]^+$ cations can be used in the future to stabilize demanding anions, like for example $[PPN\text{-}3^F]_2[I_4Cl_4] \cdot 4\ CH_3CN$ presented here.

# 6 Zusammenfassung

Im Rahmen der vorliegenden Arbeit wurden neuartige Polyhalogenide und Polyinterhalogenide synthetisiert und charakterisiert. Zum ersten Mal konnten fluorierte Bis(triarylphosphoranyliden)iminiumsalze, eine neue Art schwach koordinierender Kationen, hergestellt und vollständig charakterisiert werden.

Es wurden Polybromiddianionen und -netzwerke $[(C_6H_5)_3PBr]_2[Br_{14}]$, $[(C_6H_4F)_3PBr]_2[Br_{14}]$, $[(C_6H_4F)_3PBr][Br_{11}]$ und $[(C_6H_2F_3)_3PBr]_2[Br_{16}]$ erhalten. Diese ließen sich in die Reihe der bekannten Verbindungen $[(C_6H_5)_3PBr][Br_7]$ und $[(C_6F_5)_3PBr]_2[Br_{20}] \cdot Br_2$ eingliedern. Die beiden neuartigen Polyhalogenid Netzwerke mit den Wiederholeinheiten $[Br_{14}]^{2-}$ und $[Br_{16}]^{2-}$ erweitern die strukturelle Vielfalt der Polybromiddianionen. Es konnte gezeigt werden, dass durch Fluorierung des Bromo(triphenyl)phosphoniumkations höhere Bromgehalte für die resultierenden Polybromide erreicht werden können. Der P–Br···Br Abstand nimmt in der Reihe $P(C_6H_4F)_3 > P(C_6H_3F_3)_3 > P(C_6F_5)_3$ ab. Dies konnte durch quantenchemische Rechnungen und der Untersuchung des elektrostatischen Potentials, wie z. B. des $\sigma$-Lochs untermauert werden. Ein Überschuss an Brom (≥5 Äquivalente) spielt für die Bildung der erwähnten Polybromide eine untergeordnete Rolle. Die schwach gestörten $Br_2$-Einheiten, aus denen die Polybromide aufgebaut sind, erlaubten es, einen Zusammenhang zwischen ihren Bindungslängen und ihrer Frequenzverschiebung im Raman Spektrum herzustellen. Diese Korrelation wurde durch quantenchemische Rechnungen bestätigt, ist mit den Werten aus der Literatur konsistent und macht daher die Raman-Spektroskopie zu einer ausgezeichneten Charakterisierungsmethode für diese Art von Polybromiden. Des Weiteren wurden die $[Br_{20}]^{2-}$ Dianionen $[BMDIM][Br_{20}]$ und $[AsPh_4]_2[Br_{20}] \cdot ½\ Br_2$ sowie $[CoCp_2][Br_{11}]$, das erste Undecabromid, das eine Kristallstruktur ohne ein weiteres eingebettetes $Br_2$-Molekül aufweist, strukturell charakterisiert.

Im Bereich der Polyinterhalogenide konnte auch eine Vielfalt neuer Verbindungen synthetisiert werden. So konnte mit $[NMe_4][I_4Br_5]$ das bislang größte Iodbromid-Monoanion synthetisiert und charakterisiert werden. $[I_4Br_5]^-$ weist ein strukturelles Motiv auf, das unter den Nonahalogeniden bislang nicht bekannt war. Es besteht aus einem V-förmigen $[I_2Br_3]^-$ Anion, das zwei IBr-Moleküle über Halogen-Halogen-Wechselwirkungen koordiniert, was im Einklang mit quantenchemischen Rechnungen steht. In Abhängigkeit vom gewählten Lösemittel wurde eines der folgenden Isomere gebildet: *syn*-$[NMe_4][I_4Br_5]$ in der ionischen Flüssigkeit [HMIM]Br und *anti*-$[NMe_4][I_4Br_5]$ in Dichlormethan. In weiteren Untersuchungen konnten die Iodbromide $[NEt_4][I_5Br_2]$ und $[CoCp_2]_2[I_3Br_4]_2 \cdot CH_2Cl_2$ erhalten werden. Durch die Reaktion von $[PPh_4]Cl$ mit ICl konnte eine Reihe an

Iodchloriden erhalten werden, nämlich $[ICl_2]^-$, $[I_2Cl_3]^-$, eine neue kettenförmige Struktur von $[I_3Cl_4]^-$, das Dianion $[I_6Cl_6]^{2-}$, sowie $[CoCp_2][I_2Cl_3]$. Diese Vielzahl an Interhalogeniden ergänzt die bisherige Raman-Spektrenbibliothek und kann daher zukünftig zur Charakterisierung dieser Verbindungsklasse beitragen.

Die Struktur der erhaltenen Polyhalogenide hängt neben dem Verhältnis von Halogenid zu Halogen stark vom verwendeten Kation ab. Daher beschäftigt sich diese Arbeit auch mit der Synthese und vollständigen Charakterisierung der teilfluorierten Bis(triarylphosphoranyliden)iminiumkationen $[PPN\text{-}1^F]^+$, $[PPN\text{-}2^F]^+$ und $[PPN\text{-}3^F]^+$. Diese Verbindungen konnten erstmals im Zuge einer neu entwickelten sogenannten Eintopf-Reaktion erhalten werden. Durch Berechnung des elektrostatischen Potentials und der Fluoridionenaffinität konnte gezeigt werden, dass innerhalb dieser Serie das $[PPN\text{-}3^F]^+$ die am schwächsten koordinierenden Eigenschaften aufweist. Diese fluorierten $[PPN]^+$ Kationen können zukünftig zur Synthese anspruchsvoller Anionen eingesetzt werden, wie zum Beispiel dem hier vorgestellten $[PPN\text{-}3^F]_2[I_4Cl_4] \cdot 4\ CH_3CN$.

# 7 Publications and Conference Contributions

## Publications (Part of this work: 1–3)

[4] S. Hämmerling, L. Mann, S. Steinhauer, M. W. Kuntze-Fechner, U. Radius, S. Riedel, submitted. Investigation of Organonickel-Pentafluoroorthotellurates

[3] L. Mann, G. Senges, K. Sonnenberg, H. Haller, S. Riedel, *Eur. J. Inorg. Chem.* 10.1002/ejic.201800404. Polybromide Dianions and Networks Stabilized by Fluorinated Bromo(triaryl)phosphonium Cations.

[2] L. Mann, S. Steinhauer, E. Hornberger, S. Riedel, *Chem. Eur. J.* 2018, *24*, 3902–3908. Further Developments of Weakly Coordinating Cations: Fluorinated Bis(triarylphosphoranylidene)iminium Salts.

[1] L. Mann, P. Voßnacker, C. Müller, S. Riedel, *Chem. Eur. J.* 2017, *23*, 244–249. $[NMe_4][I_4Br_5]$: A new Iodobromide from an Ionic Liquid with Halogen–Halogen Interactions.

## Conference Participation (Poster Contributions as Presenting Author)

09/2017 GDCh Scientific Forum Chemistry 2017, Berlin, Germany

Poster title: Fluorinated $\mu$-Nitridobis(triphenylphosphorus) Cations

09/2016 18. Vortragstagung der Wöhler-Vereinigung, Berlin, Germany

Poster title: Interhalogen Anions – A New Nonainterhalide and Novel Weakly Coordinating Cations

09/2016 17. Deutscher Fluortag, Dorfweil, Germany

08/2015 ISFC & ISoFT Como 2015, 21st International Symposium on Fluorine Chemistry, Como, Italy

Poster title: Partly Fluorinated Cations for Stabilisation of Polybromide Anions

09/2014 16. Deutscher Fluortag, Dorfweil, Germany

## Conference Organization (Book of Abstracts)

09/2016 18. Vortragstagung der Wöhler-Vereinigung, Berlin, Germany

11/2014 X. German-Russian-Ukrainian Symposium on Fluorine Chemistry, Berlin, Germany

## Oral Presentations

04/2017 GRK 1582 "Fluorine as a Key Element", Seminar

Title: Fluorinated $\mu$-Nitridobis(triphenylphosphorus) Cations

03/2017 GRK 1582 "Fluorine as a Key Element", Workshop

Title: Novel Fluorinated Bis(triphenylphosphine)iminium Salts

04/2016 GRK 1582 "Fluorine as a Key Element", Workshop

Title: Poly- and Interhalides of the Cobaltocenium Cation

11/2015 GRK 1582 "Fluorine as a Key Element", Seminar

Title: Partly Fluorinated Cations for Stabilisation of Polybromide Anions

10/2015 GRK 1582 "Fluorine as a Key Element", Workshop

Title: Stabilisation of Polybromide Anions by Different Substituted Bromotriphenylphosphonium Cations

# 8 Curriculum Vitae

The curriculum vitae is not included for reasons of data protection.